CLEAN AIR TASK FORCE

CASCADE INSTITUTE

Cornell Atkinson Center for Sustainability

Prospecting for superhot rock energy: A technology gap analysis for siting and characterizing superhot rock energy resources

Authors: Chanmaly Chhun, Cornell University; Rebecca Pearce, Cascade Institute; Pascal Caraccioli Salinas, Cornell University; Seth Saltiel, Cornell University; Carolina Munoz Saez, Cornell University

Executive summary

Superhot Rock (SHR) geothermal systems are attracting significant interest from governments, industries, and academia due to their high energy density and potential for large-scale, low-cost electricity production. SHR systems are defined by the temperature at which water becomes supercritical (>374°C), and are typically accessible at depths of 15 km or less. However, these temperatures can be found within 5 km depths in areas of active magmatism, such as subduction zones, extensional regions, and hot spots. In order to develop SHR geothermal systems, it is necessary to characterize the physical properties of the subsurface that hosts the geothermal resource, which is achieved by conducting geological and geophysical studies of the prospective site. Siting and resource characterization are essential to identify drilling targets, mitigate project risks, and improve project economic projections. This report focuses on the geophysical methods that effectively characterize SHR geothermal resources, identifies technology gaps that must be closed to improve SHR resource characterization, and suggests strategies to close these gaps.

We review the subsurface characterization technologies relevant to SHR geothermal resources, including potential field (gravity and magnetics), electromagnetic (EM), seismic, remote sensing, geodesy, well-logging, rock physics experimentation, and fluid geochemistry analysis methods. We then review data analysis techniques that optimize data integration and model interpretation, including joint inversion, value-of-information, machine learning, and play fairway analysis methods. Applications to SHR systems are highlighted with an assessment of state-of-the-art technologies and gaps that would contribute to limiting the risk and improving the scalability of SHR energy development. The report then explores techniques to resolve the crucial subsurface properties that determine the economic feasibility of a SHR resource: temperature at depth, fluid transport mechanisms (permeability), stress regime and proximity to tectonic and volcanic structures. We performed this analysis by grouping the relevant technologies by their optimal spatial sensitivity, progressing from the exploration scale (100s-10s km), reservoir scale (10s-1 km), validation and monitoring scale (1 km-1 m).

At the exploration scale, geodynamic settings provide context for interpreting heat sources/magma, reservoir rock conditions, stress states, and the presence of seismogenic faults. Different SHR play sub-types may require varied approaches. Increasing the granularity of models is a key technological advancement needed for SHR. Heat mapping at the exploration scale is best achieved by integrating a range of geophysical datasets, including thermal conductivity properties, surface heat flow, seismic velocity models, sediment thickness, electromagnetic conductivity, and more. Improving data granularity and modelling capacity of convective heat flow will improve thermal model accuracy. The 3D stress state at depth can be captured by detailed stress maps, but increased data resolution is also necessary. Greater data resolution is crucial for drilling design and engineering permeability enhancement at prospective SHR project sites. Structures and permeability are vital for understanding fluid transfer and ambient stress fields, which can be derived from fracture imaging, locating natural and induced seismicity, anisotropy, and focal mechanism analyses. Seismic methods show promise for mapping these structures, but current technical gaps remain in obtaining robust data analysis and methods in hard-rock and heterogeneous SHR geothermal fields.

At the reservoir scale (i.e., using dense data surveys to increase model resolution and building 3D geological conceptual models for siting), estimating temperature at depth involves direct measurements from exploratory boreholes and proxies for thermal conductivity. There is a strong correlation between thermal model accuracy and data density, elevating the need for high resolution well-log sampling at SHR sites. Stress measurement and pore fluid pressure estimation are essential for reservoir borehole design and preventing drilling complications. Crosswell seismic/EM tomography and logging are promising for mapping structures and permeability with high resolution in the vicinity of the boreholes.

Monitoring induced seismicity provides detailed information about reservoir state and mitigates reservoir development/extraction risks. Adaptive Traffic Light Systems (ATLS) for balancing fluid injection and production need to be developed for SHR fields to limit the intensity of seismicity. Real-time microseismic, EM, gravity monitoring arrays, and remote sensing can also map (sub)surface deformation due to changes in reservoir mass balance. Long-term lifecycle analysis (e.g., numerical reservoir simulation, tracer, transient tests) is necessary to track heat depletion, mass balance, and fluid-rock interaction geochemistry, requiring more field demonstration sites and long-term production data.

Overall, many geophysical methods required for SHR exploration are developed and ready for application, but limited validation in relevant locations hampers robust conclusions. Data-driven analysis methods, including machine learning, show potential but are constrained by a lack of sufficient data. More field-validated datasets and laboratory experiments are needed to establish robust connections between geophysical observables and the key rock properties and conditions.

By addressing the following challenges and advancing the needed technologies, SHR geothermal systems can become a viable and significant source of clean energy transition solutions, contributing to a sustainable energy future:

- **Refining and advancing subsurface SHR site characterization technologies**: Target SHR plays by integrating various datasets to identify favorable conditions for superhot EGS reservoirs within sustained elevated heat flow areas. Incorporate high-resolution and integrated data analysis for a SHR-specific field and develop good models/practices by both data- and expert-driven analyses targeting any SHR geological setting.
- **Standardized and shared data collection and analysis**: Establish a sharing approach of SHR site characterization to de-risk exploration (e.g., Play Fairway Analysis) and improve extrapolation of lessons learned between projects. Conduct retroactive studies with archival datasets to identify optimal geophysical techniques.
- **Investment and policy support**: Substantial subsidies, tax incentives, research funding, and company investment are needed to support the development of next-generation technologies and promote public understanding and acceptance of SHR geothermal energy.

Table of contents

Acronyms and abbreviations

AAS: Atomic Absorption Spectroscopy

AGG: Airborne Gravity Gradiometry

AI: Artificial Intelligence

BDT: Brittle Ductile Transition zone

CDP: Curie Depth Point

CFN: Cloud Fracture Network

CLG: Closed-Loop Geothermal

CSEM: Controlled-Source Electromagnetics

DAS: Distributed Acoustic Sensing

DOAS: Differential Optical Absorption Spectroscopy

DTS: Distributed Temperature Sensing

EGS: Enhanced Geothermal Systems

ERT: Electrical Resistivity Tomography

FTG: Full Tensor Gradiometry

GNSS: Global Navigation Satellite System

HTHP: High Temperature High Pressure

IC: Ion Chromatography

ICP-MS: Inductively Coupled Plasma Mass Spectrometry

InSAR: Interferometric Synthetic Aperture Radar

ML: Machine Learning

MSA: Micro Seismic Array

MT: Magnetotellurics

PFA: Play Fairway Analysis

Q: Quality factor

SEE: SeismoElectric Effect

SHF: Surface Heat Flow

SHR: Superhot Rock

TEM: Transient Electromagnetics

TIR: Thermal infrared

TMI: Total Magnetic Intensity

VSP: Vertical Seismic Profiling

XRD: X-Ray Diffraction

1. Introduction

1.1 Background

There is growing governmental, commercial, and academic interest in high enthalpy, Superhot Rock (SHR) geothermal resources due to their high energy density and potential for large-scale electricity production. SHR geothermal reservoirs are defined as resources with temperatures above the supercritical point of pure water, ~375°C. These temperatures exist everywhere on Earth but are only readily accessible in areas of active magmatism—subduction zones with volcanic arcs, extensional regions and rift structures, or hot spot mantle plumes (Manzella et al., 2019). To develop SHR resources beyond these geological domains, significant advances in reservoir permeability enhancement and deep (>7 km) drilling into crystalline rock must be achieved (Cladouhos & Callahan, 2024a). All SHR prospects, regardless of geological setting, must undergo extensive siting and characterization studies to assess the project's technical feasibility, risks, economic cost, and return on investment.

The site-specific aspects of geothermal resources introduce significant risk to developing SHR resources. Geothermal wells must be drilled into uncertain subsurface conditions at great expense, and their failure can terminate a project. While this challenge is not shared by modular renewable technologies such as wind and solar, other subsurface resources such as minerals and hydrocarbons face similar exploration risks. Techniques to mitigate these risks are well-developed by the mining, oil and gas, and conventional geothermal sectors, which can be leveraged and adapted for SHR siting and characterization procedures. This report reviews state-of-the-art geophysical, geochemical, and geological methods that can characterize SHR geothermal resources; identifies technical gaps in these methods for SHR characterization; and suggests strategies to close these gaps. This report is one of a five-part series that analyzes technology gaps for SHR resource development (see companion reports on heat extraction, drilling, well completion, and surface equipment on the Clean Air Task Force Superhot Rock landing page). The technology gap analysis series was facilitated by the Clean Air Task Force, with the *Drilling* report and this *Siting and Resource Characterization* report done in collaboration with the Cascade Institute.

The Earth's crust is a complex system that offers little observable evidence of subsurface conditions. Geoscientific methods strive to illuminate these conditions with instruments that sense specific physical or chemical properties at depth. Sampling multiple properties and performing different types of geoscientific data analysis increase confidence in model outputs, iteratively reducing uncertainty and exploration risk. The properties targeted by an exploration program are specific to the prospected resource (Beardsmoore & Cooper, 2009). In the case of SHR geothermal, the primary properties to constrain are heat, stress, permeability/fluid content, and geological structures. These parameters are first-order controls of the commercial viability of a resource, as they inform: 1) the temperature and thermal transfer mechanism at depth; 2) the drilling program required to access the resource, including depth to target, well configuration, and orientation; 3) requirements to enhance reservoir permeability; and 4) the risks of induced seismicity. It is, therefore, crucial to constrain the key properties to the highest degree of confidence or risk substantial project failures.

Exploration risks are particularly difficult to estimate and manage without costly exploration drilling and core analysis. Surface geophysics can indirectly estimate these properties at a broad range of scales with sufficient data coverage from coeval surveys, but each method can be compromised by poor data quality or invalid assumptions. Lastly, there are only a handful of SHR resources that have been extensively characterized by geophysics and verified with exploration drilling. Therefore, it is difficult to conclusively determine best practices for SHR resource characterization.

1.2. Report organization

As this report covers a wide range of material, with varying levels of detail, it is not designed to be read from beginning to end in sequence. We suggest that the reader use the table of contents and provided references and links to navigate to topics of interest. We begin with a review of available geophysical/geochemical properties and measurement methods (Section 2.1), and data analysis / interpretation techniques (Section 2.2) for characterizing the subsurface conditions of a geothermal resource. Applications to SHR systems are highlighted with an assessment of state-of-the-art technologies and gaps that would contribute to limiting risk and improving the scalability of SHR energy development. Section 2 provides background that is referenced throughout the rest of the report. The way that characterization data are utilized varies greatly depending on their applicable scale and resolution.

From there, the report follows the chronological use of these techniques from initial exploration at the regional scale (Section 3), through detailed reservoir scale surveys and well-logging methods to validate the inferred properties (Section 4). Characterization techniques are needed to assess reservoir changes throughout the full development and operational phases of a project, referred to as monitoring (Section 5). Each of these sections is organized according to the most important reservoir characteristics and how they are constrained at each scale: heat, stress, fluids/permeability, and structures. We conclude by highlighting investment, policy, research, and development priorities for enabling economic SHR energy production (Section 6).

2. Methods

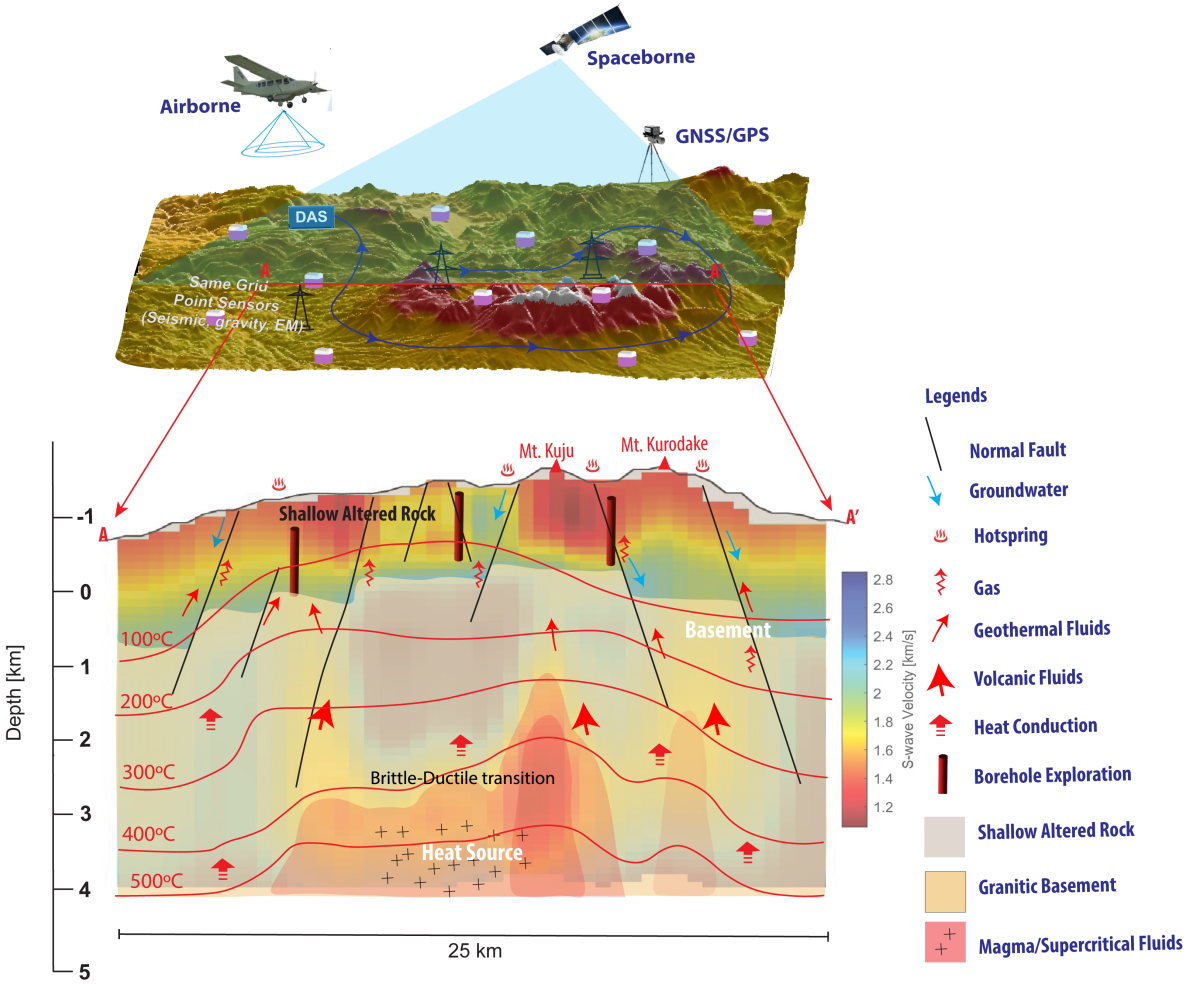

Figure 1. Conceptual representation of current technologies applied to SHR geothermal resource characterization and how these data of the subsurface are mapped and interpreted, modified from Chhun et al., 2024.

2.1 Geophysical rock properties and measurement techniques

2.1.1 Density (gravity)

Rock density, or total rock mass per unit volume, relates to rock composition, crystallinity, fluid saturation, and porosity. Gravimetry can detect contrasts in rock density at depth, a geophysical method that measures changes in the surveyed gravitational potential field with a gravimeter (Hinze et al., 2013; Kana et al., 2015; Telford et al., 1990). Gravimetry is a mature, relatively low-cost, non-invasive geophysical method that provides insight into subsurface geology, such as those hosting geothermal resources, including SHR plays. Common geothermal features resolved by gravity data are generally, 1) basement geometry and sediment-crystalline rock contacts; 2) surface lithologic deposition (such as tuffs and lavas); 3) structural offsets in lithologies with contrasting density, an indicator of fault

structures; 4) hydrothermal precipitation or alteration that densifies silica (Folsom et al., 2020), 5) diapiritic intrusions of magma, salt, and shale; and 6) deeper crustal transitions. Deeper lateral contrasts create longer wavelength variations in gravity, whereas shallow lateral changes can create short to long wavelength variations depending on the scale of the features (Kana et al., 2015; Omollo & Nishijima, 2023). As a potential field method, gravity data loses sensitivity with depth, and is challenged with non-uniqueness, where an infinite number of density models can fit the observed gravity data (Gasperikova & Cumming, 2020).

These challenges are well-known, and there are many techniques to improve depth resolution and mitigate non-uniqueness, such as informing gravity data inversions with *a priori* information or jointly inverting residual gravity data with complementary datasets (Ars et al., 2019; Y. Li & Oldenburg, 1998; Soyer et al., 2018; Witter et al., 2016). These techniques apply to SHR geothermal plays; however, technology gaps remain, as SHR reservoirs are typically deeper, and structures at depth may not exhibit gravity signatures.

2.1.1.1 Scalar gravimetry

Scalar gravity surveys recover an array of point measurements of absolute gravity values. Gravity data are collected by spaceborne satellites, airborne fixed-wing aircraft, or through land-based surveys, progressively decreasing spatial coverage and density of measurements, but increasing their resolution and precision (Hardwick et al., 2019; Hinze et al., 2013; Kana et al., 2015; Telford et al., 1990). The data undergo a series of corrections to produce a map of residual gravitational anomalies, referred to as a Bouguer Anomaly map, which can be inverted (Section 2.2.3) to produce a 2D or 3D density model of the subsurface (Telford et al., 1990). Including *a priori* information in the model can reduce the non-uniqueness of gravity data (Faulds et al., 2021; Omollo & Nishijima, 2023; Siler et al., 2020; Witter et al., 2016).

In non-magmatic, hot-dry rock SHR plays, gravity residuals lose resolution with increased depth, increasing model non-uniqueness. As well, the densities of hard rock become more uniform with increasing depth, thus deeply buried geological contacts and structures may not exhibit detectable gravity signatures at the surface. This was observed at the DOE-funded research initiative Utah FORGE (Section 3.1). Long-wavelength gravity anomalies revealed basin geometry consistent with MT and seismic models. Short-wavelength anomalies were related to dipping interfaces between bedrock and sediment boundaries (Hardwick et al., 2019). However, a blind fault plane that separates impermeable and permeable rock units was not revealed in the gravity data (Interview with lead researchers at Utah FORGE). Mapping fault planes at depth is essential to seismic risk assessment. Extensive modelling with archival or synthetic datasets of SHR-analog sites will prove the use of gravity for locating blind, deep structures.

Advanced gravity modelling techniques such as edge detection may improve the sensitivity of gravity measurements to structures at depth. Omollo & Nishijima (2023) conducted a gravity survey of the Olkaria geothermal reservoir in Kenya, a high-temperature (>300°C), rift-system play geothermal resource that supplies the 799 MW Oklaria geothermal plant. They computed residual (high-frequency)

and regional anomaly (low-frequency) trends and applied additional filtering techniques such as horizontal derivative (HD) for horizontal edge detection and improved normalized horizontal tilt angle (INH) for further edge resolution and noise suppression. These additional filters, HD and INH, improved the resolution of fault structures and dips, fractured lithologies due to faulting, and other deep reservoir structures. In another case, Folsom et al. (2020) conducted a multi-geophysical study of the blind geothermal system in San Emidio, Nevada, incorporating gravity, magnetics, and MT to characterize a drilling-confirmed geothermal reservoir. Computing the first vertical derivative and maximum horizontal gradient yielded a density structure not resolved in the scalar gravity residual. Furthermore, the first vertical derivative residuals identified a gravity low related to hydrothermal alteration that was highly correlated with a coeval magnetic study (Figure 2). Similar methods were applied by Faulds et al. (2021) to resolve blind geothermal systems and fault planes, which show no expression of geothermal resources at the surface, analogous to EGS-type SHR plays. Sufficient receiver distribution is required to perform edge detection and mitigate spatial aliasing; otherwise, the faults and structures generated through deriving grid data may be artifacts, not true structures.

2.1.1.2 Full tensor gravity gradiometry

Full tensor gradiometry (FTG), also known as airborne gravity gradiometry (AGG), captures the gravitational potential field in 3D. The rate of change of the gravitational field is represented as a third-rank tensor, yielding three primary components: the vertical gradient, horizontal curvature, and horizontal gradient. Each component resolves aspects of the gravitational field that are not captured by a classic scalar gravimetry survey, such as direct geological contacts, the curvature of geological structures such as fault blocks, carbonates and ore bodies, and high-frequency (shallow) changes in the vertical gradient that are lost when processing classic scalar gravimetry data (Kohrn et al., 2011). Due to increased spatial coverage, FTG is less prone to spatial aliasing that can occur in sparsely sampled scalar gravity surveys. However, FTG is at higher risk of noise than scalar surveys. In an airborne survey, k-space Fourier filters may be applied to correct instrument and flight path noise.

Few studies have been conducted on the applications of FTG for geothermal resource characterization. One example is the study by Kohrn et al. (2011), which computed the FTG forward calculations of the Salton Sea Geothermal Field, and successfully resolved known structures through geological mapping and scalar gravimetry, such as high-density hydrothermal alteration along fault zones and basin bounding faults. Further studies in the applicability of FTG for SHR resource characterization should be conducted.

Gaps:

- An infinite number of density models may produce the observed gravity signatures—this is referred to as *non-uniqueness*.
- Gravimetry may not resolve the density contrasts of deep lithologies, which may impact the seismic risk assessment of SHR projects. Complex overburdens further challenge poor depth resolution as they mask the signatures of deeper density contrasts.
- The trade-offs between airborne and land-based gravity are substantial, with airborne surveys prioritizing efficiency, coverage and data density, while land-based surveys prioritize accuracy and cost.

Current technology:

- Scalar and full-tensor gradiometry are mature geophysical methods for constraining density variations at depth. Ideal targets are geological contacts with contrasting densities, such as sediment-crystalline offsets from faults or basin geometry.

- In both academics and industry, gravimetry methods are a highly common first-stage study for characterizing geothermal or other resources and their hosting geology. Geosoft Oasis Montaj by Seequent™ is a common, industry-standard gravity data processing and modelling tool. A common, industry-standard handheld gravimeter is the Scintrex CG6. Zonge and Quantec Geoscience Ltd. are established geophysical contractors that conduct gravity data collection and analysis.

Technology/approach needed to develop SHR:

- Conducting coeval geophysical studies, particularly magnetics, EM methods, and seismology, may improve the delineation of deep geological structures with low-density contrasts and reduce non-uniqueness.
- Confirm the sensitivity of gravity to SHR reservoir targets, particularly blind fault planes. This is best achieved with forward modelling experiments of SHR settings.
- Researchers should conduct synthetic and in-field experiments with FTG gravimetry on known SHR resources to verify its applicability to SHR characterization.

2.1.2 Magnetic susceptibility

Magnetic susceptibility measures material magnetization per unit volume when exposed to a magnetic field. The magnitude of rock magnetization is measured by detecting anomalies in the Earth's magnetic field, or *primary field*. The magnetic susceptibility of a rock relates to its composition—particularly if it is rich in magnetite or iron-ore—and rock temperature. The magnitude of magnetic susceptibility depends on the present-day primary field, as well as the magnetic traces of the historic primary field at the time of the rock formation, referred to as remnant magnetization (Georgsson, 2009; Hinze et al., 2013; Kana et al., 2015; Núñez Demarco et al., 2021; Pandarinath et al., 2014; Telford et al., 1990). Like gravimetry, magnetic potential field mapping is one of the most accessible and available geophysical observables, measured primarily by satellite for continental scale resolution, or airborne-mounted systems for regional scale resolution (Mather & Fullea, 2019).

In the SHR context, magnetic anomaly data covering hundreds of kilometers of spatial distribution can be used to resolve the Curie Depth Point (CDP) (Kolker et al., 2022) (Section 3.2.2). At the regional scale, structural trends, magmatic intrusions, and hydrothermal alteration from geothermal fluids can produce a recoverable magnetic susceptibility signature (Folsom et al., 2020; Pandarinath et al., 2014). The latter two signatures can also be detected by EM methods in 3D.

2.1.2.1 Total magnetic intensity (TMI)

The magnetic susceptibility of rocks can be inferred by measuring the distribution of total magnetic intensity (TMI) over a target formation through land or airborne surveys with fluxgate, proton

precession, or optical absorption magnetometers (Carrillo et al., 2022; Georgsson, 2009; Kana et al., 2015). The data undergoes a series of corrections, and residual magnetic contours indicate magnetic susceptibility anomalies. Gravity and magnetic potential field methods can be collected coevally (Figure 2) and jointly inverted to reduce model non-uniqueness inherent in both potential field methods (Section 2.2.3). However, joint inversions cannot be performed if the surveys do not have similar receiver distributions, which is the case if TMI surveys are acquired with airborne units and gravity surveys are acquired with land-based units.

Magnetic signatures of intrusive units tend to be positive due to magnetic material, while hydrothermally altered units are demagnetized and show non-magnetic signatures (Kana et al., 2015; Maubana et al., 2019; Zahedi et al., 2022). In the SHR context, TMI surveys can resolve fault structures, intrusive units, hot springs and fumaroles, upflow zones, and evidence of high-temperature mineral alteration (Faulds et al., 2021; Georgsson, 2009). Its primary use when characterizing SHR resources will be through continental-scale surveys for depth to CDP estimation.

Gaps:

- Modelling TMI data are challenged by non-uniqueness, and should be paired with complementary geophysical methods to improve model confidence.
- The magnetic signatures of EGS-type SHR resources require further study. Archival TMI datasets from existing SHR or analog locations should be cross-referenced and compared to identify distinct signatures of SHR reservoirs.

Current technology:

- Magnetic susceptibility surveys are mature, industry-standard methods for mapping magnetic properties at continental to reservoir scales. Datasets covering hundreds of kilometers can be used to estimate depth to CDP, whereas regional-scale datasets can resolve some structural, geological, and geothermal features that contextualize a geothermal reservoir.
- Quantec Geoscience Ltd. and Zonge are established data acquisition firms. Oasis Montaj (GeosoftTM), ModelVision, and Viridien Multiphysics (Li & Oldenburg, 1998) are established data processing modelling software.

Technology/approach needed to develop SHR:

- Forward calculations should be performed to verify the applicability of TMI surveys for SHR resource characterization. The optimal spatial density required to detect target resources at depth should be modelled.
- Potential field methods, such as TMI, work most effectively when coupled with datasets that resolve the 3D geometry of subsurface structures, such as MT or passive seismology. Where these complementary datasets are available from SHR or analog locations, a series of modelling experiments should be performed with cross-gradient inversion techniques (Section 2.2.3).

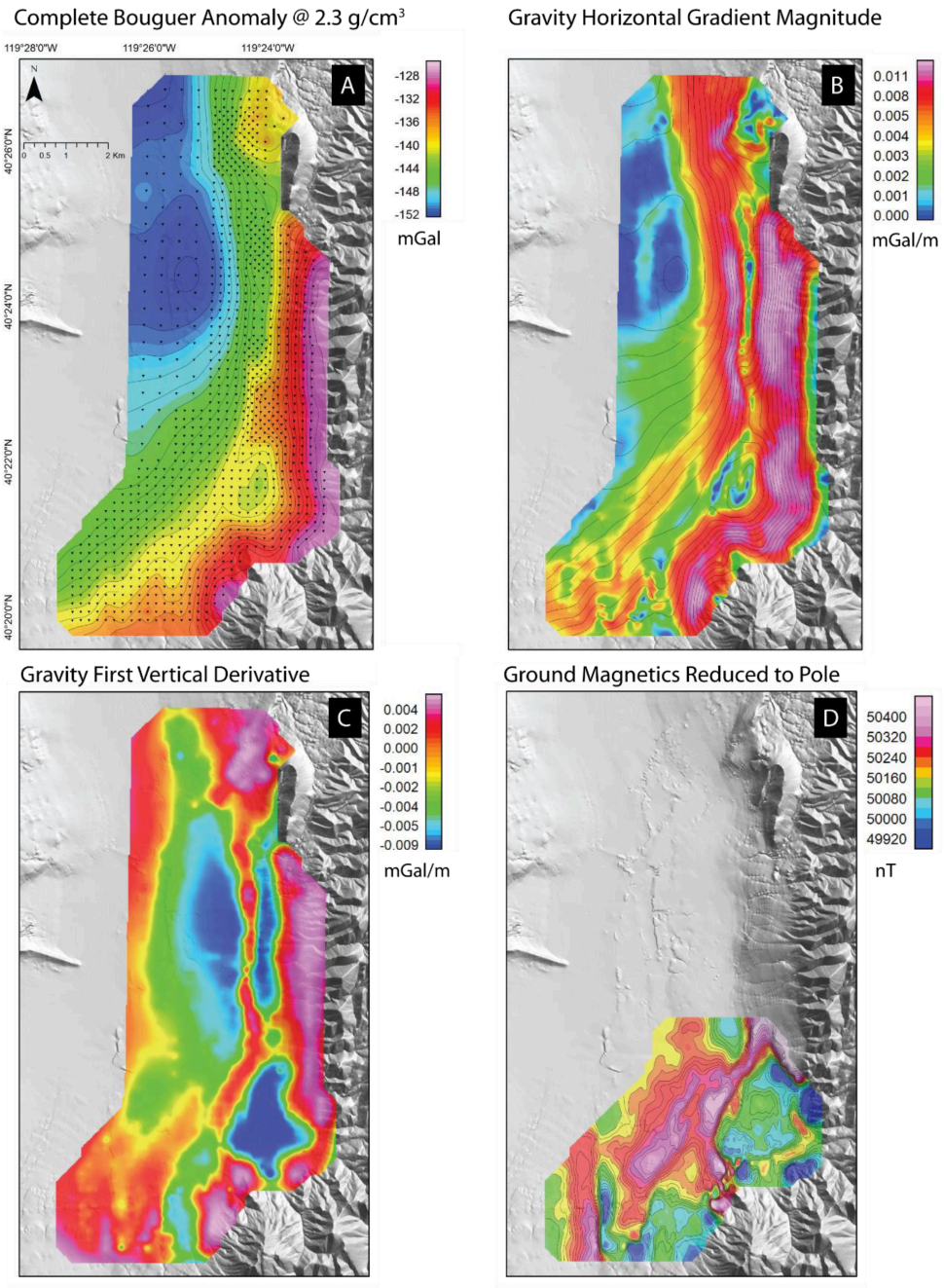

Figure 2: (Top left) Bouguer anomaly map of residual gravity, black triangles denote gravity receivers; (top right) gravity horizontal gradient magnitude; (bottom left) gravity first vertical derivative; and (bottom right) ground magnetics reduced to pole residuals from the San Emidio Geothermal Field, Nevada. Strong correlations between low density and low magnetic anomaly are observed in the first vertical derivative gravity and ground magnetics data, indicating the value of multi-geophysics characterization and joint interpretation of the resource, as well as the additional information yielded from the advanced processing of gravity data (Folsom et al., 2020).

2.1.3 Electrical conductivity

Electrical resistivity (Ohm.m), or inversely electrical conductivity (S/m), measures the flow of electric charges through a material exposed to an electric field. Electrical conductivity relates to a unit of rock's water content, temperature, porosity, pore fluid salinity, mineral alteration, and metalliferous mineral content (Ars et al., 2019; Börner et al., 2015; Cumming, 2009; Didana et al., 2017; Kalberkamp, 2007; Peacock et al., 2012; Soyer et al., 2018). A rock's bulk resistivity relates to its permeability, porosity, and composition, subsurface properties crucial to SHR geothermal siting (Darnet et al., 2020; Didana et al., 2017; Gasperikova et al., 2011). The EM methods applicable to SHR geothermal resource characterization are magnetotellurics (MT), controlled-source electromagnetics, and transient electromagnetics. We have omitted Ground Penetrating Radar, Direct-Current, and Induced Polarization from this analysis as they do not have sufficient depth penetration to characterize SHR sources.

2.1.3.1 Magnetotellurics

The Earth's magnetosphere is continually perturbed by natural sources of EM energy from solar wind, and lightning discharges. These perturbations induce EM currents that transmit through the subsurface, generating EM induction responses that are proportional to the resistive properties of the mediums at depth. Magnetotellurics passively measures EM induction at depth by sensing secondary EM fields at the surface in the frequency domain. The 3D inductive response is represented as a second-rank EM impedance tensor (Z) at a range of frequencies (10^4 Hz to 10^{-5} Hz). High-frequencies capture shallow resistive structure, and low-frequencies capture deep resistive structure (Chave & Jones, 2012; Simpson & Bahr, 2005). MT can resolve subsurface EM resistivity structure from <1 km to >1,000 km, depending on the receiver, deployment time, and resistivity at depth – deeper for resistive mediums, and shallower for conductive mediums that attenuate EM waves.

MT is considered the most effective EM method for geothermal exploration due to its 1) depth sensitivity, 2) 3D resolution of magmatic/hydrothermal systems and clay caps, and 3) resolution of contrasting resistivities between crystalline and permeable lithologies (Gasperikova & Cumming, 2020; Munoz, 2014; Peacock et al., 2012; Santilano et al., 2015). A low signal-to-noise ratio can compromise MT data due to near-field or coherenttelluric distortion (Bedrosian et al., 2004; Didana et al., 2017; Faulds et al., 2021; Munoz & Ritter, 2013; Rosenkjaer et al., 2015; Santilano et al., 2015). Deploying a remote reference for all MT datasets and using advanced signal processing techniques can mitigate noise and reduce its influence on the data (Chave & Jones, 2012; Chave & Thomson, 2003). In hot-dry-rock plays, MT may prove capable of monitoring reservoir permeability enhancement pre- and post-EGS stimulation (Section 5.2.2). In hydrothermal SHR plays, MT can delineate low-resistivity clay caps that contain hydrothermal reservoirs (Árnason et al., 2010; Cumming & Mackie, 2010; Munoz, 2014; Spichak & Manzella, 2009; Ardid et al., 2021; Samrock et al., 2023; Sewell et al., 2015), identify magmatic bodies that feed hydrothermal or volcanic systems (Bertrand et al., 2015; Gasperikova et al., 2011; Hanneson & Unsworth, 2023; Ishizu et al., 2021; Ogawa et al., 2014; Pearce et al., 2020; Wannamaker et al., 2009), and provide insight into the temperature, permeability, composition and fluid content of the reservoir using Archie's law (Section 2.2.2) (Faulds et al., 2021; Folsom et al., 2020; Jenkins et al., 2023; Trainor-Guitton et al., 2017). Fluid-filled fault systems that channel magmatic fluids along strike can also be

resolved, an observation best supported by coeval seismic studies (Faulds et al., 2021; Pearce et al., 2020; Sewell et al., 2015; Wannamaker et al., 2009).

It is well demonstrated that MT can image magmatic systems at depth (Hjörlefisdóttir et al., 2023; Bertrand et al., 2015; Hanneson & Unsworth, 2023; Kalberkamp, 2007; Munoz, 2014; Pearce et al., 2020; Rowland & Simmons, 2012), however mishaps can occur. The IDDP-1 research well in the Krafla geothermal field unexpectedly encountered magma at 2.1 km depth, the outcome of a 3D resistivity model produced from MT data that did not resolve this feature (Árnason et al., 2010; Gasperikova et al., 2011). This highlights that MT lacks the resolution to resolve magma migrating through faults, fractures or fissures. Lee et al. (2020) verified this by re-examining the Krafla MT data with modern joint inversion techniques and concluded that MT can only resolve very large and very low resistivity sills. Another concern in magmatic settings is the attenuation of EM signals in conductive mediums, which reduces the sensitivity of MT measurements beneath conductors and increases model non-uniqueness. Additional methods that retain their sensitivity beneath conductors should be deployed in magmatic settings. Altered clay-caps can also generate ambiguous indications of temperature, as high resistivity structures interpreted to be chlorite/epidote alteration (>240°C) may equally be dry, cold, basement rock. Otherwise, conductive clay-caps may have since cooled but retain their conductive properties, as observed in Samrock et al. (2023).

It may be possible to infer supercritical temperatures at depth with MT. For deep structure, the K-horizon can be demarked as a low-resistivity transition coherent with seismic results (Munoz, 2014; Santilano et al., 2015). In shallower hydrothermal systems, high temperatures increase the dissolution of electrolytes into geothermal brine, creating a low-resistivity signature (Ishizu et al., 2021; Munoz, 2014; Spichak & Manzella, 2009). However, geothermal brine exhibits a high-resistivity signature once it reaches a supercritical state due to a decrease in viscosity and dielectric constants, and an increase in thermal expansion (Kummerow & Raab, 2015a, 2015b). This was observed in laboratory experiments (Section 2.2.2) and at the Reykjanes geothermal field in Iceland, where brine resistivity increased from a factor of 5 to 7 when temperatures increased over 405°C (Darnet et al., 2020; Reinsch et al., 2017). It is thus difficult to distinguish high-resistivity, cold, crystalline rock from high-resistivity, supercritical fluids. A study of the Kakkonda geothermal system in Japan demonstrates this ambiguity. The resource hosts an 80 MWe geothermal plant sourced from a reservoir 1–3 km deep, where bottom hole (3,729 m) temperatures are 500°C and at supercritical conditions (Ogawa et al., 2014). Analysis and synthetic testing of this geothermal system revealed that it was difficult to delineate temperature changes of supercritical fluids at depth from resistivity variations (Ishizu et al., 2021).

Gaps:

- MT can fail to detect smaller resistive features such as magma intrusions or sills. The resolution of MT decreases with depth, so these features will be increasingly difficult to resolve with increasing depth.
- MT data lose sensitivity beneath conductors, such as a hydrothermal reservoir, as EM fields attenuate in conductive mediums. This may pose an issue for SHR resources located below conventional geothermal systems, where supercritical temperatures occur.

- It is feasible to resolve temperature at depth with MT. However, further work is needed to distinguish ambiguous resistivity signatures, such as indicators of cold, resistive basement versus supercritical, resistive fluids.

Current technology:

- MT can resolve conductive properties due to hydrothermal alteration, fluids or metallic minerals from <1 km to >1,000 km in depth. In hydrothermal systems, MT is adept at locating low-resistivity smectite clay-caps or magmatic feed zones. MT can also delineate lithospheric scale features such as the K-Horizon or lithospheric base, which may constrain temperature horizons relevant to SHR.
- MT is an industry and academic standard EM method for imaging hydrothermal systems. Common data acquisition systems and data processing programs include Phoenix Geophysics (instruments) and EMPower (data processing); Quantec Geoscience Ltd. (acquisition, processing and modelling); Geotools-RML3D (Viridien/CGG Multiphysics); MTPy (data visualization), Jif3D (single or joint inversion) (Moorkamp et al., 2011); and ModEM (Inversion, Kelbert et al., 2014).

Technology/approach needed to develop SHR:

- The resistivity signatures of supercritical fluids at depth should be studied with synthetic modelling and petrophysical experiments, as this would be a powerful tool for mapping temperature at depth if successful.
- Archival MT datasets from SHR systems should be reprocessed and remodelled to test their sensitivity to small-scale magmatic features, fluid conduits (such as faults) or temperature horizons with modern data analysis techniques.

2.1.3.2 Controlled-Source EM

Controlled Source MT (CSMT), also referred to as Controlled Source EM (CSEM), uses the same principles and instruments as MT. CSEM differs as it is active source, measuring time-varying EM signals injected into the ground or a current loop by a transmitter. The advantage of CSEM is its higher signal-to-noise ratio, which can be optimized by increasing the sample time, transmitter-receiver offset, or signal strength controlled by the transmitter. Resistive structure is thus better resolved by CSEM than MT, but only within <3 km penetration depth (Darnet et al., 2020). Its disadvantages are in deployment logistics, as the survey requires installing a current loop as well as an array of MT receivers. It is also still susceptible to coherent EM noise, similar to MT. Darnet et al. (2020) show that CSEM has a higher sensitivity than MT to frequencies <0.1 Hz with a transmitter-receiver offset of 10 km, and yields lower errors and higher sensitivity to shallow resistive structure than MT. Its applicability to SHR reservoir monitoring is explored in Section 5.2.2.

Gaps:

- CSEM has limited depth resolution (<3 km), and thus should be paired with a complementary EM method with greater depth sensitivity for site characterization, typically MT.
- CSEM is repeatable and yields an improved signal-to-noise ratio. However, it is complex logistically and is susceptible to noise in highly developed areas that host geothermal plants.

Current technology:

- CSEM can resolve conductive properties of the subsurface within 3 km depth. There is an improved signal-to-noise ratio due to the injection of a controlled current into the ground. CSEM uses the same receivers as classic MT systems; however, the logistics of CSEM are more complex as a current loop and transmitters must also be deployed.

Technology/approach needed to develop SHR:

- The applicability of CSEM should be tested at existing SHR or analog sites, likely for reservoir monitoring.
- If CSEM successfully resolves changes in subsurface resistivity due to stimulation, further testing must be conducted to refine and improve monitoring techniques.

2.1.3.3 Transient EM

Transient EM (TEM), or Time-Domain EM (TDEM), methods send a direct current through an insulated wire loop, creating a magnetic field that enters the subsurface and generates secondary EM fields in conductive material at depth. The current is repeatedly shut off and on, and the rate of decay (V/s) of the secondary, *transient* EM fields provides insight into the resistivity of the shallow subsurface (<1,000 m) (Börner et al., 2015; Cumming & Mackie, 2010; Hardwick et al., 2019). TEM can demark the same resistive properties as MT within a 1,000 m penetration depth (Cumming & Mackie, 2010). At these depths, varying resistivities may be due to 1) low-resistivity (10-30 Ohm.m), clay-rich valley fill, the water table, or water-laden sediments; 2) high-resistivity (100-1,000 Ohm.m) sand and gravel-rich alluvial fans; or 3) very-high-resistivity features such as igneous rock (1,000 - 100,000 Ohm.m) (Hardwick et al., 2019). Airborne acquisition of TEM data offers and more consistent coverage than land-based surveys such as MT (Cumming & Mackie, 2010; Santilano et al., 2015). TEM may correct statically shifted MT data resulting from near-surface conductive features (Cumming & Mackie, 2010; Gasperikova et al., 2011), although this can be achieved with modern 3D inversions (Cumming & Mackie, 2010). While no SHR-specific TEM studies exist, researchers have explored the application of TEM for EGS reservoir monitoring synthetically (Section 5.2.2).

Gaps:

- TEM has a penetration depth (<1 km) that is too shallow to image SHR resources.

Current technology:

- TEM is an airborne EM method used to survey near-surface (<1,000 m) conductivity properties, typically used in mining exploration or to correct statically shifted MT data.
- Resistivity contrasts in the shallow subsurface are related to geological contacts, outcropping faults, alluvium, the water table, water-laden sediments, etc.

Technology/approach needed to develop SHR:

- None applies for SHR resource characterization as TEM is generally too near-surface to adequately image SHR reservoirs.

2.1.3.5 Seismoelectric effect (SEE)

SEE has been applied in other geo-resources, but it is relatively new in geothermal fields. This method aims to better map fracture and fluid properties, which are not well resolved by traditional seismic (rock moduli sensitivities) and EM (resistivity, permeability, and dynamic fluid viscosity sensitivities) imaging (Grobbe et al., 2020; Morency et al., 2022). SEE uses the natural interaction between seismic waves and electromagnetic fields or the seismic-to-electromagnetic conversion to provide insights into the physical rock properties of porous media (Grobbe et al., 2020; Thompson, 1936).

SEE is a coupling of seismic and EM principles. A shot point source generating a seismic wave passes through porous fluid media, causing pore fluid flow to generate an electrical current. This current creates an electromagnetic field, known as a coseismic field, which moves with the seismic wave. When this coseismic field encounters subsurface variations, such as differences in mechanical or electrical properties, it forms an electric dipole. The dipole generates a separate electromagnetic field that can be captured at a distance by the electrode array (Grobbe et al., 2020; Morency et al., 2022), which is later used in the electrical resistivity inversion.

Morency et al. (2022) conducted a SEE study in Sioule-Miouze geothermal fields. Their approach integrated numerical simulations (theoretical SEE modelling); experimental analysis to characterize SEE signals from saturated porous rock samples considering temperature, salinity, and permeability; and a proof-of-concept field survey. This integrated approach resulted in a 3D electrical resistivity map, which they used to interpret geothermal fluid and fracture-bearing zones. They identified fracture zones at a reservoir depth as areas of low resistivity, which are consistent with fault zones and microseismicity observed in the study area.

Gaps:

- Active seismic sources in heterogeneous media can affect wave propagation, which can influence the induced electrical signals.
- Variations in fluid, temperature, and pressure due to structural/strata changes can further affect the electrical conductivity and permittivity of the EM field.
- These factors can scatter and attenuate the SEE signals, posing a challenge for data processing and modelling.

Current technology:

- SEE is a relatively new method, currently under study in geothermal fields.
- SEE is being improved by integrating numerical modelling, laboratory experiments, and field surveys.
- The reflection signals from the SEE survey should be stacked and migrated for seismic structural interpretation.

Technology needed to develop SHR:

- The relationship between seismic and electromagnetic data requires advanced modelling and interpretation for many field applications, tests, and validations for SHR. This includes noise filtering, S/N signal enhancements, and continuous equipment improvement.

2.1.4 (An)elasticity (Seismic)

Elasticity and anelasticity refer to the rock deformation properties at small strains. Elasticity is instantaneous and purely reversible, so no energy is lost, while anelasticity refers to deformation that is time-delayed but recoverable, so seismic energy and amplitude decays with wave propagation. In practice, seismic waves are used to probe the rock stiffness (elasticity), which is manifest in the wave speed, and energy absorption (anelasticity), manifest in wave amplitude. There are also multiple body and surface wave types that propagate through the ground, providing at least two independent elastic parameters (such as moduli). If there are directional differences (such as due to faults and fractures oriented by the local stress field), then there can be more (see Section 2.1.4.3.5. on anisotropy).

The following section discusses the usefulness and limitations of seismic methods for SHR resource investigation. Seismic monitoring of induced seismicity and permeability enhancement are covered in sections 5.1 and 5.2.1, respectively. Seismic (wave propagation) methods are especially important because they give some of the most detailed information, with resolutions determined generally by the seismic wavelength and/or density of ray paths. Rock (an)elasticity is more closely related to important potential permeable structure properties such as rock strength, fluid content, fracture density, and orientation, than some of the other geophysical properties. Seismic methods have a wide range of applications in resource exploration, production, and monitoring: 1) Depth constraints for supercritical and SHR at BDT conditions as well as magmatic structures; 2) high-resolution 3D velocity models to improve the absolute locations of induced seismic events; 3) mapping of potentially active faults using microseismicity in the project area to avoid greater induced seismicity risk (see sections 3.4 and 5.1); 4) imaging other structures or non-fractured zones (e.g., intrusions, dikes, basement depth) that would impact drilling and stimulation plans; 5) stress orientation and regime determination from the focal mechanism analysis and anisotropy (e.g., shear wave splitting or azimuthal anisotropic ambient noise); and 6) open fracture orientations (i.e., seismic and/or borehole analysis).

Seismic sensors vary in their cost and sensitivity, from standard broadband seismometers to low-cost accelerometers for economic, dense deployment. Surface nodal seismometers or geophones (at the surface or in boreholes) can be deployed relatively easily for short-term deployments but are not designed for permanent monitoring. One emerging method for acquiring dense seismic data are Distributed Acoustic Sensing (DAS) to probe optical fibers for dynamic strain. Pulses of laser light are continuously scattered along the fiber's length, which is interrogated over time to measure very small changes in the cable's strain, with the precise location attributed based on travel time of the scatter light in the fiber. This provides a truly distributed record of motion along the cable, digitized as strain of one-to-ten-meter gauge lengths on meter-spaced channels (Lindsey & Martin, 2021). Fiber optic cables can be deployed along the surface or along borehole casing in optimized survey designs, while locations with existing, unused telecommunications fiber (so-called 'dark fiber') can be turned into a dense string of sensors. Fiber optic cables are also able to withstand higher temperatures than conventional sensors (~300 C), although not yet SHR conditions.

2.1.4.1. Reflection seismic

Active seismic reflection is commonly used in the oil and gas industry. The seismic reflection method is dependent on high-frequency sources (Vibroseis or air gun, < 500Hz) to generate waves that travel and are reflected back from interfaces between rock strata and structures; however, this method is more likely to be applicable in layered sedimentary basins, not in heterogeneous geology such as deeper (crystalline) structures or geothermal fields. Because these geothermal strata are complex and SHRs are deep, body wave (P-wave or S-wave) propagation in these environments tends to lose energy and attenuate the signal, making the reflected wave difficult to retrieve or process (Barison et al., 2023; Chhun et al., 2024). General seismic data processing includes raw data acquisition and pre-processing (i.e., geometry, muting, static correction), followed by processing such as trace editing, bandpass filter, f-k filter, demultiple, sort to common-midpoint gathers, normal-moveout correction (velocity analysis), migration, and stacking (pre- and post-stack time/depth velocity analysis). Finally, additional analyses are conducted for quantitative and qualitative seismic analysis and interpretation (Hutapea et al., 2020; Stockwell, 1999; Vernik, 2016).

The K-horizon is a seismic reflector associated with high-temperature geothermal reservoirs, interpreted as indicating the presence of supercritical fluids in Larderello, Italy (Bertani et al., 2018; De Franco et al., 2019; Piana Agostinetti et al., 2017). Reflection seismic imaging techniques are used to map this horizon, providing high-resolution information on the depth and extent of the geothermal reservoir (Piana Agostinetti et al., 2017). Seismic reflection methods can provide the most detailed information at depth, as the resolution is only limited by the wavelength of the reflected seismic wave. Although short wavelengths are attenuated before they reach deeper structures, reflection methods are capable of achieving meters-scale resolution down to a few kilometers' depth. High-quality seismic reflection data are costly and difficult to collect in volcanic regions and can be particularly challenging to interpret. A reflector represents a contrast in acoustic impedance properties, but there are multiple potential physical explanations for such a contrast at depth. The K-horizon is also limited in applicability to those locations where an existing supercritical reservoir is expected.

The K-horizon was a major piece of evidence for the presence of supercritical fluids in the DESCRAMBLE project at Larderello, Italy (De Franco et al., 2019) but deepening of a local well (Vendelle-2) did not confirm this interpretation of the resolved reflector. More drilling validation is needed for these geophysical signatures of SHR targets. Legacy 2D seismic reflection lines were reprocessed and interpreted using relevant geologic and geophysical data from the super-hot Los Humeros geothermal field to reveal basement structure and caldera faults (Barison et al., 2023). Collecting new seismic reflection lines for exploration is labor- and energy-intensive, so is likely not the most cost-effective method to characterize a new SHR resource, but when existing data are available, they can provide important constraints on subsurface structure, potential targets, and hazards.

Gaps:

- Data acquisition and processing in SHR, depending on the active source, can be limited in achieving high-resolution imaging of SHR sites. The challenges stem from difficulty retrieving reflected body waves in complex and hard-rock environments.

- The significant acoustic contrast in seismic reflections within deep and hard-rock environments, such as basement structures and various deep lithostratigraphic formations, can complicate the interpretation and differentiation of acoustic impedance or strong reflection contrasts associated with supercritical fluid reservoirs.

Current technology:

- Automated velocity and advanced migration techniques (Fomel, 2009) have been developed, but they are still challenging to apply in SHR fields.
- Machine learning has been integrated to analyze seismic data processing and interpretation (i.e., auto horizon picking/interpretation).

Technology/approach needed to develop SHR:

- Many steps of the seismic reflection data processing scheme could be enhanced to retrieve body waves in hard rock environments or SHR deep structures. Although challenging, advancing methods and theories through testing and application in known geological structures of geothermal fields or SHR regions can validate and improve the results.
- Body reflection using passive seismic interferometry can retrieve body waves, which can enhance seismic reflection imaging in the SHR regions as well as k-horizon identification. However, data processing is still under-developed for accurately revealing true subsurface structures.

2.1.4.2 Microseismic monitoring and locations

Seismicity, or lack of seismicity, is a key source of information (as well as potential hazard) in geothermal projects of all types. This is especially true for SHR resources due to their potential proximity to the brittle-ductile transition (BDT). The BDT can serve as a depth marker to constrain temperature at depth but also significantly impacts the permeability and hydrothermal circulation within the reservoir. BDT is a boundary where rock deformation changes from localized brittle failure to distributed ductile flow. This transition is also commonly assumed to change the strength of the crust, from increasing with depth due to increased stresses holding together any fractures at brittle depths, to decreasing with depth from lower rock viscosities at increasing temperature in the ductile regime, an active area of research in rock mechanics and tectonics (Bürgmann & Dresen, 2008). The conditions of the brittle-ductile transition depend on the strain rate, temperature, effective stress, microstructure, porosity, and mineralogy of the rock and fluids (Davarpanah et al., 2023). Since ductile conditions are assumed not to sustain seismic stress drops, the bottom of the seismogenic zone is often associated with the brittle-ductile transition. This is not strictly the case, as much deeper earthquakes have been observed, but the frequency of events decreases below a certain depth, providing the opportunity for well-located earthquakes to constrain the depth of this transition. Depth resolution is the worst-resolved dimension in absolute earthquake locations, so refined velocity models and improved earthquake location techniques are key to constraining the BDT depth. The development of SHR reservoirs in the ductile zone has the potential to minimize induced seismicity hazards, in addition to increasing energy capacity.

Ductile rock masses are expected to have relatively homogeneous stress states and to fail in distributed micro-fractures. Initial lab-scale experiments of supercritical water injection into granite found significant permeability increase due to distributed *cloud fracture network* (CFN) generation (e.g., Meyer

et al., 2024; Watanabe et al., 2019). Distributed fracture networks could represent an ideal situation for extracting heat from a rock mass, but whether or how these fractures can remain open is a crucial area of research, both in the lab and in field settings. More fundamental studies are also needed to understand the characteristics of seismicity associated with injection of cold fluid into nominally ductile or semi-brittle SHR reservoirs (Asanuma et al., 2020; Bromley et al., 2020; Cladouhos & Callahan, 2024a).

Passive seismic monitoring requires installation of a microseismic array (MSA). The instruments and array type will depend on budget, timeline, permitting, and requirements. The MSA installed during this phase will likely inform design parameters for the permanent array to be installed during well stimulation and maintained during EGS operations (sSection 5.1). Potential temporary and permanent array types include a surface array with many (>1,000) nodes, near surface instruments (e.g., Newberry array of eight seismic 250 m deep boreholes), fiber optic-based DAS in offset wells, geophones in offset wells, etc.

2.1.4.3. Seismic tomography

2.1.4.3.1. Travel-time tomography

Body-wave travel-time tomography (P-wave, S-wave, Vp/Vs) based on either active or passive sources (e.g., earthquake or ambient noise sources) has been substantially applied for the study of the interior of the deep earth to the shallow crustal zones (Kamei et al., 2012; Rawlinson & Sambridge, 2003). Earthquake sources can be used when present, while ambient noise source (low-frequency sources such as wind, oceans, and cars) can be used in any location. Travel time tomography uses the picked travel times of seismic waves, assuming that seismic waves travel along ray paths. Based on a ray theory approximation and inversion tomography, a model of the Earth's subsurface structure (e.g., Vp) can be derived in an iterative process by back projecting the travel time differences along rays in the current velocity model (Kamei et al., 2012; Rawlinson & Sambridge, 2003; Van Leeuwen & Mulder, 2010).

Many travel time tomography studies have been applied to investigate heat sources or volcanic structure (Koulakov et al., 2020, 2021, 2023; Mhana et al., 2018; Preston, 2010; Ulberg et al., 2020). For example, local source Vp and Vs tomography, based on Ulberg et al. (2020), has been used at Mount Saint Helens to map fluids using Vp/Vs anomalies. They deployed 70 broadband stations as part of the Imaging Magma Under St. Helens (iMUSH) project, utilizing local source arrival time tomography from earthquakes and explosions. They identified the heat source or magmatic fluids beneath Mount Saint Helens, which is 5-7 km wide and 6-15 km deep, based on low-velocity anomalies of Vp and Vs or an increase of Vp/Vs anomaly.

2.1.4.3.2. Full-waveform inversion imaging

This method is similar to travel-time tomography but offers a higher resolution because it utilizes the full seismic waveform, not just the travel times, to image subsurface structure. In practice, travel-time tomography can provide a good starting model for full waveform inversion, especially in cases where seismic data lack low-frequency signals (Kamei et al., 2012). This initial model can help mitigate the issue of cycle-skipping in full-waveform inversion.

To study supercritical geothermal reservoirs, Kasahara et al. (2019) conducted numerical simulations using full-waveform inversion with DAS arrays deployed along the borehole. They simulated imaging a supercritical geothermal reservoir using both active buried sources and natural earthquake passive sources. The simulation tests yielded promising results, demonstrating the feasibility of applying full-waveform inversion at a real demonstration site if the locations and sizes of earthquakes can be appropriately chosen. They also emphasized the importance of ACROSS (Accurately Controlled Routinely Operated Signal System), which can separate signals from background noise. Using ACROSS as source signals can enhance full-waveform inversion analysis, improving subsurface structure imaging (Kasahara et al., 2019; Tsuji et al., 2021). However, further field testing and validation are needed.

Gaps:

- Travel time and full-waveform inversion techniques are mostly used to study large-scale structures such as crust-Moho-mantle structure, or in large volcanic areas. Small-scale target of superhot rock regions requires dense sensors, survey geometry, acquisition, processing, and application in the SHR region.

Current technology:

- Seismometer networks on both land and ocean have been intensively developed, and can be applied to any SHR region.
- DAS is a high sampling rate sensor that can be used, but its application in SHR study has not been tested.

Technology needed to develop SHR:

- Innovative approaches that integrate dense sensor networks and advanced data-processing techniques are essential to enhance the resolution and accuracy of subsurface imaging in SHR regions. This includes the development of new algorithms for data interpretation and the use of machine learning to identify patterns in seismic data that are indicative of SHR formations.

2.1.4.3.3. Surface wave tomography

Surface wave tomography is another tomographic technique for 3D imaging that offers higher resolution in the shallow region of upper crustal structure. Surface wave tomography is based on a passive seismic source, which captures dominant surface waves. Surface waves (Rayleigh or Love waves) sense different depths depending on their frequency/wavelength, longer wavelengths or low frequencies reach deeper and thus give information about deep seismic velocities. Dispersion modes give the surface wave velocity as a function of frequency. Due to its dependency on different frequency/depth and complex wave interaction, surface wave dispersion can exhibit multiple modes, including the commonly used fundamental mode and higher modes. Passive (ambient) seismic noise, continuously generated by natural sources like wind and ocean waves at low frequencies, can be analyzed using seismic interferometry, but have limited frequency bands that define their sensitivity to different depths.

The seismic interferometry method involves extracting the propagation of surface waves between two seismometer stations from ambient noise data, using both passive and active/controlled sources. Passive-source seismic interferometry is based on the idea that seismic waves from natural sources

travel between sensor pairs. By continuously measuring at different receiver locations, the cross-correlation function of ambient seismic noise between a pair of receivers can be computed. This function helps recover the Earth's response between the receivers, known as the impulse response or Green's function estimate. The Green's function represents seismic/cross-correlation waveforms by treating one station as a virtual receiver and the other as a virtual source, and vice versa (Campillo & Paul, 2008; Obermann & Hillers, 2019; Shapiro & Campillo, 2004). Then, surface wave dispersion velocities (e.g., Rayleigh or Love waves) can be extracted by various techniques such as frequency–time analysis or a multiple filter technique (e.g., Lehujeur et al., 2018; Planès et al., 2020), a continuous wavelet transform (e.g., Jiang & Denolle, 2020), or a zero-crossing approach (e.g., Ekström et al., 2009; Martins et al., 2020; Sadeghisorkhani et al., 2018). Finally, surface wave dispersions can be obtained and converted into S-wave velocity model (Chhun et al., 2024; Fang et al., 2015; Nimiya et al., 2020). The 3D S-wave velocity structures can be derived using either conventional or direct surface wave tomography techniques (Fang et al., 2015; Nimiya et al., 2020). Conventional surface wave tomography (e.g., Lehujeur et al., 2018) involves inverting dispersion data into a 2D phase/group velocity profile by performing point-wise inversion of 1D S-wave at each grid, which are then combined to create a 3D S-wave velocity model. In contrast, direct surface wave tomography (e.g., Fang et al., 2015; Nimiya et al., 2020; Nthaba et al., 2022; Suemoto et al., 2022) bypasses the step of constructing a phase/group velocity map and directly inverts surface wave dispersion travel times into a 3D S-wave velocity structure.

There are many case studies of geothermal fields in various volcano tectonic settings using ambient noise tomography based on fundamental modes of surface waves (e.g., Cabrera-Pérez et al., 2023; Chhun et al., 2024; Lehujeur et al., 2018; Martins et al., 2020; Sánchez-Pastor et al., 2021; Toledo et al., 2022a). An advanced technique is multi-modal surface tomography. (Nimiya et al. (2023) successfully used this technique to detect the boundary of the basin between sediment and bedrock in the Kanto basin. Although this method has not yet been applied in deep geothermal fields, future research should conduct this analysis to map supercritical vs. non-supercritical fluid boundaries, brittle-ductile transition layers, and the boundaries of magmatic or non-magmatic structures. Another detailed resolution technique that can detect fine-scale structures is based on full waveform inversion (see Section 2.1.4.3.2) using wavefield gradient measurements (e.g., from DAS or rotational sensors). This novel technique considers heterogeneous or small-scale effects smaller than the minimum wavelength, based on homogenization theory (Capdeville et al., 2020; Mukumoto et al., 2024). Newly developed DAS or rotational sensor data should be applied using this method to obtain detailed resolution Vp, Vs, Vp/Vs, or Q for imaging heterogeneous SHR geothermal and magmatic structures.

Gaps:

- S-wave velocity is sensitive to fractures but not to fluids, making it highly effective for studying fractured zones that host geothermal, SHR, and magmatic structures. However, this sensitivity can pose challenges in differentiating types of fluid contents (i.e., supercritical fluids associated with magmatic chambers). Therefore, a Vp/Vs model should be used.
- The ambient noise source is commonly inhomogeneously distributed, and surface waves can be scattered, attenuated, or affected by instrument noise, nearby loud noise sources, or topographic effects. Additionally, dispersion curve analysis exhibits multiple modes due to the

frequency-dependent behavior of surface waves traveling through the heterogeneous subsurface.

Current technology:

- Various tomography models based on surface wave analysis have been applied and can be used to distinguish fractures, fluids, and strata at SHR sites.

Technology/approach needed to develop SHR:

- Advanced methods have been developed to improve and correct the noise source distribution (Eikonal tomography) (e.g., Lin et al., 2009), zero-crossing methods (Ekström et al., 2009; Sadeghisorkhani et al., 2018), and F-J methods or multi-modal surface wave tomography (Hu et al., 2020; Jiang & Denolle, 2020; Z. Li et al., 2021; Nimiya et al., 2023) to be used for surface wave dispersion measurement and inversion. Since SHR can be located more than 5 km deep, dense seismometer networks or array spacing geometry setup needs to be designed to investigate this target depth.

2.1.4.3.4. Attenuation tomography

Seismic attenuation, or quality factor (Q) tomography, based on active or passive seismic sources, has been applied to investigate Earth's interior, volcanic structures, or potential petroleum reservoirs. Seismic waves tend to weaken or decrease their signals as they travel through the Earth's interior. This is because seismic wave energy can be attenuated over distance, due to differences in temperature, stress, fluid saturation, or rock type in the Earth's interior, which affects seismic amplitudes, phases, and frequency. By measuring how amplitude varies with frequencies/depths, we can estimate the attenuation (or inverse Q) factor (Hurst et al., 2016). For SHR regions, ductile zones or partial melt can cause large seismic attenuation or energy loss (i.e., a low Q factor).

Gaps:

- The high spatial resolution of seismic attenuation tomography is limited by density and distribution of seismic sources and sensors. Achieving high-resolution imaging requires a dense network of seismometers, which can be logistically challenging and costly to deploy. In addition, Q resolution can be limited to capture the fine-scale SHR reservoir fractures or drilling location.
- Complex interactions between rock and fluids can introduce wave scattering and noise into the data, which can be challenging for data processing and interpretation, in addition to the inherent complexity of Q models.

Current technology:

- DAS and multiple component sensors have been developed, but not yet widely applied to study Q structure in geothermal/SHR reservoirs. Further research and field trials are needed to validate their effectiveness and integrate them into the standard SHR site characterization.

Technology needed to develop SHR:

- The advanced approach, including high-precision Q modelling and Q migration technology (Xu et al., 2024), can improve Q factor results and be applied to SHR regions, where brittle-ductile transitions give contrast in Q factor. Other advanced geophysical techniques should be used for

joint inversion to obtain high-resolution Q tomography or improvement of SHR reservoir-drilling scales.

2.1.4.3.5. Anisotropy

The Earth's interior is highly heterogeneous, causing seismic waves to travel through its layers at different speeds depending on the direction of the Earth's structure (Boness & Zoback, 2006). This variation can be attributed to alignments of minerals or pore shapes, fracture or crack orientations, and other geological factors such as stress or strain rates, temperature or pressure conditions, or fluid accumulations (Sayers, 1994). Due to these structural alignments in the Earth's interior, seismic waves travel faster parallel through fracture direction compared to when they are not aligned (Boness & Zoback, 2006; Nthaba et al., 2023). Specifically, there are four types of seismic anisotropy in the subsurface media: Vertical Transverse Isotropy (VTI), where seismic velocities vary vertically but are constant horizontally; Horizontal Transverse Isotropy (HTI), where seismic velocities vary horizontally but are constant vertically; Tilted Transverse Isotropy (TTI), where seismic velocities vary with direction in a tilted plane; and Orthorhombic TI, where seismic velocities vary in both azimuthal and polar directions (Tsvankin et al., 2010). Thus, a degree of seismic anisotropy can be used to identify areas with varying fracture intensity and orientation, providing valuable information for SHR resource development and drilling.

Azimuthal ambient noise tomography versus shear wave splitting tomography

Both methods are used to investigate anisotropic structure or anisotropy of the Earth depending on the topic (for example, rock foliation, crack or fracture orientation, fluid flow pathways, or contrast of litho-strata). Azimuthal ambient noise tomography, based on Liu et al. (2019), uses a direct inversion technique for 3D shear wave speed azimuthal anisotropy derived from surface wave travel time (i.e., ray paths relative to their direction), whereas shear wavesplitting tomography (Richards et al., 2021), known as seismic birefringence, involves analyzing the polarization and propagation direction of shear waves (S-waves) in the anisotropic media, as recorded at broadband seismometers.

These two methods are mostly applied at the deep-Earth, crustal, or basin scale. A local (10 km x 10 km) case study was conducted in the Kuju volcano (Chhun et al., 2024). These methods are useful for superhot rock because, in ductile or active zones, we try to avoid areas that are cold and faulted/fractured regions (which can display high anisotropic structure in low-velocity zones), and target areas with high velocity and high anisotropy, or low anisotropy, depending on the litho-strata of the ductile subsurface.

Gaps:

- In heterogeneous fractured media, wave propagation can vary and scatter in multiple directions, posing challenges for specific types of VIT, HTI, or TTI.
- Contrast lithologies and strata can give strong anisotropy, which can be challenging for structural interpretation.
- The resolution can effectively detect faulted and fractured zones, but mapping individual fractures or faults remains challenging.

Current technology:

- Seismic anisotropy approaches have been developed and should have been substantially applied in superhot rock (SHR) environments.

Technology needed to develop SHR:

- S-wave and anisotropic analyses require a high density of seismometers to adequately cover the ray path density across various wave propagation directions. This comprehensive coverage is essential for capturing detailed and accurate data on seismic wave velocities and anisotropic properties, which are critical for distinguishing fractured and non-fractured zones.
- Dense ray paths and appropriate survey coverage (array spacing) are essential for imaging SHR reservoir depths.
- Both techniques can be applied to SHR regions, where ductile or homogeneous rock states can result in low anisotropy identification. This is important to identify non-faulted and faulted zones in brittle and ductile environments.
- DAS has not yet been applied to study anisotropic structure.

2.1.5 Remote sensing and geodesy

Surface deformation and structure detected by remote sensors can provide information such as lineaments, alteration zones, surface temperature, or volcanic or reservoir deformation (e.g., uplift and subsidence) (Reath et al., 2019; van der Meer et al., 2014). Remote sensing is an imaging technique based on satellites or aerial sensors, which identify objects on Earth by the radiation they emit or reflect (Wang et al., 2024). There are two primary types of remote sensing based on passive and active techniques. Passive sensors detect naturally emitted and reflected radiation, while active sensors emit energy at predetermined wavelengths and measure the reflected or backscattered signals (Maliva & Missimer, 2012). Remote sensing has many methods depending on the type of satellites and sensors, which can cover an extensive area. Thermal infrared (TIR) remote sensing is often used to obtain surface temperature for signatures or delineation of geothermal fields. The main data processing is first to obtain raw data (thermal infrared data from satellite), then undergoing pre-processing techniques (e.g., atmospheric, elevation correction), followed by processing to determine surface land emissivity, then surface temperature inversion based on inversion algorithms (e.g., hyperspectral algorithm) in an area of interest (Muanza et al., 2024). The application also extends to the mapping of surface rock alteration, fault, or lineament based on the radiation reflected or emitted by their ground structure, which are captured by remote sensors.

InSAR (Interferometric Synthetic Aperture Radar) is another type of remote sensing technique, which is often used for the investigation of surface deformation. Because geothermal, volcanic, or earthquake activity can lead to surface deformation, this tool is widely applied in geothermal exploration and seismological studies (Biggs et al., 2016, 2021; Sandwell et al., 2011). InSAR takes into account the phase shift between images taken at different times, which can later be used to determine ground deformation once sources of error are assessed. InSAR and GNSS (Global Navigation Satellite System) are both used for ground deformation monitoring. While InSAR covers a large area based on satellite radar, ground station-based GNSS sensors offer high precision measurement at a specific area or point

with a much higher temporal sample (e.g., every second or several times per second with GNSS compared to days or weeks between InSAR images) (Hamling et al., 2022). Tilt meters and strain meters are other ground motion sensors used to measure angle change of the ground and strain, respectively. They are frequently used in boreholes (Tsuji et al., 2023).

Gaps:

- Remote sensing and geodesy provide an indicator of the presence of a heat or pressure change source and subsurface structure, but can be limited in depth resolution.
- While remote sensing/InSAR may face limitations in resolution and can be influenced by atmospheric, orbital, and phase unwrapping errors, it is important to note that GNSS and tiltmeters, despite their higher accuracy, can be costly and time-consuming to deploy due to the required instruments and deployment density.

Current technology:

- Remote sensing/InSAR technologies cover large and inaccessible areas, indirectly reflecting the dynamics of volcanic-geothermal systems. The accuracy of these results can be enhanced by combining or calibrating them with GNSS or tiltmeter data.
- The surface faults resulting from the subsurface structure and tectonic stress, which are also utilized in the rock stress model.

Technology needed to develop SHR:

- While remote sensing/InSAR has depth limitations, it remains a valuable tool for monitoring large-scale deformation as well as during SHR reservoir development and extraction.
- Further advancements are required in integrating surface deformation data with subsurface models to improve the accuracy of locating and characterizing superhot rock reservoirs, including the development of new algorithms or the application of machine learning.

2.1.6. Borehole geophysics

Borehole tomography such as cross-well tomography, vertical seismic profiling (VSP), and electrical resistivity tomography (ERT), represent advanced approaches of geophysical borehole exploration. Seismometers or optical fiber sensors on the surface and/or the along the borehole have been used to obtain Vp or Vs structure or others using body wave tomography or full wave form inversion (see Section 2.1.4.3). This data can be interpreted for reservoir fractures, fluid changes, or reservoir behavior states (e.g., fluid flow) in detailed resolution, or using rock physics to translate elasticity parameters into temperature, saturation, or permeability (see Section 2.2.2). The distance to which it can be measured depends on the sensor spacing and array geometries. Cross-well tomography is a similar technique, but may offer higher resolution at a specific depth, and time-dependent changes as in monitoring (see Section 5), due to at least two wells being used to conduct tomography along the cross-section of the boreholes (Nibe & Matsushima, 2022).

2.1.7. Fluid geochemistry

In the deeper levels of a hydrothermal system, close to the heat source, temperatures and pressure can surpass 374 °C and 22 MPa, respectively, which is above the critical point for pure water (Scott et al., 2016). Supercritical and superheated fluids are relevant for SHR systems, but there are few good constraints for their chemical composition and processes due to the limited amount of available data. Few examples of drilling into supercritical fluids include Krafla in Iceland, where supercritical fluids have similar volatiles as the surrounding subcritical geothermal fluids, suggesting the same meteoric origin, but at temperatures of 440 °C, fluids were found to be depleted in rock-forming elements such as Si, Na, K, Ca, Mg, Al, and Fe (Heřmanská et al., 2019a; 2019b). The isotopic signature of oxygen and hydrogen in the supercritical fluid also indicates a meteoric source that has a small degree of water-rock interaction (Heřmanská et al., 2019a; 2019b). The main mechanism proposed for Krafla superheated fluid is conductive heating of geothermal fluids close to the intrusion, with minor input of magmatic gases. However, in Japan and Iceland (Reykjanes), highly concentrated brines in supercritical zones have been associated with enrichment in magmatic gases (Henley & Seward, 2018). The incorporation of magmatic volatiles into deep hydrothermal systems will depend on supply—from fluid solubility and magma composition (Wallace et al., 2015; Webster et al., 1999), and transport dependent on permeability at brittle-ductile depths allowing fluids to reach the brittle crust (Fournier, 1999; Halter & Webster, 2004; Hurwitz & Lowenstern, 2014). Modelling proposed that episodic stress perturbations can promote failure in the brittle-ductile low-permeable zone (Dingwell, 1997; Lavallée & Kendrick, 2021), enhancing transport of magmatic volatiles and heat in the deeper level of the hydrothermal systems (Fournier, 1999; Uno et al., 2022).

Although at subcritical conditions, equilibrium conditions for single and multi-mineral reactions are well established under supercritical conditions, the chemical reactions controlling the fluid composition are still poorly understood. Few experiments and geochemical simulation of conductive supercritical fluid formation in basaltic systems indicate precipitation of silicates instead of dissolution, which deplete the concentration of rock-forming elements in the fluids, but volatile elements remained unchanged (Heřmanská et al., 2019a; 2019b). The limitation of those experiments is that except for quartz and some common salts (Driesner & Heinrich, 2007), the solubilities of minerals are poorly known. Some of the most powerful geochemical exploration tools used in conventional geothermal systems, such as geothermometers, work under the assumption of temperature-dependent reactions between the fluids and surrounding minerals in the host rock, which occurs under equilibrium without chemical re-equilibration upon fluid ascent. Thus, the applicability of these techniques in superheated fluids is limited due to the lack of understanding of equilibrium reaction and mineral conditions in deeper levels of hydrothermal systems. Thermodynamic formulations generally do not apply at extreme temperatures and low pressures/fluid densities (Chambefort & Stefánsson, 2020). Although to date there are no good geothermometers adapted for temperatures above the supercritical limit, new research is targeting elevated temperatures.

The Na/Li geothermometer (Sanjuan et al., 2014), is used broadly in volcanic environments, being adapted to temperatures close to supercritical, up to 365 °C. Some volatiles and isotopes present little variability between supercritical and subcritical fluids, providing important insights about the origin of

the fluids (Bégué et al., 2017; Heřmanská, Kleine, et al., 2019; Heřmanská, Stefánsson, et al., 2019). However, applications of classical geochemical methods over surface manifestations are limited due to mixing processes, cooling, boiling, and water-rock interaction occurring in a rising fluid, which commonly mask the geochemical characteristics of supercritical fluids. Supercritical chemical reactions are still poorly understood due to the lack of access to extreme environments and difficulties of experimental setting with highly reactive gas mixtures, elevated temperature, and low pressures. Further modelling and fluid-rock-interaction experiments, combined with drilling in different volcanic settings, can present a complete picture of the characteristics and origin of the fluids and the subsurface processes occurring deep into the crust.

Hydrothermal systems interact with evolving magma exsolving volatiles, and exsolution of volatiles from magmas is linked to mechanisms like decompression during ascension, eruptions, cooling, and precipitation of minerals. Advances in volcanology such as continuous measuring of volatiles and studying melt inclusions trapped in minerals associated with porphyry and epithermal deposits can also offer important records of the compositions of deep hydrothermal environments.

Better understanding fluid geochemistry can be beneficial for drilling and environmental assessment of SHR development. Drill string fatigue and corrosion has been associated with high pressures, temperatures, and acidity in supercritical fluids (Gunnlaugsson et al., 2014; Miller, 1980; Sanada et al., 2000). Both precious metals and toxic metals from deep hydrothermal systems can potentially reach the surface due to SHR development posing potential economic benefits as well as hazards to the environment.

Gaps:

- Conventional geochemical exploration tools may not apply in SHR regions.
- Lack of the chemical data of supercritical fluids in different geological settings to establish a general characterization and understand the mechanisms occurring in the deeper levels of hydrothermal systems.
- Lack of understanding of chemical processes expected in wells under supercritical conditions.
- Lack of thermodynamic formulation for supercritical temperature and pressure conditions.

Current technology:

- Geochemical laboratory analysis for geothermal fluids (gas and liquid) and rocks includes gas chromatography, Inductively Coupled Plasma Mass Spectrometry (ICP-MS), Atomic Absorption Spectroscopy (AAS), Ion Chromatography (IC), Stable Isotope Analysis, X-Ray Diffraction (XRD) and Fluorescence (XRF).
- In active volcanoes, *in situ* measurement of gases record long-term time series. Instrumentation includes Differential Optical Absorption Spectroscopy (DOAS), or custom-made multi-component gas analyzer systems that measure major components of volcanic gases: CO2, SO2, H2S, and pressure-temperature-humidity sensors are typically included in a package.

Technology/approach needed to develop SHR:

- Geochemical tools development in areas of active volcanic-geothermal activity or supercritical fluids zones will be relevant for SHR resources.

2.2 Data analysis and interpretation techniques

2.2.1. Resource exploration and assessment

This section begins by introducing the concept of geothermal play fairway analysis (GPFA) a methodology borrowed from the oil and gas industry and applied to conventional geothermal resources. It then discusses the potential applications of the technique in the SHR context, and the advancements required for its application. The section continues by examining the state-of-the-art use of machine learning (ML) in geothermal resource exploration, reservoir assessment, and subsurface data integration, highlighting its prospective application for the development of SHR. Lastly, the section ends by emphasizing the decision-enhancing value (VOI) of utilizing statistically and data-driven approaches for SHR exploration and assessment.

2.2.1.1. Play fairway analysis

Play fairway analysis (PFA) is a methodology borrowed from the oil and gas industry, where it is used to identify hydrocarbon reservoirs. Play refers to an exploration target in an area governed by similar geological conditions where the resource is projected to exist (Doughty et al., 2018). The main goal of the PFA is to identify the areas (fairways) with the greatest likelihood of hosting the resource of interest and thus prioritizing areas for future development. To achieve its main goal, the PFA methodology first identifies the key conditions that characterize the occurrence of the resource, then compiles the relevant datasets that can inform a future model. Lastly, it systematically evaluates the data to identify areas with high favorability.

For a geothermal play, the PFA evaluates the unique regional or basin scale conditions in which geothermal systems manifest. The relevant datasets to characterize the systems will depend on the specific geologic setting and data availability but generally include a mix of geological, geophysical, and geochemical evidence aiming at identifying the presence of fluid, heat source, and reservoir permeability (Pauling et al., 2023). Since the PFA integrates multiple datasets to find favorable intersections of the required elements (e.g., fluid) for a geothermal system to exist, it is particularly useful for identifying blind or hidden resources (Pauling et al., 2023).

To date, and as part of a Funding Opportunity Announcement (FOA) from the US Department of Energy (DOE) to locate blind geothermal resources, 11 research teams in the United States (e.g., Bennett et al., 2015; Bielicki et al., 2016; Faulds et al., 2015, 2017; Lautze et al., 2017; Shevenell et al., 2015; Wannamaker et al., 2016; Shervais et al., 2021) adapted the PFA methodology in regions such as the Great Basin in Nevada (Faulds et al., 2015), the Hawaiian Islands (Lautze et al., 2017), the Appalachian Basin (Jordan 2015), and Central Cascades (Wannamaker et al., 2016). All but one of these projects (Jordan 2015) aimed to identify conventional hydrothermal resources for electricity production. In this report, we refer to those that target temperatures high enough to produce electricity as geothermal PFA (GPFA or PFA). Although the methodologies varied across these DOE FOA awardee projects, the GPFA workflow began with the compilation, curation, and processing of the datasets deemed relevant by each research team to characterize the respective key geothermal play factors. Specifically, most of these projects aimed to identify the potential for a heat source, reservoir permeability, the presence of fluid,

and in some cases, the presence of a rock seal. Each of these factors is represented through evidence layers.

For instance, Lautze et al., (2017) incorporated gravity, groundwater geochemistry, groundwater temperature, electrical resistivity, and volcanic feature location data to define the evidence layer for heat. Once these evidence layers are constructed, they are combined into a composite map using a weighting approach and then used to create geothermal favorability maps. This composite or summed map identifies locations with the required play components for a geothermal resource. Areas identified as having high favorability (intersection of key elements) are considered targets for further exploration. From the 11 DOE-funded GPFAs, 5 projects were selected to validate their results by conducting exploratory drilling campaigns using the PFA model to select surface targets, most of which were successful in discovering anomalously high temperatures and gradients (Pauling et al., 2023).

Despite the successful development of GPFAs, the methodology has various limitations that can affect its implementation for SHR. The GPFA methodologies varied significantly from one research team to another, because of limitations in data availability, differences in geologic setting, and different validation techniques. Consequently, methodologies that are effective in one region may not be applicable or successfully validated in others. Furthermore, all the previously mentioned methodologies apply to conventional geothermal systems and do not assess resource exploration for enhanced geothermal systems (EGS).

Recent work from the DErisking Exploration for multiple geothermal Plays in magmatic ENvironments (DEEPEN) project re-evaluated the PFA methodology to target superhot EGS (Taverna et al., 2024). The work by Taverna et al. (2024) modified the PFA approach and applied it in the Newberry Volcano, USA. Using the key components identified by Kolker et al. (2022) for superhot EGS plays (i.e., heat, thermal insulation, and the reservoir potential to create and maintain fractures [producibility]) and integrating the 3D PFA methodology developed by Poux & O'Brien (2020), Taverna et al. (2024) created 3D favorability models for each of the key components and a 2D geothermal favorability model. In addition, the research team integrated existing exploration datasets with a MT and gravity joint inversion and explored expert-driven and statistically driven weighting approaches. Despite the positive results, the DEEPEN EGS PFA models faced some limitations that are critical for SHR development. For instance, DEEPEN's focus on supercritical fluid reservoirs meant that datasets relevant to identify and define superhot EGS reservoirs were not well characterized or studied. In addition, the uncertainty of some of the datasets used to characterize producibility couldn't be quantified (e.g., earthquake data, velocity models), increasing exploration risks. A non-technical limitation is the use of paid software. Currently NREL is developing open software to assess this issue (Taverna, N., Personal Communication).

Although DEEPEN EGS PFA addressed the limitations of the PFA methodology for EGS, it faces similar challenges to those found in conventional GPFA when applied to superhot enhanced systems. SHR resources are believed to exist in many geodynamic settings (Section 3.1). These various environments define SHR play sub-types (e.g., SHR resources in extensional environment and SHR resources hosted in compressional environments) with unique characteristics. Consequently, the exploration datasets may vary in the degree of contribution or usefulness for a particular SHR-play based on the specific geological environment. Therefore, datasets should be tailored to each specific sub-SHR play.

Another challenge results from the process of combining datasets to create evidence layers and then a composite favorability map. The PFA uses a weighting approach where layers are combined to emphasize the significance of more contributing layers and de-emphasize those deemed to be less significant. The DOE-funded PFAs used a combination of expert opinions with statistically driven approaches (Pauling et al., 2023). DEEPEN EGS PFA combined both approaches and created separate models to compare the results. Expert-guided weighting can impart higher confidence in the modelling process, but it may introduce biases in the resulting models and potentially reduce their predictive skills. Applying data-driven methods has the advantage of reducing potential bias, but requires sufficient training data, which is currently limited to a few sites with SHR evidence (a couple dozen).

Finally, there is the limitation of the data itself. Transforming discrete datasets into continuous ones requires geostatistical functions (Pauling et al., 2023). Some interpolation methods used in the DOE-GTO funded GPFA resulted in data that are geospatially smooth whereas geological conditions do not necessarily exhibit this behavior, resulting in input data that do not reflect true geological conditions. Some models that included structural information such as distance to fault (e.g., Taverna et al., 2024) relied upon surface observations which potentially hide older faults covered by younger material.

Adapting the PFA approach to SHR requires overcoming various challenges. For a 3D PFA, such as the one developed by Taverna et al. (2024), the methodology should focus exclusively on SHR targets and identify the relevant datasets to characterize permeability. This includes further studies to understand SHR plays in various geodynamic settings. A 2D PFA, such as those initially funded by DOE, needs to incorporate evidence layers specific to EGS systems (e.g., producibility). Shifting from an expert-opinion-weighting approach to a data-driven one requires addressing the challenge of a limited number of training sites. This issue may be mitigated by augmenting the training sites with analogous systems. Lastly, improving granularity, continuity, and quality of the input data are crucial to accurately represent true geological conditions.

2.2.1.2. Machine learning

Machine learning (ML) is a subdomain of artificial intelligence (AI) that uses statistical and mathematical functions to identify patterns in input datasets. The name *machine learning* refers to the process where the computer discovers (i.e., learns) these patterns autonomously with minimal human intervention (Mordensky et al., 2022). Depending on the paradigm, ML is in turn subdivided into supervised, unsupervised, and reinforcement learning. Supervised ML approaches consist of utilizing labelled examples to identify patterns in the data for classification and regression tasks. Unsupervised ML approaches instead identify patterns on unlabelled data. Lastly, reinforcement learning uses a system of rewards and punishments in the training process in the modelling process.

Since 2018, the use of ML in geothermal research has increased exponentially (Okoroafor et al., 2022) in areas such as exploration (e.g., Brown et al., 2020; Mordensky et al., 2023a; Vesselinov et al., 2022) and reservoir characterization (e.g., Zhang et al., 2020; Siler et al., 2021).

Data-driven approaches offer an alternative to expert-driven geothermal assessments. Mordensky et al. (2023a) successfully employed supervised ML in the data from the U.S. Geological Survey's latest

moderate-to-high-temperature geothermal assessment (Williams et al., 2008) and compared the results with those found by Williams et al. (2008). Despite selecting a supervised ML approach, the research team had positive labels in the dataset and unlabelled data (i.e., no negative sites) and a tailored under-sampling strategy to select negative training sites from the unlabelled data. The research team applied the under-sampling strategy to create favorability maps. The results were consistent with the previous expert-informed assessment from Williams et al. (2008) and in particular cases surpassed the identification of known geothermal labels.

The results from Mordensky et al. (2023a) demonstrated that data-driven ML algorithms could be used to remove or minimize the need for expert feature-weighting decisions. Similarly, the Nevada Machine Learning Project (NVML; Brown et al., 2020; Faulds et al., 2021) used an artificial neural network (ANN) to identify geothermal favorability in the Great Basin (i.e., supervised classification problem). The results were consistent with those from the Nevada PFA, demonstrating that ML methods can be successfully used in geothermal resource evaluation. However, NVML faced some fundamental challenges (e.g., low number of training sites) with infusion of expert knowledge in the selection and engineering of input features and model evaluation. The positive sites defined by NVML corresponded to known geothermal sites, while the negative labels were selected using relatively deep and cool wells from previous oil and gas exploration.

More recently, Caraccioli et al. (2023) revisited the NVML data and applied supervised ML techniques to predict geothermal favorability. The research team hypothesized that the location of negative and positive sites in NVML (preferentially in the east and west, respectively) geospatially biased the model. Using the customized under-sampling approach for Mordensky et al. (2023a), Caraccioli et al., (2023) trained models to reflect the expected distribution and conditions of hydrothermal systems. When utilizing the under-sampling approach, the models by Caraccioli et al. (2023) outperform NVML ANN, demonstrating that simpler physics-informed ML models can outperform more complex models, emphasizing the value of integrating domain-specific knowledge into the ML process.

The unsupervised ML study by Vesselinov et al. (2022) discovered hidden geothermal signatures using non-negative matrix factorization with customized k-means clustering (NMFk). They used 18 geological, geophysical, hydrogeological, and geothermal attributes at 44 locations in the southwest New Mexico region (SWNM), including low- and medium- temperature hydrothermal systems. This study uncovers hidden patterns and relationships in the SWNM geothermal dataset to improve the understanding of regional hydrothermal conditions and the favorability of energy production. They identified the medium-temperature hydrothermal systems in the study areas and the most favorable regions for future exploration located in the Rio Grande rift and northern Mogollon-Datil volcanic field.

Other work based on NMFk includes Siler et al. (2021), where they used the technique to successfully identify the structural signatures controlling hydrothermal circulation in productive wells in the Brady geothermal field. Mudunuru et al. (2022), meanwhile, developed an unsupervised deep learning and cloud computing (GeoThermalCloude) pipeline for geothermal resource exploration or ePFA. The methodology was validated using data from the Great Basin in Nevada, UtahFORGE, Tularosa Basin, Tohatchi Hot Springs in New Mexico, and Hawaii. The results from Mudunuru et al. (2022) were consistent with the ones identified by their respective PFAs. In a subsequent work, Mudunuru et al.

(2023) used their GeoThermalCloud method for modelling EGS to estimate the undiscounted cashflow of different EGS reservoir behaviors. They designed the training and scalable deep learning model. The database consists of EGS design parameters (inputs to the DL model) and their undiscounted cashflow (output of the DL model) in uncertain geologic systems. The EGS design parameters for constructing this training database are based on UtahFORGE, including well configuration and completion cost, production, thermal properties, NPV, economic factors, etc. They further worked to improve and suggest the promising results of undiscounted cashflow prediction in hidden EGS reservoirs.

Despite these advancements, the application of supervised ML to SHR poses some challenges. One critical issue is having a sufficiently large number of positive-labelled training sites (i.e., locations that host geothermal systems) and determining representative negative-labelled sites.

Positive sites (or labels, in ML jargon) are crucial to identify SHR resources by allowing ML algorithms to detect the geophysical and geological signals that characterize SHR resources. A small dataset with a low number of positive sites may lead to overfitting, where the model fails to identify meaningful relationships in the data and performs poorly when tested in new, unseen data. The small number of training sites combined with the diverse geological settings where they are located (e.g., Los Humeros, Mexico; Larderello, Italy; IDDP-1 [Krafla], Iceland) exacerbates this issue, making it difficult for ML models to generalize findings across different SHR plays. The issue of training sites extends to the selection of negative training sites. In classification tasks, models need to identify positive and negative sites, but there are various conditions in which hydrothermal systems fail to manifest, making the selection of negative training sites prone to bias (Caraccioli et al., 2023). These limitations suggest that while ML offers significant potential, expert domain or a shift towards a physics-based modelling approach may still be needed until these challenges can be addressed.

2.2.1.3. Value of information and feature engineering

Value of Information (VOI) is a metric used in decision analysis that quantifies how relevant a source of information is, given an uncertain outcome (Trainor-Guitton et al., 2013). Geochemical, geological, and geophysical datasets are limited to the accuracy of measurements, data processing, and non-uniqueness issues for inversion methods in geophysical data. Geologic datasets are composed by a combination of numerical and categorical data (Brown et al., 2020). The latter includes, for example, rock classification and field descriptions that need to be encoded before applying ML techniques. Addressing the limitations in the data and increasing its quality can reduce uncertainty and provide greater value to decision-makers (Trainor-Guitton et al., 2013).

Feature engineering involves a series of techniques to transform predictor data and enhance its predictive power, and thus reduce uncertainty. Using fewer, but more informative, features is preferred over more datasets that are highly correlated when working with few labelled examples (Mordensky et al., 2023b). In geothermal research, feature engineering focuses on developing features that can better characterize the subsurface and reflect accurate geological conditions.

The Innovative Geothermal Exploration through Novel Investigations of Undiscovered Systems (INGENIOUS) project in the Great Basin, for example, aims to integrate PFA methodologies, ML VOI

analysis, geo-statistics, conceptual modelling, and other methodologies to develop a PF workflow for the region. As part of the feature engineering efforts, Hart-Wagoner et al. (2023) integrated two attributes from fault data from the Great Basin into a single feature to emphasize the role of Quaternary faults in controlling hydrothermal systems in the region. DeAngelo et al. (2023a) used a simple interpolation method to create a detrended elevation map for the region that isolates the signal for local valley-scale topography (i.e., basins and ranges) from the regional elevation trend. DeAngelo et al. (2023b) developed a conductive heat flow map using well data and an iterative process to separate convective influences. Using the heat flow map from DeAngelo et al. (2023b), Burns et al. (2024) updated previous temperature at depth maps. These improved features can aid ML efforts to identify hidden geothermal resources in the Great Basin.

Mordensky et al. (2023c) trained ML models using DeAngelo et al. (2023b) conductive heat flow signals as labelled data to identify areas of hydrothermal upflow. ML thermal modelling for geothermal resources extends outside the Great Basin. Aljubran & Horne (2024) used a graph-based, physics-informed neural network to create a thermal model for the conterminous United States (interPIGNN). The Stanford Thermal model (STM) has a resolution of 18 km^2 with depths up to 7 km at 1 km increase intervals and predicts temperature at depth, thermal conductivity, and surface heat flow. Aljubran & Horne, (2024) used temperature data from 400,134 bottom holes, as well as other input data, such as magnetic anomaly, sediment thickness, elevation, and gravity anomaly. The results from Aljubran & Horne (2024) predict temperature at depth with a mean average error of 4.8°C. In Japan, Chhun et al. (2024) extend work to improve the 3D temperature model estimation of the Mount Kuju geothermal reservoir based on various ML models. The input feature data included eight temperature logs, 3D S-wave velocity, 3D resistivity, and 3D seismic anisotropy as fracture orientations (Azimuth, Amplitude). They obtained a 3D temperature variation of up to 250°C within the identified geothermal reservoirs. Ishitsuka et al. (2021) used two methods based on Bayesian and neural network approaches to estimate the 3D temperature distribution derived from borehole, 3D resistivity data, observed geological/mineralogical boundaries, and microseismic observations in a supercritical geothermal system in Kakkonda, Japan. In Colombia, Mejía-Fragoso et al. (2024) used a gradient-boosted regression tree algorithm to create a geothermal gradient map for the country within 12% accuracy.

The previous examples describe the applications of feature engineering for geothermal resources. Some approaches consist of linear or simple interpolation methods, while others use mathematically complex neural networks with hundreds of thousands of examples to create a single feature. The complexity of the approach does not necessarily relate to the predictive skills of the feature.

Increasing the quality of geothermal datasets is crucial to characterize, develop, and reduce exploration risks for SHR resources. However, the specific feature engineering approaches discussed in this section have not yet been validated in SHR demonstration sites, highlighting the need to establish benchmarks for data processing and engineering workflows in SHR environments. Identifying the most informative datasets will enable the development of innovative techniques of data enhancement.

Current technology:

- PFA: 3D PFA (multi-play) and 2D PFA (hydrothermal, low T).

- ML: Supervised ML approaches for exploration.
- Feature engineering: Clustering, dimensionality reduction, interpolation, ML driven feature engineering, 3D joint inversions.

Gaps:

- Limited number of SHR data (training sites or benchmarks for both ML and PFA).
- Low data granularity/resolution which increases uncertainty (low VOI).
- 3D EGS PFA not exclusive for SHR targets (producibility datasets are not well constrained).
- 2D PFA were not developed to include evidence layers for EGS.
- Lack of data availability (repository) for SHR.
- Lack of open-source software.

Technology/approach needed to develop SHR:

- Use of free/open software.
- Training data augmentation (analogous).
- Improve the quality of input datasets.
- Identifying which methods/surveys can better characterize SHR.
- Integration of physics-based modelling and physics-informed machine learning.

2.2.2. Rock physics and laboratory core analysis

Geophysical imaging provides structural information about the spatial, or temporal, differences in rock properties (elastic properties, density, electrical conductivity, magnetic susceptibility, etc.) across the region of interest, but a quantitative interpretation about what those geophysical properties represent is needed to fully utilize the data. Converting the measured geophysical properties to petrophysical conditions is the job of rock physics, using theoretical and empirical relationships confirmed by and derived from controlled laboratory experiments (Mavko et al., 2009). Experiments can provide further confidence in the interpretation by using direct core samples from the reservoir of interest or analogs (e.g., Wenning et al., 2018). But the HPHT conditions of SHR resources can be difficult to reach in the laboratory for relatively large rock sample sizes, so analog materials can also be used, for example acrylics that exhibit a brittle-ductile transition at lower temperatures and pressures (Parisio et al., 2021). Utilizing 3D CT scans of cuttings, chips, and core samples, digital rock physics provides the ability to model continuum-scale (representative elementary volume, or REV) petrophysical rock properties (e.g., Khodaei et al., 2022); these effective medium methods must be further expanded to SHR conditions and processes.

Electrical conductivity, or resistivity, is the geophysical property with the most direct dependence on temperature. Hokstad & Tanavasuu-Milkeviciene (2017) performed a temperature inversion of MT data, with gravity to further constrain porosity, at the IDDP-2 well site. This Bayesian rock physics inversion assumed experimentally derived relations for conductivity and density as a function of temperature. Temperature-with-depth predictions were made in anticipation of drilling, under-predicting by 50-100°C the while-drilling updates, and were corrected with log data as they became available. Archie's Law can be used to interpret electrical conductivity values as a combination of fluid conductivity (which depends on salinity and temperature), matrix conductivity (dependent on temperature and mineralogy, as clay

minerals surface conductivity often dominates), and pore connectivity (given by a formation factor). Since opposite charged ions in electrolytes recombine near the critical point, conduction was assumed to be negligible at supercritical conditions, providing a clear contrast when supercritical temperatures are reached, but fluid-rock interactions complicate this by introducing new charge carriers (Kummerow et al., 2021). So, while clear resistive anomalies might represent low permeable supercritical zones, with limited fluid-rock interaction, highly permeable locations are expected to exhibit hydrothermal alternation that will overprint with conductive mineralogy. Thus, these supercritical fluid zones might be difficult to identify with EM methods.

Rock physics interpretations more often focus on seismic properties (velocity and attenuation) because seismic surveys provide the most detailed resolution of structural differences and can give information about some of the most useful parameters for geothermal development (temperature, fluid content and connectivity, and porosity and pore shape). Even isotropic rock elasticity provides two independent elastic constants (for example, in Vp and Vs), so seismic data further constrain petrophysical conditions if these two properties are interpreted together, as well as with attenuation. Hutchings et al., (2019) provide a detailed interpretation framework for possible combinations of these properties in a steam-dominated geothermal setting, with examples given from seismic tomography of the Geysers geothermal field in California.

Since the measured properties depend on these rock types and conditions interdependently, it is important to undertake a complete sensitivity analysis to determine the likely constraints each measurement provides. Poletto et al. (2018) provides the sensitivity of seismic properties to temperature in geothermal settings, using a viscoelastic Burgers constitutive model with Arrhenius temperature equations, Gassman fluid substitution, pressure dependence, and permeability effects, such as frequency-dependent squirt flow. This model shows that seismic velocity and attenuation are expected to be very sensitive to temperature in the melting zone and at the fluid supercritical point, and thus particularly useful for exploration and monitoring the temperature of SHR relative to conventional geothermal resources. The model also shows that seismic exploration methods should be able to distinguish between conductive and convective heat flow in the reservoir (Farina et al., 2019), and seismic monitoring should be sensitive to temperature draw-down from cold water injection over the project lifecycle (Farina et al., 2022). Along with the theoretical model, empirical relationships between seismic velocity and temperature have been analyzed in the Los Humeros and Acoculco fields as part of the GEMex project, showing a statistically significant correlation but an indirect relationship between seismic velocities and temperature (with a common dependency on pressure). Borehole DAS/DTS and VSP measurements have been proposed to test and improve these relationships (Mendrinos et al., 2020).

Experiments on, and analysis of, rock core from the reservoir or outcrops from the field site is one of the most direct ways to develop and test quantitative interpretations of geophysical data. One example is a set of experiments on rock core from the Grimsel Test site underground laboratory, a well-studied analog site for SHR crystalline reservoirs. The Grimsel granodiorite hosts a mylonitic fault core that exhibits brittle-ductile transition fabric. Seismic anisotropy and permeability measurements at high pressure and temperature conditions show how ductile deformation can control the matrix elastic and

fluid flow properties. In this way, seismic measurements are sensitive to variation in complex ductile flow structures that control permeability in these settings (Wenning et al., 2018). Other laboratory experiments (Meyer et al., 2022, 2024; Petrini et al., 2021; Watanabe, Egawa, et al., 2017; Watanabe et al., 2019, 2021; Watanabe, Numakura, et al., 2017) have studied the fracture and dissolution processes for creating and maintaining permeability at superhot ductile conditions (as was summarized in the Heat Extraction report), but few have attempted to tie these lab observations to geophysical measurements that can be made in the field, as has been done at conventional reservoir conditions (Tomac & Sauter, 2018).

Goto et al. (2021) conducted the first hydrofracturing experiment with supercritical water in granite under true triaxial stress with Acoustic Emission (a laboratory scale analog to seismicity) monitoring to confirm the creation of a distributed 'cloud-fracture network' (CFN). They also utilized before-and-after changes in P-wave velocity to show that the damage was distributed throughout the sample (Figure 3). Marie Violay's group has developed a new HPHT loading rig (TARGET) at EPFL. Similar to a Paterson rig but adapted to handle larger sample sizes, their initial results do not include acoustic data (Meyer et al., 2024), but upcoming work will incorporate active and passive acoustic monitoring.

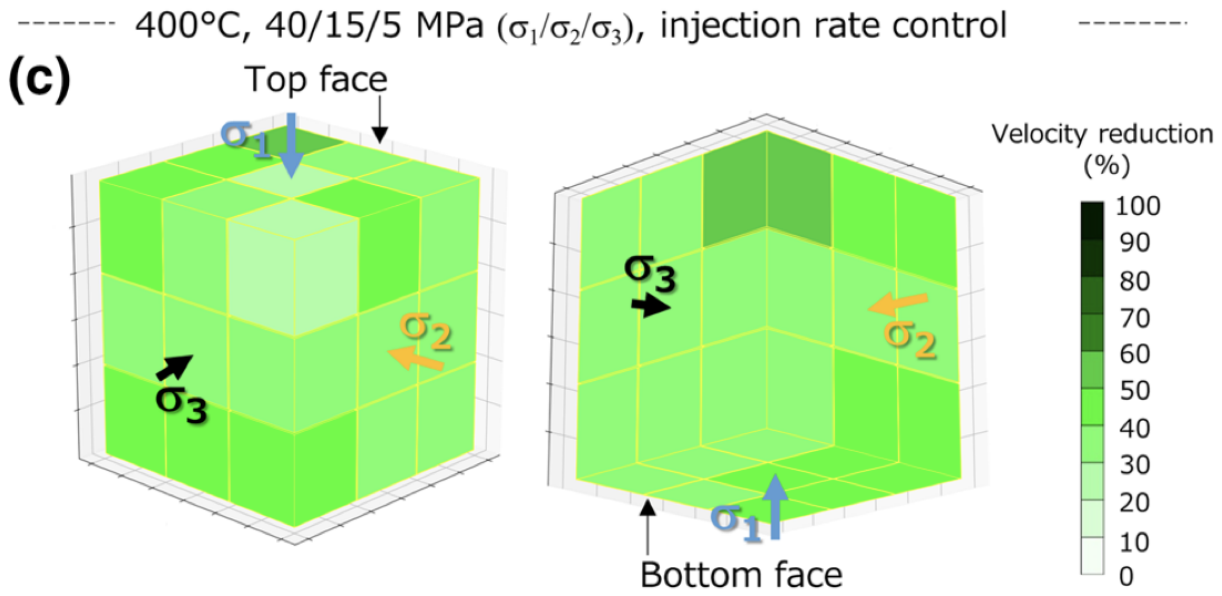

Figure 3: from Goto et al. (2021), seismic velocity changes show that damage after hydrofracturing with supercritical water at SHR conditions produces distributed damage over the entire sample, developing a 'cloud-fracture network' as opposed to localized fracture observed at lower, brittle temperatures.

Other relevant experiments in the literature focus on the sources of volcano seismicity and interpretation of seismic tomography from these settings. Lab experiments of volcanic rocks at SHR temperatures show a significant change in P-wave velocity, an increased seismicity rate, and low-frequency content Acoustic Emissions (AEs) when crossing the glass-transition temperature in volcanic rocks, consistent with observations of volcanic tremor (Benson et al., 2020). Partial melting experiments have been conducted by the academic community, where seismic velocity and attenuation are used to

argue for high melt-fractions in the upper mantle but are inconsistent with geochemical constraints. Recent rock analog experiments and polycrystal anelasticity models provide more consistent interpretations (Takei, 2017), which could be applied to interpretation of seismic attenuation of superhot geothermal and underlying magmatic systems.

Gaps:

- Geophysical data are most often used to image structures, but could provide more quantitative interpretations given rock physics relationships and core analysis.
- Most current experiments to understand fracture permeability at SHR ductile depths do not incorporate measurements with field deployable geophysics analogs.

Current technology:

- Electrical conductivity has the most direct temperature dependence, although uncertainty in porosity complicates interpretation.
- Supercritical conditions should limit conductivity, but overprinted hydrothermal alteration can reintroduce charge carriers and mask supercritical resistive bodies. Overlying conductive layers (such as clay-caps) will also limit resolution of resistive layers below.
- Theoretical constitutive models and empirical relations suggest that seismic velocity (especially Vp/Vs) and intrinsic attenuation should be very sensitive to temperature at SHR conditions (while having a mutual dependency on pressure and other rock properties), but experimental verification is limited.
- Permeability can be controlled by complex ductile deformation fabrics, which exhibit seismic anisotropy, so could be identified and characterized with seismic methods.
- 'Cloud-fracture networks' of distributed damage suggested by supercritical water hydrofracturing experiments can be confirmed with active and passive acoustic monitoring techniques.

Technology needed to develop SHR:

- Laboratory experiments of anisotropic (an)elastic and electrical properties at SHR conditions to develop robust relations between geophysical observables and temperature, permeability, fractures, and stress in reservoir rocks and analog materials.
- Further development of constitutive models across the brittle-ductile transition that incorporate monitoring of evolving geophysical properties.
- Digital rock physics expanded to SHR field conditions to estimate and understand petrophysical rock properties using SHR cuttings, chips, and core samples/images.
- Field validation with downhole seismic monitoring and temperature fiber optic sensing (DAS/DTS).

2.2.3. Joint interpretation/inversion

Each individual geophysical method and measured property can be highly non-unique, since many different combinations of materials and the conditions we are interested in (temperature, stress, permeability/fluid content, etc.) within a resolved volume can produce the same average or effective measured property. For this reason, these methods must be utilized jointly to maximally constrain the subsurface. In practice, this is often done by overlaying the mapped geophysical data together in data

visualization programs, such as LeapFrog or petrel, and then interpreting jointly by trained humans. Although not regularly used for decision making due to issues with obtaining robust solutions, these data sets can be combined more quantitatively with joint inversion schemes.

The concept of joint inversion arises from the inherent complexity of geophysical inverse problems and models, coupled with uncertainties from data processing and interpretation analysis. To mitigate these issues, various inversion methods are used together with external constraints, such as prior geological information, smoothing, stochastic regularization, or inversion for a specific model type. The inversion workflow techniques aim to reduce model misfit and increase accuracy by applying model smoothing, regularization, synthetic model evaluation, and inversion algorithms based on non-linear, deterministic, or stochastic approaches (Hokstad & Kruber, 2023; Keilis-Borok & Yanovskaja, 1967; Treitel & Lines, 2001).

Despite these efforts, inversion models still face challenges or limitations due to the number of deployment sensors, spacing, survey topography/coverages, frequency of sources, data quality, computation time, and model complexity (Spichak, 2020). Therefore, geophysicists often use geologically constrained inversions. Geologically constrained inversion significantly enhances results and interpretation, including hypothesis testing of conceptual or prior knowledge, by integrating different sources of information, such as geological maps, known subsurface structure, outcrop data, or borehole data.

Often the variables that are estimated in the inversions (e.g., resistivity or seismic-wave speed) are not the variables of interest (e.g., heat or permeability), but rather are correlated with them in some way. Separating the effect of the variable of interest from other variables that affect our measurements can be challenging and often requires simultaneous estimation of several variables that depend on the variable of interest. In order to explicitly extract the variable of interest, joint inversion of two or more geophysical datasets has been developed as a powerful tool for quantitative data integration (Simirdanis et al., 2019). Data combinations among the different types of geophysical data are used for joint inversion, including electrical resistivity with seismic, cross-hole electrical resistance with ground penetrating radar, magnetotelluric and seismic travel-time data, seismic with gravity and electromagnetic data, and others. Joint inversion can be applied to obtain independent physical parameters (e.g., seismic, gravity) or jointly estimate petrophysical parameters (e.g., porosity, permeability, or heat).

There are many types of joint inversion, such as sequential, simultaneous, structural constraint or petrophysical constraints, or Bayesian inversion. However, the various joint inversion types can be grouped into two classifications based on petrophysical and structural approaches (Tu & Zhdanov, 2021). The petrophysical-based joint inversion requires *a priori* knowledge between different petrophysical parameters and correlate them based on theoretical, empirical, or statistical petrophysical relationships using field-, well-log-, or lab data (Section 2.2.2). Structural-based joint inversion is used to model different physical properties considering similar spatial structures or structural resemblance in the study area (i.e., low velocity correlating with low density refers to geothermal structures or magma chambers). Other advanced joint inversion algorithms have also been developed, such as Multimodal Deep Learning-Based Methods (JointNet by Huang et al., 2024) and the Gramian Constraint Method

(Vatankhah et al., 2022). The program jif3D (Moorkamp et al., 2011) is open-source with capabilities to singly or jointly invert scalar gravity, full-tensor gradiometry, total-field magnetics, three-component magnetization, magnetotellurics, DC resistivity, and long-offset seismic data. It has multiple methods to couple the various datasets, specifically the widely used cross-gradient approach established by Gallardo & Meju (2011), and lesser-known mutual information methods.

One case where joint inversion was applied to better characterize an EGS resource was the study by Ars et al. (2019). The authors jointly inverted MT, gravity, and ambient noise surface wave seismic data to characterize a non-conventional geothermal resource in the French Massif Central within 15 km depth. The resistivity, density, and shear wave velocity information were coupled linearly in various combinations, using the MT-derived resistivity model as a starting model for the density and velocity model, to improve constraints of deep geological domains, as well as depth to the BDT revealed by a sharp increase in density and velocity, indicating plastic behavior. This transition was between 6 and 8 km and is estimated to demark the 400°C isotherm. Their results showed some correlation between the three integrated datasets, but they concluded that more complex, non-linear statistical relationships should be explored. In the case study of the Newberry volcanic structure evaluated by PFA (Taverna et al., 2024), one of the datasets used was a joint inversion of magnetotelluric (MT) and gravity data. However, many other datasets (e.g., digital elevation model, earthquake catalogs, seismic velocity, geothermal well data, and geological modelling) were also utilized in the PFA (Shervais et al., 2024; Taverna et al., 2024). This approach aimed to use joint data to model the heat, fluid, and permeability maps for resource favorability evaluation. This example is described in more detail in the PFA section (2.2.1.1.

Joint analysis can also be performed based on ML, incorporating multi-modal data. Machine learning or Deep Learning (DL) techniques have two main approaches: supervised learning for classification and regression models, and unsupervised learning for finding patterns/groups in unlabelled data. There are many types of classification and regression models, and to –date, they have been applied to many geothermal field studies, from global, field, and development scales to reservoir monitoring.

For example, the paper by Aljubran & Horne (2024) estimated the 3D temperature structure across the US using InterPIGNN (Thermal Earth Model using interpolative physics-informed graph neural networks). They used bottomhole temperature measurements for training data and other input data such as depth, geographic coordinates, elevation, sediment thickness, magnetic anomaly, gravity anomaly, gamma-ray flux of radioactive elements, seismicity, and electrical conductivity. From these various input data and BHT data as a training model via InterPIGNN, they produced the spatial temperature distribution of the US at depths of 0-7 km with a vertical resolution of 1 km and a horizontal resolution of 18 sq km. The sections on Machine Learning in Resource Exploration and Assessment (2.2.1.2.) and Heat Mapping (3.2 and 4.1) give more examples and details.

Technology needed to develop SHR using ML: ML incorporating multiple data sources demonstrates an innovative tool for exploring and developing various geothermal resources, including SHR. Uncertainty can arise from the different model resolutions of various geological and geophysical data or limited data availability. Funding and conducting geothermal well data collection, particularly in deep boreholes, should be prioritized in many regions to advance the understanding of temperature and stress fields in

SHR. In the US, well data collection is already widespread, but accessibility varies. The borehole data should be made accessible worldwide for researchers to develop, improve, and advance research and field applications on a broad scale, especially for predicting 3D large-scale temperature, permeability, and stress.

Gaps:

- Prior information is needed in the joint inversion based on petrophysical approaches.
- Data survey, processing, and resolutions are often different based on various geological/geophysical surveys or geological settings.

Current technology:

- Advanced techniques such as JointNet, based on deep learning (Huang et al., 2023) or Gramian Constraint Method (Vatankhah et al., 2022).
- There are many developed 3D geological modelling tools, such as kinematic structural modelling, PyNoddy; discrete element methods, MOVE; and potential field methods, GemPy. Additionally, software like Leapfrog Geo and Oasis montaj are widely used in this field.

Technology needed to develop SHR:

- Account for diverse datasets and incorporate multi-spatial geo-data resolution and combability.
- Develop effective methods of joint different resolutions of different geological/geophysical methods.
- Commercialize academic joint inversion codes and improve usability.

2.2.4. Data availability/repositories

The availability and accessibility of data from existing and future SHR projects is key to sharing and progressively improving siting and characterization procedures for SHR resources. The existing repositories are extremely important and useful, but even data that are needed to meet funding requirements are often not truly accessible to other researchers in the field due to unclear metadata and context. In practice, someone involved in the collection or analysis of the data are needed to guide the use of existing data. Useful analysis is often left in internal reports and not published due to time constraints and a lack of incentive. More metadata and publication requirements would improve this situation but can be an onerous time commitment and potentially an unrealistic expectation. A widely agreed-upon, standardized approach to data collection and curation would also greatly improve the accessibility of available data. The table below lists existing relevant open data repositories and how they can be accessed.

Type	Authors	Sources
Lithoref18	Afonso et al. 2019	https://www.juanafonso.com/software
The Global Heat Flow Database	Fuchs et al. 2021	https://ijthfa.com/index.php/journal/article/view/62

SMU Geothermal Heat Flow Database		https://www.smu.edu/dedman/academics/departments/earth-sciences/research/geothermallab/datamaps
National Geothermal Data System (NGDS)	DOE-Geothermal Technologies Office	https://www.re3data.org/repository/r3d100011016
Data, results, papers, projects, methods, reproducible papers	Geothermal Data Repository, OpenEI,	https://gdr.openei.org/home
	SHR resource map, CATF	https://www.catf.us/shr-map/
	IDDP Iceland Deep Drilling Project	https://iddp.is/
	DEEPEN	https://www.or.is/en/about-or/innovation/deepen/
	FORGE	http://energy.gov/eere/geothermal/forge
	Krafla Magma Testbed	https://www.kmt.is/
	GEMex	https://ec.europa.eu/inea/en/horizon-2020/projects/h2020-energy/geothermal/gemex
	DESCRAMBLE	http://www.descramble-h2020.eu/
	DEEPEGS	https://deepegs.eu/
	GNG, New Zealand	https://www.geothermalnextgeneration.com/
	Supercritical fluid resources of Japan, NEDO	https://www.nedo.go.jp/english/index.html
Various project data locations	IRIS, FDN	https://www.fdsn.org/networks/
GeoMap™ Surface and subsurface modules, a suitability analysis tool, and a Techno-Economic Sensitivity Tool	Google Earth; Project Innerspace	https://geomap.projectinnerspace.org/map-selection/

US Array, Federally funded EarthScope Project	Seismic and magnetotelluric data across the contiguous USA	http://www.usarray.org/
International Heat Flow Commission (IHFC)	Heat flow data repository	https://www.ihfc-iugg.org/
Stanford Thermal Model (STM)	Stanford thermal model for the contiguous USA	https://gdr.openei.org/submissions/1592
EMAG2	Curie Point Magnetic Anomaly Map	https://www.ncei.noaa.gov/products/earth-magnetic-model-anomaly-grid-2
Global Heat Flow Database (GHBD) (Hasterok, 2019)	A compilation of the Lucazeau (2019) and Hasterok & Chapman (2008) heat flow estimates with thermal conductivity, thermal gradient, temperature, and heat generation datasets	http://heatflow.org/

3. Exploration scale (100s to 10s of kilometers)

The data analysis techniques discussed above rely on a wide range of data types and are limited by the availability and uncertainty in these data. In the next three sections (3, 4 & 5), we highlight key methods and data for constraining SHR resources. Some of these methods and data have been applied to supercritical geothermal systems, although these applications are limited to a few locations. The sections are organized by the scale/scope of data; as the characterization process is undertaken, more detailed and smaller-scale data are incorporated.

This section focuses on the large-extent, low-resolution data that are often the only data available in the early exploration stages of a project. Reservoir and validation scale (Section 4) describes more detailed data that can be collected once a location is determined to be a promising resource. These data are key for refining geological conceptual and reservoir models and limiting drilling risk, which can be confirmed by well-logging methods. These data should be incorporated into exploration and development processes.

3.1 Geological/geodynamic setting

To start, we address the larger geological/geodynamic context of an SHR play. Geothermal/SHR resources can exist in 15 geodynamic settings (Afonso et al., 2019; Ball et al., 2024; Hasterok & Chapman, 2008; Moeck, 2014). Many of these are found in volcanic arc and orogenic belt settings, such as the USA/Cascadia, New Zealand, Japan, Indonesia, the Andes, and the Philippines, which are among the first prospective regions where potential energy resources have been estimated. Shields, accretionary complexes, wide rifts, and margins are also expected to contain considerable reserves. For example, the East African Rift systems (Biggs et al., 2016) in Kenya and Ethiopia, and Mid-Oceanic ridges, such as those in Iceland, hold significant potential. Globally, two-thirds of the Geothermal/SHR resources are located within compressive domains, while one-third are in tensile and stable domains, including the eastern USA (Peacock & Siler, 2021), parts of Europe (Planès et al., 2020), and Southeast Asia (e.g., Thailand).

Ball et al. (2024) classified 33 EGS/SHR geothermal projects based on their geodynamic setting, to improve risk forecasting for future SHR resource development per geodynamic setting. The classification scheme included historical data such as drilling penetrations and drilling operation success, hydrothermal proxies, a global map of geologic provinces (Hasterok & Chapman, 2008), a lithospheric reference model to draw the 450°C isotherm (LithoRef18, Afonso et al., 2019, see Section 3.2.1), and surface heat flow estimates (Fuchs et al., 2023; Lucazeau, 2019, see Section 3.2.3). The geothermal heat transfer mechanism (convection or conduction) for each SHR resource and their geological domain depend on radiogenic heat diffusion, mantle dynamics, bulk rock porosity, water content, and permeability. Robust heat flow estimates in steady-state domains are provided by Lucazeau (2019) and Fuchs et al. (2023), and the distribution of hydrothermal proxies are incorporated to capture non-steady-state heat flow regimes, which are often missed by coarse, steady-state heat flow maps. Overall, based on depth estimation to the 450°C isotherm, an area of 20-35% of all geodynamic settings host feasible sites for SHR geothermal development, with volcanic arc and orogenic belts offering the highest

success. Further work on stress state mapping related to geodynamic setting, as well as non-steady state heat flow dynamics, is needed to improve this estimation.

Geothermal energy play types in different geological/geodynamic settings provide distinct heat source locations, reservoir/altered rocks, temperature ranges, fluid geochemistry, fractured / non-fractured systems, energy output capacity, and longevity. Here we review some key examples for different geological settings which have been studied for supercritical and SHR geothermal resources.

DESCRAMBLE in Larderello geothermal field, Italy (intrusive volcanic structure in subduction/collision)

The Larderello geothermal field has been renowned for its geothermal power production and research for over 100 years. Since the 1900s, the power plants in the area have operated with a capacity of about 800 MW, supporting approximately one-third of the region's energy needs. The Larderello geothermal field is part of the Northern Apennine volcanic arc of Italy, where the African plate collides and subducts beneath the European plate at a rate of 1 cm/year. This region has experienced compressional regimes due to the subducting plate, which caused magmatic intrusion and the formation of strike-slip fault blocks. These factors subsequently led to extensional tectonic phases in the shallow crust of Northern Apennine section, currently characterized by a back-arc basin extensional setting (Gola et al., 2017; Minissale, 1991). Unlike other extrusive volcanic regions in central and southern Apennine of Italy, the Larderello geothermal field has only been influenced by intrusive magmatic activity without eruption.

Due to the continuous tectonic compressive regime, numerous magmatic systems (4 Ma - present) have intruded into the shallow regions, creating complex litho and metamorphic strata (Gola et al., 2017). The heat source is recent partial-melt granites located at depths greater than 5 km, serving as the heat convection and conduction medium for the geothermal reservoirs of the Larderello field. The main structure comprises a series of major extensional fault zones. The stratigraphy, including geothermal and magmatic structures, consists of Neogene sediments underlain by Tuscan units and a tectonic wedge complex, which includes phyllitic, quartzitic, mica schist, and gneiss complexes, followed by Pliocene granite. These rock complexes can host reservoir temperatures ranging from 200°C to 550°C within depths of 2-5 km (Bertani et al., 2018; Gola et al., 2017).

DESCRAMBLE is an international geothermal project undertaken in the Larderello geothermal field. The project aims to develop advanced drilling technologies and test the feasibility of reaching supercritical geothermal resources. The well reaches a depth of 3 km, successfully achieving supercritical conditions (Bertani et al., 2018; Davide & Luca, 2019). This project has demonstrated innovative drilling techniques and detailed characterization of chemical and thermo-physical conditions in supercritical fluid reservoirs.

Iceland Deep Drilling Program (IDDP) in Krafla caldera (volcanic and rift structure in Mid-Atlantic Ridge)

Iceland is situated above a hot mantle, indicative of a deep-sourced mantle plume. This region lies along the mid-Atlantic spreading ridge, resulting from the divergence of the North American and Eurasian plates and the creation of new oceanic crust. This ridge extends roughly north to south through Iceland,

with an average spreading rate of 2 cm per year (White et al., 2019). The structure of Iceland is shaped by active volcanic rift zones. The northern part of Iceland consists of five en echelon spreading segments, each featuring a fissure swarm with predominantly north/south extensional fractures and a central volcano that drives volcanic activity and high-temperature geothermal resources (Toledo et al., 2022b). In contrast, the southern part of Iceland is split into two branches of the Eastern and Western volcanic rifts (Toledo et al., 2022b; White et al., 2019).

The Krafla Magma Testbed (KMT) is located within the Krafla caldera in northern Iceland. The project aims to drill and directly access a magma chamber to initiate the world's first magma research facility for observations and experiments in magma dynamics, volcanic risk, and superheated geothermal energy (Hersir et al., 2021). This volcano spans roughly 20 km in diameter, featuring an 8 by 10 km caldera formed by the last eruption around 110 ka (Gudmundsson & Mortensen, 2015). Most eruptions are bimodal, consisting primarily of basaltic magma with little silicic or rhyolitic content. The Krafla Fissure Swarm extends about 50 km north and 40 km south from the caldera's center. At the center of the Krafla caldera lies the hill Leirhnjúkur. A few kilometers southeast of Leirhnjúkur is Leirbotnar, the primary production site for the Krafla geothermal power plant (60 MW). Additionally, Bjarnarflag, another high-temperature geothermal area used for energy extraction, is located to the south of the Krafla caldera (Ilic et al., 2020). This region is known for its magmatic heat source, which can reach temperatures of approximately 1,000°C and is situated as shallow as 2 kilometers below the surface. Many regions of Iceland exhibit high geothermal gradients, with most brittle-ductile transition zones occurring at depths of 6 to 8 kilometers. Beyond these depths, the hotter crust typically remains aseismic (White et al., 2019). However, some earthquakes, including induced seismicity, can occur at these depths or beyond due to magmatic intrusion or the accumulation of volatiles or gas, which generates excessive stress and strain. This can create cracks or faults, subsequently triggering deep seismicity.

Japan Beyond Brittle Project (volcanic and rift structure in subduction zones)

Kuju volcano is part of the Japan Beyond Brittle project. A national research and development agency in Japan (NEDO) has been intensively studying this area for supercritical fluid exploitation by 2050. Kuju, an active volcanic group located in the Beppu-Shimabara Graben in central Kyushu, Japan, hosts the biggest geothermal power plant, Hatchobaru (110 MW), and a low capacity Otake power station (12.5 MW). These power stations have been operational since the 1960s. The energy has been extracted only from shallow reservoirs (up to 250°C) less than 2 km deep.

The Kuju volcanic group (2 Ma – present) consists of more than 20 Quaternary lava domes and stratovolcanoes over an area of approximately 10 x 10 km. The Beppu-Shimabara Graben is a subsidence zone resulting from compressional to extensional conversion induced by a major series of strike-slip faults and volcanism. These geological processes are driven by the oblique subduction of the Philippine Sea Plate beneath the Japanese Islands, at a rate of 6 cm/year (Moreno et al., 2016; Sudo & Matsumoto, 1998).

Exploration boreholes, geochemical analyses, and geophysical imaging have identified a heat source at depths greater than 3.5 km below the surface, associated with supercritical fluid and SHR reservoirs exceeding 380°C. This supercritical reservoir is above a magma body in the granitic basement, forming the shallow brittle-ductile transition zone (Aizawa et al., 2022; Chhun et al., 2024; Kitamura et al., 2023). This heat source acts as a significant conductive body for geothermal fluids, which migrate fluids from recharge zones through major northwest/southeast-trending fault zones beneath the power stations. The shallow reservoir zones contain geothermal structures and fluid accumulations, with temperatures reaching up to 250°C below sea level. The Kuju stratigraphy includes volcanic rocks (Middle–Upper Pleistocene), Hohi volcanic rocks (Lower Pleistocene), the Usa group (Miocene), and basement rocks (pre-Tertiary). The reservoir rocks beneath the power stations consist of low- (alunite), intermediate- (chlorite, wairakite, kaolinite), and high-temperature alterations (montmorillonite) (Aizawa et al., 2022; Momita et al., 2000).

Utah FORGE, geothermal basement structures below back-arc sedimentary basin

The Utah FORGE site is a cutting-edge facility for testing and validating EGS technologies. The reservoir is not at SHR conditions but is exemplary of extensional settings and is among the best characterized locations for EGS development. The target reservoir, located at depths of 2-5 km and temperatures up to 250°C, consists of fractured granitic rocks from the tertiary-age Mineral Mountains intrusion (Simmons et al., 2019). Situated on the eastern margin of the Great Basin, this region is part of the back-arc extensional setting of the Cascade subduction zone, which is moving at a rate of 4 cm/year. Similar to other subduction regions, the Great Basin features magma underplating and strike-slip faults resulting from plate collision and subduction. During the Middle to Late Cenozoic, the area transitioned from compressional to extensional tectonism, leading to a series of normal faulting systems, with most structures oriented in northwest/southeast and northeast/southwest directions (Pérouse & Wernicke, 2017).

The Great Basin exhibits ongoing magmatic underplating and volcanism. It has experienced both paleo-hydrothermal processes, which have contributed to its mineral resources, and present hydrothermal systems (Peacock & Siler, 2021; Pérouse & Wernicke, 2017). The major BDT layer is located approximately 15 km below the surface. Below this basin, magmatic underplating replenishes the lower crust with mafic melt, which becomes trapped around the BDT (Peacock & Siler, 2021). Magmatic fluids are released through the BDT via major strike-slip and normal fault zones, acting as conductive pathways for the Great Basin geothermal systems. This mechanism controls the movement of heat and fluids through fault systems, while some faults are self-sealed by ore minerals. These (ore) mineral deposits may have also contributed to retaining, promoting, and transferring heat conduction from deep to shallow geothermal reservoirs in the region (Kirkby et al., 2022).

3.2. Heat mapping

Heat mapping determines the thermal properties at depth for a prospective geothermal resource, commonly quantified as the geothermal gradient (°C/km), temperature at depth (T(z)), or heat flow

(mW/m^2). The Earth's internal heat is the result of radioactive decay, exothermic chemical reactions, latent heat from the Earth's formation, and kinetic friction, which diffuses from the Earth's interior to the surface (Batir & Richards, 2020; Fuchs et al., 2023). Geothermal heat flux is dependent on the conductive, convective, and radiative heat transfer properties of the geological province (such as continental margin, sedimentary basins, shield-type cratons, or orogenic belts), geological properties (such as composition and porosity), and mantle dynamics that impact basal heat flow (Kirbky et al., 2024; Fullea et al., 2021; Fuchs et al., 2023; Grasby et al., 2011). Thermal properties at depth can be directly measured by exploration drilling. However, these measurements are cost-intensive, relatively shallow, and highly localized. Global-to-regional-scale heat flux values must otherwise be indirectly estimated by integrating a range of datasets, such as surface heat flow measurements, geological domain characteristics, EM conductivity, soil temperature, gravitational and magnetic potential, seismic velocity, and other datatypes (Kana, 2015). The depths to thermophysical horizons, such as the Brittle-Ductile transition (BDT), the K-Horizon, or the Curie Depth Point (CDP), can be leveraged to estimate temperature properties at the crustal scale.

Thermal properties at depth are complex to resolve, yet essential for proposing and de-risking geothermal projects, including SHR plays (Lucazeau 2019). We review some state-of-the-art thermal mapping techniques that can be applied to SHR site characterization, identify gaps in these methods, and suggest strategies to close these gaps.

3.2.1 Global scale thermal model LithoRef-18

LithoRef18 models lithosphere dynamics by jointly inverting gravity, elevation, seismic velocity, thermal conductivity, and petrological data from the upper mantle and lithosphere (Afonso et al., 2019; Sellars et al., 2023). The model calculates steady-state heat transfer at depth using the thermophysical parameters of the upper crust, lower crust, and lithospheric mantle. These parameters include the thermal conductivity of geological provinces (craton, convergent margin, rift system, oceanic crust, etc.) and rates of radiogenic heat diffusion. The 2°-x 2° (correlating to 230 km x 230 km) discretization resolves first-order lithospheric scale temperature variations. While applicable for thermal mapping at the exploration scale, LithoRef18 is too coarse to capture short-wavelength geothermal anomalies at the reservoir scale (Ball et al., 2024; Tester et al., 2006; Aljubran & Horne, 2024). Depth to the specific isotherms (such as the supercritical temperature threshold, 375°C) can be estimated using LithoRef-18 within the upper 410 km of the Earth (Afonso et al., 2019). Sellars et al. (2023) and Ball et al. (2024) used LithoRef18 to map the 450°C isotherm at global or continental scales (discussed in Section 3.1). Both studies produced results that were well-correlated with surface heat flow maps (Section 3.2.3), supporting model results. However, Ball et al (2024) and Sellars et al. (2023) observed discrepancies in temperature-at-depth estimations between LithoRef18 and other global thermal models.

The global LithoRef18-generated 450°C isotherm (Figure 4) tends to be shallower than the CDP-generated isotherm in orogenic domains (Section 3.2.2), and deeper in cratonic domains by +/- 10 km. This domain variance may be due to underestimated subsurface temperatures, oversimplified assumptions of radioactive heat production in continental margins by LithoRef18, or unrealistic CDP estimates in thick lithospheric regions by EMAG2 (Ball et al., 2024). Discrepancies between the 450°C

isotherm from LithoRef18 and CDP mapping highlight the challenge of constraining high-temperature isotherms at inaccessible depths with little to no direct measurements. LithoRef18 also assumes conductive heat transfer, but some regions of the crust within 5 – 8 km depth exhibit transient or advective heat transport related to magma transport through fractures or highly permeable zones. Ball et al. (2024) incorporated data from hydrothermal proxies to more accurately model regions of advective heat flow, a strategy that can be adopted by future studies that use LithoRef18. Model improvements are required to incorporate more complex, realistic assumptions of lithospheric/crustal heat transfer properties until both LithoRef18 and CDP model converge.

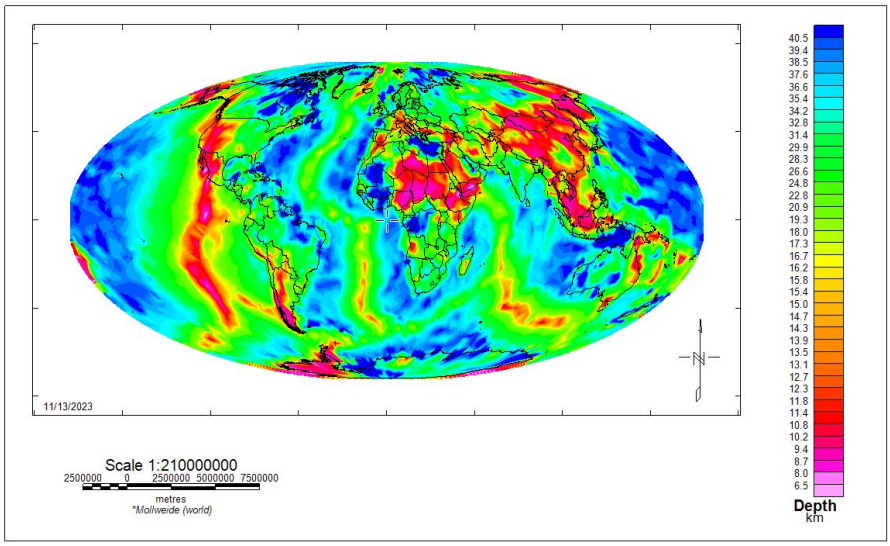

Figure 4: LithoRef18 computed 450°C isotherm calculated, Mollweide Projection. This is the first global representation of the 450°C steady-state conductive isotherm (Ball et al., 2024)

Gaps:

- The LithoRef18-generated 450°C isotherm tends to be shallower than the CDP generated isotherm in orogenic domains, and deeper in cratonic domains by +/- 10 km. This may be due to underestimated subsurface temperatures, oversimplified assumptions of radioactive heat production in continental margins by LithoRef18, and unrealistic CDP estimates in thick lithospheric regions.
- The 2°-x 2° (correlating to 230 x 230 km) discretization resolves first-order, lithospheric scale temperature variations, but is too coarse to capture short-wavelength geothermal anomalies.
- The depth uncertainties of the 450°C isotherm are 20% for the LithoRef18. Accuracy may be improved by incorporating detailed thermophysical parameters in the crust and modelling advective heat transfer.
- LithoRef18 assumes conductive heat transfer, which does not apply to advective thermal diffusion found in magmatic regimes.
- While models provide valuable insight into the heat flow dynamics of large-scale geological provinces that can assist in the decision on where SHR geothermal projects should be developed, models are not datasets. The propagating effects of modelling assumptions, data

processing, and data scarcity may lead to a high margin of error.

Current technology:

- LithoRef18 is a 2° x 2° resolution lithospheric model (correlating to 230 x 230 km) produced by the joint inversion of 3D density, elevation, seismic velocity, thermal conductivity, and petrological data from the upper mantle and lithosphere.
- LithoRef18 can be used to estimate heat transfer properties of the lithosphere and shallow crust that have been shown to correlate well with surface heat flow maps. Depths to specific isotherms (such as the SHR temperature threshold of 375°C) can be estimated with LithoRef18.
- The model assumes that steady-state conductive heat transfer and lithospheric thickness are the primary control of geothermal heat flow, which is not valid for some magmatic provinces or regions with high thermal diffusion rates.

Technology/approach needed to develop SHR:

- Increased detail for domains that do not exhibit steady-state heat transfer, such as rift systems, volcanic margins, and hot spots, should be adopted by the LithroRef18 model. This could involve a weighting scheme that adjusts heat transfer controls depending on the geological domain, rather than assuming lithospheric thickness to be the primary control. Experts are needed to deliberate what alternative lithospheric-scale controls on heat transfer should be integrated into the model.
- Increasing the LithoRef18 resolution from 2° x 2° gridding would more effectively capture high heat flow anomalies. This may require intensive acquisition of global-scale geophysical datasets to increase data density, requiring substantial time, financial investment, and expert capacity. The authors of LithoRef18 must be consulted on missing data, followed by an audit of global datasets that could fill identified data gaps. Alternatively, to improve the resolution of high-temperature anomalies in active geothermal areas, integrating geothermal proxies into LithoRef18, as demonstrated by Ball et al. (2024), may provide a near-term solution to the low resolution of these domains.

3.2.2 Curie depth point mapping

The Curie depth point (CDP), approximately 580° C, is where pure magnetite loses its permanent magnetic properties and changes from a ferromagnetic to a paramagnetic phase, which can be used to estimate the depth to supercritical temperatures (Telford et al., 1990; Langel & Hinze, 1998; Fuchs et al. 2023; Li et al., 2017). CDP estimation is performed with the spectral analysis and inversion of magnetic anomaly data. Nunez-Demarco (2020) discusses various published spectral analysis methods, including their strengths and limitations. CDP mapping is commonly performed with EMAG2, EMAG2v3, or satellite lithospheric model (LCS-1). EMAG-2 assumes CDP to be at 550°C and uses the Earth Magnetic Anomaly grid at 2-arc-minute resolution at three different window sizes (98.8 km2, 195.0 km2 and 296.4 km2) that offer increasingly deeper but coarser depth resolution (Li et al., 2017).

Surface heat flow data from the IHFC and CDP-generated models shows a strong correlation in regions with elevated surface heat flow data and shallow CDP. Discrepancies are observed in craton or shield

domains from heat flow data, possibly due to thermal perturbations in the asthenosphere that have not breached the surface (Li et al., 2017). Uncertainties in CDP estimation can be +/-30 km in depth, thus it does not apply to inferring local or near-surface heat flow as it is too coarse to map short-wavelength thermal features. CDP mapping better serves to constrain crustal geometry to inform surface heat flow estimates, which must be validated with borehole temperature data (Mather & Fullea, 2019).

Furthermore, while the CDP temperature is generally assumed to be 580°C, the true CDP threshold depends on crustal composition. For example, the Curie point is 580° C for pure magnetite, 300° C for titanium magnetite, and 620-1,100°C for Fe-Co-No alloys (Elbarbary et al., 2022; Nunez-Demarco et al., 2020). CDP can also be misestimated due to a decrease in magnetic content as a result of non-magnetic mantle material mixing with the asthenosphere, creating the same magnetic signature as demagnetization. In other cases, the upper mantle can influence the geomagnetic field in rift zones or can cause a sharp rise in magnetic susceptibility due to the phase transition from ferro- to paramagnetic states, which may complicate the correlation of magnetic horizons with the CDP isotherm (Nunez-Demarco et al., 2020). This demonstrates that the assumptions used for CDP mapping may result in inaccuracies depending on mantle dynamics, which must be considered when applied for SHR resource characterization.

Gaps:

- CDP estimates often incur uncertainties of +/-30 km, and generally only capture the heat flow regime at the 100's of km scale.
- The CDP is highly dependent on crustal composition and heat flow characteristics, which are not captured by standard CDP mapping techniques that tend to assume a constant CDP temperature. For example, EMAG-2 assumes that the global CDP is constant, and 550°C, which may be invalid in some regions.
- Heat flow values sourced from the International Heat Flow Commission are averaged per 1° (~100 km) cell and cross-referenced with EMAG-2 generated CDP values. Discrepancies are observed, particularly in cratons or shield provinces. Further study to improve CDP in thick lithospheric settings is needed.

Current technology:

- Several algorithms that analyze spectral signatures of magnetic anomaly maps can be used to estimate CDP or DBMS, such as EMAG2 and LCS-1. These thermophysical horizons can be better estimated if the dominant magnetic mineralogy in the crust is known.
- CDP mapping can be used to infer high-temperature isotherms in the crust. However, assumptions in thermal conductivity, crustal composition, and spectral analysis may yield inaccurate CDP estimations.

Technology/approach needed to develop SHR:

- CDP mapping offers insight into lithospheric scale thermal dynamics; however, significant discrepancies exist between highly robust (although imperfect) lithospheric scale heat modelling techniques. Incorporating more thermophysical parameters into CDP modelling, such as crustal composition and lithospheric thickness, may improve the convergence of crustal-scale heat models.

- Further work must be done to examine the spectral analysis of magnetic anomalies in different geological settings, guided by the work done by Nunez-Demarco (2020).

3.2.3 Surface heat flow mapping

Surface heat flow (SHF) measurements measure the diffusion rate of the Earth's internal heat through its surface. SHF can be used to infer temperature and heat flux at depth using Fourier's Law, which relates vertical thermal gradients to the thermal conductivity properties of the crust (Li et al., 2017; Lucazeau, 2019; Batir & Richards, 2022). Heat flow density models typically assume steady-state conductive heat transfer and an equilibrated vertical temperature profile, which does not accurately represent convective heat transfer mechanisms associated with magmatic domains (Fuchs et al., 2023; Li et al., 2017). Mantle dynamics are considered the primary control of geothermal heat flow at depth, while surficial geodynamic processes such as sedimentation, erosion, or climate may also influence SHF measures (Fuchs et al., 2023). Continental heat flow values and thermophysical properties are sampled from hydrocarbon and mining well logs (Section 4.1). In marine settings, heat flow is measured with shallow temperature probes, or short probes mounted on submarine engines for mid-ocean ridges (Lucazeau, 2019; Fuchs et al., 2023). Commonly referenced SHF data repositories include the International Heat Flow Commission Global Heat Flow Database (IHFC-GHFD) (Figure 5) and the New Global Heat Flow (NGHF) (Lucazeau, 2019). Refer to Section 2.2.4 for more SHF repositories. NGHF is used as an example of how global heat flow maps are compiled. NGHF was selected as the heat flow map incorporated into the frontier geothermal exploration de-risking initiative, GeoMap™.

The NGHF is discretized into a 0.5° x 0.5° grid (approximately 55 km x 55 km) and relies primarily on direct thermal measurements from exploration wells to derive heat flow on land. Lucazeau (2019) uses a statistical similarity method to incorporate lithological proxies and literature data to supplement regions without consistent data coverage. The similarity method ties cells without SHF data to cells with SHF data with data that share the same age class, topography, distance to a geological feature with a known heat threshold (such as rifts, volcanic zones, orogens, and cratons), Curie point depth, lithospheric thickness, seismic tomography, or free air anomalies. Seafloor age can be used to derive heat flow in oceanic areas with sparse data coverage. Heat flow in continents is not derivable from the tectono-thermal age of the geological province, apart from Archean or Quaternary domains, and continental rifts that resemble the heat flow-age relationship observed in oceanic crust. The NGHF global model has a misfit of observed and predicted heat flow values of 7 mWm-2, equating to an RMS of 6%.

Global SHF data has been collected over 40 years, and some archival data has uncertain data quality and/or little metadata to indicate sampling conditions. Lucazeau (2019) categorized NGHF data quality based on data variability, with a variation of <10% considered very good and datum with a variation >30% as unusable. Fuchs et al. (2023) implemented a data quality assessment scheme for the IHFC-GHFD by ranking data based on 1) numerical uncertainty; 2) a rating of data sampling methods; and 3) in situ temperature perturbations from drilling (Section 4.1). The Fuchs et al. (2023) method requires metadata on the downhole conditions when heat flow data was sampled, such as the depth interval, the time interval between drilling operations and temperature data acquisition, the techniques used for sampling, hydraulic state and other perturbing effects.

While SHF data are a useful metric for constraining near-surface thermal properties, they may not accurately represent temperature profiles at depth. High surface heat flow collected in sedimentary basins may lead to an overestimated geothermal gradient at depth, as sedimentary cover with low thermal conductivity acts as a thermal blanket relative to crystalline basement (Grasby et al., 2011). Misestimated geothermal gradients due to this thermal blanketing effect were encountered at Utah FORGE (Allis et al., 2016). The methods described by Batir & Richards (2022) (discussed in Section 4.1) demonstrate that the SMU continental scale heat flow estimates incorrectly represent true subsurface heat flow conditions by up to 40%, or +-50°C in temperature error.

Further limitations in using SHF measurements to derive thermal properties at depth were best stated by Ball et al. (2024): "It is important to remember that the difference between calculated heat flow and the measured heat flow is a convolution of a set of possible solutions: 1) error in reported heat flow measurement; 2) hydrothermal activity; 3) shallow magmatic activity; 4) natural variations in assumed U, Th, K of rocks; 5) variations in assumed thermal conductivities of rocks; 6) errors in assumed lithospheric structure; 7) thermal perturbation or intrusions that are below resolution of the model; 8) the model does not correct for transient thermal effects due to sedimentary loading in basins; 9) gridding artefacts; 10) Errors in the IHFC global heat flow database, which is still limited in its data acquisition and density, and itself may also be subject to errors in temperature reading and quality; 11) gaps in the difference model represent areas with no data."

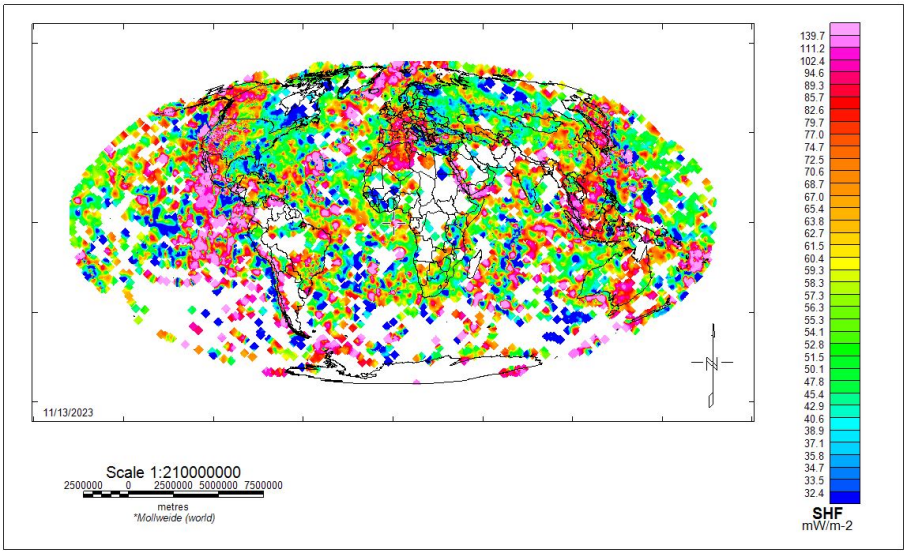

Figure 5: Measured surface heat flow from the IHFC GHFD after Fuchs et al. (2023), revealing the global distribution of surface heat flow measurements and range of surface heat flows (Ball et al., 2024).

Gaps:

- Surface thermal heat flow measurements describe the thermal conductivity of the shallowest strata. Therefore, misestimation of the geothermal gradient at depth may occur with surface heat flow measurements, in some cases to the order of 40%.

- Heat flow density modelling typically assumes steady-state conductive heat transfer and equilibrated vertical temperature profiles which may not be representative of each geological domain or region.
- There is inconsistent coverage of high-quality, high-spatial-resolution surface heat flow data. Increasing global coverage and precision of surface heat flow will improve model confidence when modelling heat flow at depth based on surface heat flow.

Current technology:

- Several extensive databases of global heat flow values exist, with robust ranking systems of data quality. They include (but are not limited to) the International Heat Flow Commission Global Heat Flow Database (IHFC-GHFD), the New Global Heat Flow (NGHF) (Lucazeau, 2019), and the SMU 2011 Geothermal Laboratory Heat Flow Map for the Conterminous USA (Blackwell et al 2011).
- Regions with high data density are where extensive exploration drilling has occurred. Methods to interpolate heat flow estimates in regions with data scarcity have been implemented, such as through the techniques described in Lucazeau (2019).
- Surface heat flow measures are generally representative of subsurface heat dynamics at a crustal-scale, and are thus an important parameter for the preliminary characterization of SHR sites, especially when integrated into more robust temperature-depth modelling schemes as described in the prior section.

Technology/approach needed to develop SHR:

- To improve temperature-at-depth estimation with SHF measurements, existing data gaps must be closed with high-density sampling. Regions that invalidate assumptions such as steady-state conductive heat transfer should be prioritized.
- Surface heat flow data repositories require extensive maintenance to ensure robust metadata and quality control. Sufficient funds should be allocated to departments conducting this pivotal research, as surface heat flow data are continuously acquired for SHR research.

3.2.4 Stanford Thermal Model

The recently released Stanford Thermal Model (STM) uses a machine learning algorithm (Section 2.2.1.2) to predict temperatures at depth, petrological thermal conductivity properties, and surface heat flow values for the contiguous USA (Aljubran & Horne, 2024). Inputs into the program include (but are not limited to) 1) >400,000 bottom-hole temperatures, 2) elevation models, 3) sediment thickness maps, 4) gravity and magnetic anomaly data, 5) gamma-ray flux of radioactive elements, 6) electrical resistivity models, 7) seismic velocity models, and 8) fault and volcano distribution. STM resolves thermal properties from 0-7 km depth at 1 km vertical intervals with a spatial resolution of 18 km2, and a temperature prediction accuracy of 6.4° C when evaluated against 40,000 non-incorporated bottom hole measurements. Datasets were upscaled or downscaled to a uniform spatial resolution of 18 km2 due to inconsistent sample densities across datasets. Heat dissipation is modelled with Fourier's law of

heat conduction with a 0.7 m/Wm2 absolute error floor. The average STM model uncertainty is 9.6% (Aljubran & Horne, 2024).

Once the thermal models (Figure 6) were produced, further analysis was conducted to evaluate which data inputs governed results for the temperature-at-depth predictions. Raw and inferred seismic features at crustal to mantle depths (20, 40 and 60 km) were particularly relevant for thermal quantity estimates, and electrical conductivity models were the most positively correlated with the heat flow maps. High concentrations of thorium radiation were correlated to regions of elevated heat flow and fault distribution, which act as channels of convective heat flow. Normalized P-wave velocities were strong indicators of decreasing temperature-at-depth, a result of increased rock rigidity and bulk modulus in higher-temperature rocks. Conversely, compressional wave velocities were inversely correlated to thermal conductivity due to increased porosity and decreased thermal conductivity (Aljubran & Horne, 2024).

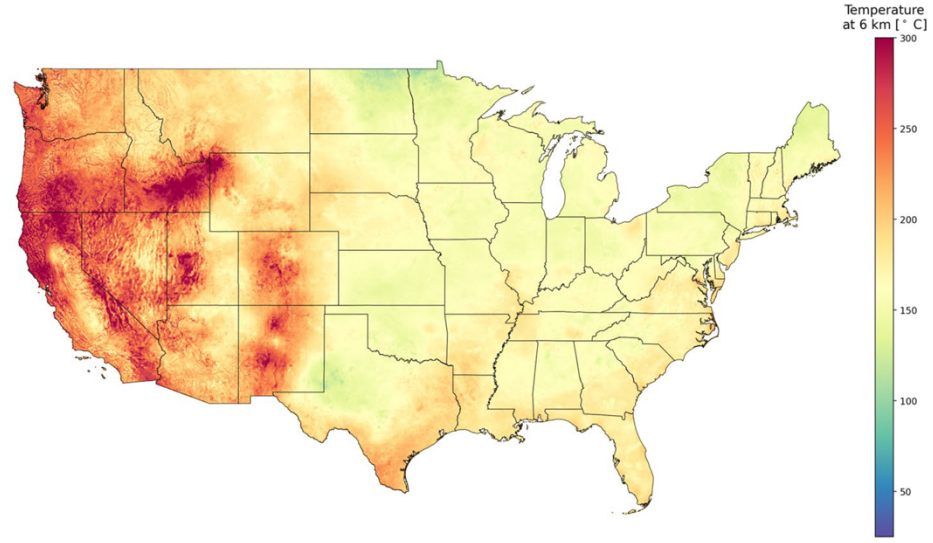

Fig. 28 Predicted temperature-at-depth map at a depth of 6 km

Figure 6: The predicted temperature at 6 km depth derived from the STM model (Aljubran & Horne, 2024)

Gaps:

- The STM should be expanded worldwide to improve global prospects in SHR project development. However, data scarcity may reduce the predictive accuracy of the thermal model when compared to those generated for the contiguous USA.
- The STM model is limited to the top 7 km of the crust. This is adequate for SHR prospecting today, but depths up to 20 km should be pursued as SHR geothermal technologies advance into deeper regimes.
- Assumptions within the model may lead to misrepresentation of heat flow at depth. Specific assumptions include Fourier's law of conductive heat transfer, which does not incorporate convective heat transfer mechanisms.
- Short-wavelength heat flow anomalies are not reliably resolved by STM such as the Socorro Magma Body (NM), Pahvant Butte (UT), and Blackfoot Volcanics (ID).

Current technology:

- STM is a new product that accurately maps temperature within 7 km depth across the contiguous USA, with an average uncertainty of 9.6% and a temperature prediction accuracy of 6.4°C.
- Integrated datasets include >400,000 well temperature and thermal conductivity measurements, elevation, sediment thickness, gravity and magnetic anomalies, gamma-ray flux of radioactive elements, electrical resistivity, seismicity, and fault and volcano distribution.
- Thermal diffusion is modelled using Fourier's Law, assuming steady-state thermal diffusion.

Technology/approach needed to develop SHR:

- Non-steady-state thermal diffusion is not modelled by STM. As suggested for LithoRef18, the representation of non-steady-state heat transfer regimes may be incorporated into STM by integrating geothermal proxies into the model, as demonstrated by Ball et al. (2024).
- The STM model should be expanded to a global scale, a major undertaking that will require significant support for the program authors using academic funding. It will also require a thorough audit of global datasets to integrate into the model that matches their current data density.
- Regions lacking adequate data should be identified and prioritized for future data acquisition initiatives. The researchers involved in GeoMapTM should be consulted as they are also striving to close global geophysical data gaps.

3.3. Stress/deformation regime

Understanding the initial stress field is crucial for designing drilling and permeability enhancement strategies. In order to create and maintain open hydrofractures, the hydrofractures should be oriented perpendicular to the least principal stress, which injected fluid pressure must exceed. Hydroshear can also be used to open existing fractures, but requires detailed knowledge of the local stress field as well as natural fracture properties. The stress field is influenced by the natural state of stress in the crust including the weight of overburden due to topography and tectonic forces, which vary regionally, locally, and with depth (Stephansson & Zang, 2014; Zang & Stephansson, 2009). Therefore, measurement of *in situ* stress and other constraints on different stress fields across regions are a key initial consideration for exploration of potential SHR resources.

The world stress map, continually refined over the last 40 years, displays the best estimated stress orientations and tectonic regimes across the globe (Heidbach et al., 2018). It is determined based on a comprehensive database that compiles information on the present-day crustal stress field including earthquake focal mechanism, borehole data (e.g., borehole breakouts, drilling-induced tensile fractures), *in situ* stress measurements (e.g., over coring and hydraulic fracturing), and surface geological structure (e.g., lineament, fault slip, volcanic axis) for indicators of stress direction. Through data integration and a quality ranking scheme, the stress data on a global scale is obtained and weighted based on the distance of the grid point to existing data and data quality.

Although data are continually added and some regions (such as Australia) have greatly improved in recent additions, there are still large parts of the world (Africa, central Asia, most of South America) with limited data due to limited seismicity or seismic network completeness and prohibitive drilling costs, requiring extrapolation over very large distances. Recent approaches in joint inversion, seismic anisotropy, and geodesy can reduce uncertainty in the orientation and magnitude of principal tectonic stresses in these regions (Coblentz et al., 2024).

To further refine the stress map (e.g, the stress field at a given site) in Figure 7, Stephansson & Zang (2014) suggested a new approach through the joint stress data analysis using field, borehole, and seismic-based methods (stress inversion from focal mechanisms). The methods combine available stress data from the Best Estimate Stress Model (BESM), new relevant data from Stress Measurement Methods on site (SMM), and available Integrated Stress Determination (ISD) data, in addition to numerical modelling. After all data are combined, an integrated stress analysis, including sensitivity analysis and model calibration, can be executed to estimate a final rock stress model (Figure 7c), FRSM (Stephansson & Zang, 2014).

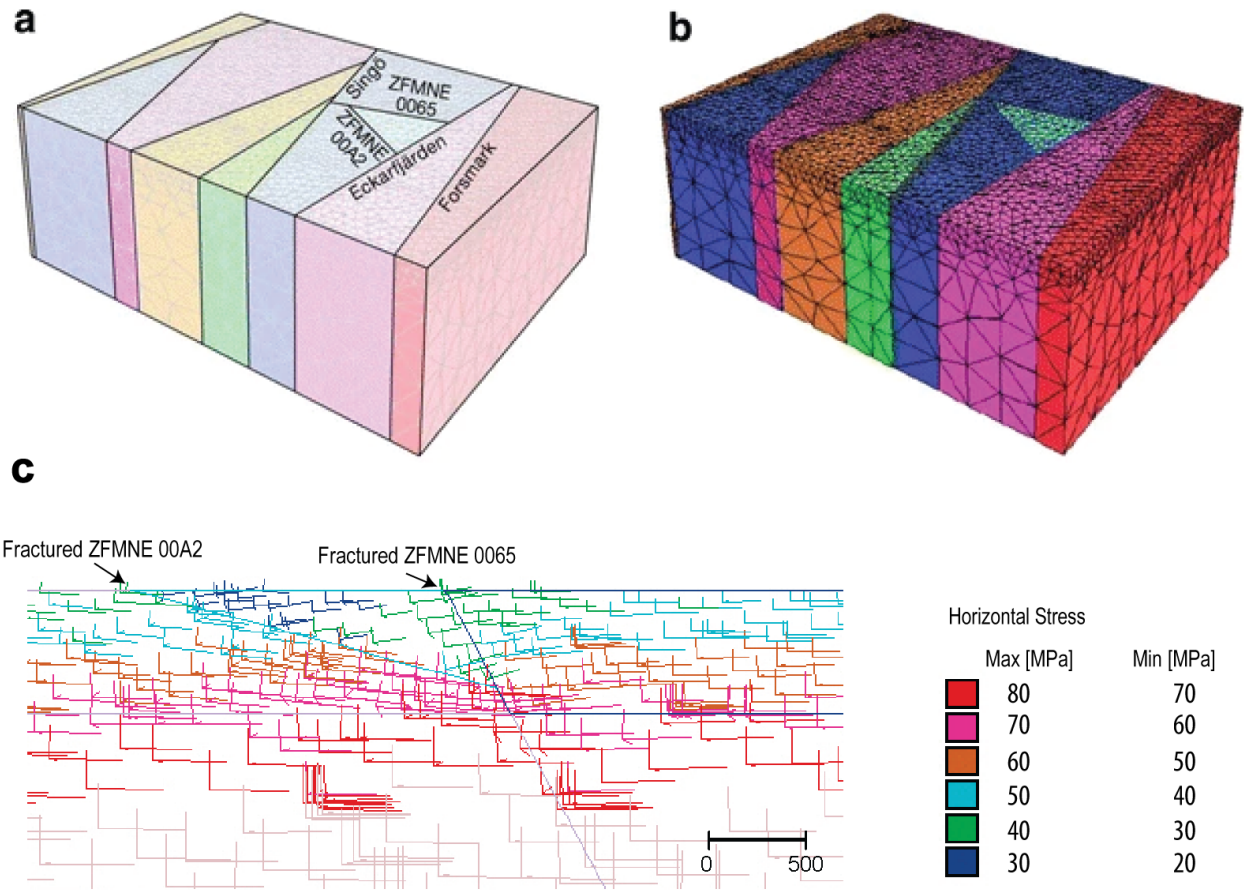

Figure 7: Numerical stress modelling with distinct element code 3DEC by Stephansson & Zang (2014): a) a model showing major fracture orientations, b) overview of 3DEC model at a site, and c) an estimated stress distribution of the orientation and magnitude of maximum and minimum principal (horizontal) stresses, after Hakami (2006).

Gaps:

- The scarcity of data and scaling effects may not accurately represent the stress state for the SHR reservoir scale. However, it is a step further to locate a promising SHR site and for identifying areas of major tectonism or high degrees of stress.

Current technology:

- Fracture due to drilling is used to determine minimum horizontal stress, which is important for a final stress model.

Technology needed to develop SHR:

- The world stress model, also known as the final rock stress model, has limited resolution. It can be further refined when a detailed study of the reservoir scale and a new dataset are obtained.
- Accurate pore pressure prediction through depth is also crucial to prevent wellbore instabilities and ensure safe and efficient drilling in SHR environments. Future research should strongly invest in accurate prediction of pore pressure distribution and *in situ* 3D rock stress model (i.e., magnitude of principle stresses, stress regimes /orientations).

3.4. Faults and other hazards

Large-scale fault mapping or monitoring is widely used in various methods, from remote sensing, to surface mapping, to deep drilling campaigns. The lineament and fault maps can be produced by remote sensing technique using ARCGIS or satellite images, geological field survey, or structural analysis (e.g., fault orientation (stereonets)), as well as by subsurface imaging such as gravity, magnetic, or seismic surveys. Active fault zones are also monitored for micro-seismicity. The International Continental Drilling Program (ICDP) and International Ocean Drilling Program (IODP) have studied the detailed deeper structure of fault behavior, for example, in the San Andreas Fault (Fulton & Saffer, 2009; Zoback et al., 2011), the Nankai trough, and the Japan trench (Tsuji et al., 2014). Despite these efforts, unmapped faults around the world routinely produce earthquakes.

Gap:

- Each method focuses on the research field or topic where large-scale faults are investigated. The resolution and results can be affected by grid survey, sparse sensor spacing, and the importance of data- and cost-based direct or indirect measurements.

Current technology:

- All the above-mentioned techniques have been combined to study large-scale or tectonic faults.

Technology/approach needed to develop SHR:

- Faults can be linked to volcanic or nonvolcanic areas. Fault monitoring by dense seismometers and accurate velocity measurement can help map the large-scale fault zone with precision. This information is important for locating safe ductile environments, without proximity to major fault zones.

4. Reservoir and validation scale (10s to 1 kilometer)

After the initial exploration stage, a location is selected for additional study. At this stage, high-resolution geophysical surveys can be undertaken to further develop a geological, conceptual model of the resource. A major goal at this stage is to identify potential drilling sites and minimize risk, as this is often one of the largest cost expenditures of the project.

Borehole exploration provides direct or *in situ* measurements of subsurface properties, which can extract core/cutting data, or run wireline logging tools while drilling, such as logs of neutron-gamma density, azimuthal density, photoelectric factor, ultrasonic caliper, elasticity, resistivity, pressure, temperature, permeability, stress, etc. To date, well-logging tools have not been fully applicable in superhot rock environments due to equipment being unable to handle high temperatures, but material development and temperature control technologies are attempting to solve these issues. The other reports in this series cover some of these efforts (Cladouhos & Callahan, 2024a; R. Pearce & Pink, 2024; Suryanarayana et al., 2024), so this section is oriented towards those measurement types that we feel are most important for SHR development: stress, temperature, fracture, and structural permeability.

4.1. Heat at depth

It is essential to precisely estimate thermal properties at depth in order to plan and de-risk an SHR geothermal project. While many of the methods described in Section 3.2 apply to reservoir-scale thermal mapping, additional strategies that rely on detailed borehole logs and geological models may enhance temperature-at-depth estimation to characterize SHR sites at the reservoir scale.

Temperature-depth (T(z)) estimations relate to lithological heat flow (Q_o), thermal conductivity (K) and heat generation (A). The petrophysical properties of core samples can be measured in laboratory facilities that measure thermal conductivity (K), thermal diffusivity (k), and heat capacity (J/kg.K) (Lachmar et al., 2019; Grasby et al., 2011; Majorowicz & Grasby, 2010; Stimac et al., 2017). When a sufficient distribution of exploration boreholes exists, thermal property measurements can be used to interpolate isotherms at varying depths. Where borehole data does not exist, literature on thermal conductivity values from geological proxies can be incorporated into regional heat flow models, supplemented by geophysical information such as mantle seismic velocity, crustal geodynamics, and geological maps (Aghahosseini, 2020; Marjorwicz & Grasby, 2010; Batir & Richards, 2022).

Downhole temperatures can be measured with wire-line tools and probes that come in direct contact with the borehole wall, thermometers mounted on drill strings, microcomputers that measure the temporal flux of temperature, and distributed temperature sensor (DTS) optical fibres that measure temperature distributed throughout a borehole (Fuchs et al., 2023). The disturbance of in situ borehole conditions due to drilling must be considered when sampling temperature at depth, and measurements should only be taken after 10-20x the time spent drilling and circulating fluid to let the well equilibrate (Fuchs et al., 2023; Batir & Richards, 2022; Blackwell et al. 2011; Shi et al., 2021). These tools must be adapted to be rated for SHR conditions, although some are nearing that threshold, such as the Kuster

temperature mechanical gauge, which features a 360°C temperature rating (Shi et al., 2021), and Sensornet DTS fibre, with a 300°C temperature rating (Khankishiyev et al., 2024).

Challenges in these techniques include: 1) downhole tools may not have temperature and pressure ratings suitable for SHR conditions; 2) thorough metadata on downhole conditions during measurement must be documented to obtain accurate temperature estimates post-temperature sampling (this is a particular concern for archival logging data); 3) thermal conductivity estimates can be measured in laboratories, but these facilities may not have adequate capacity to represent in situ conditions (Fuchs et al., 2023); 4) latency periods between drilling operations and temperature data collection is required to allow in situ borehole temperatures to equilibrate; and 5) measurements downhole may also be imperfect due to poor coupling or the presence of fluids and sediment that impair contact with the borehole. Alternative methods for estimating temperature at depth that withstand SHR temperatures and require shorter intervals between drilling and thermometry should be explored.

Where high-quality downhole temperature data exist, advanced data integration methods may significantly improve heat-at-depth estimation. Batir & Richards (2022) extrapolated temperature conditions up to 10 km depth by integrating geophysical, borehole, and petrophysical data from three counties in Texas. The extensive, densely sampled heat flow data from hydrocarbon exploration wells were supplied by the National Geothermal Data System SMU node (NGDS, 2020). Additional model inputs included 1) a steady-state assumption of heat diffusion and radiogenic heat production; 2) direct measurements of thermal conductivity and geothermal gradient to calculate heat flow; and 3) true data on sediment thickness and basement properties that were compiled into detailed stratigraphic columns with scaled thermal conductivity values. They also included crustal thickness and radiogenic flux models produced from geophysical data analyzed with the techniques described by Agrawal et al. (2015).

The regional-scale temperature-at-depth results were similar to the continental-scale SMU 2011 maps; however, discrepancies were observed, particularly in areas with high data density. A notable difference is that the heat flow estimates from the Batir & Richards (2022) study are 30-40% higher than the temperature estimates produced by the 2011 SMU estimates. This equates to a 25-50°C increase in temperature estimates at 3.5 km, and 50-100°C higher at 6.5 km, relative to the 2011 SMU estimates – overall, temperatures were 50% higher than the SMU results. The improved accuracy in these results is attributed to 13-30% higher geothermal gradient and thermal conductivity estimates, as well as the inclusion of directly sampled sedimentary and basement radiogenic heat diffusion. This reiterates the importance of data density when constraining heat flow properties at depth. Temperature estimates deeper than 5 km have errors of +/- 25% due to a lack of direct borehole temperature and thermal conductivity measurements. A strong correlation between radiogenic heat production and high geothermal gradient was also observed by Elbarbary et al. (2022) in a study that used CDP estimates and heat flow samples to map the thermal structure of Africa. The methods described by Kirkby et al. (2024) to estimate crustal thermal conductivity and heat generation at depth using crustal composition should be applied and validated in future thermal modelling studies.

Gaps:

- Sparse or incomplete datasets may cause misestimation of heat flow at depth. Where data are not available, statistical methods described by Aghahosseini (2020), Fuchs et al. (2023) and Lucazeau (2019) can be used to estimate regional to large-scale heat flow trends with the highest possible accuracy.
- Measuring thermal conductivity requires laboratory processing of collected borehole samples, but some facilities may not have the capacity to simulate *in situ* pressures and temperatures.
- Downhole measurements may be imperfect due to poor coupling or the presence of fluids and sediment that impair contact with the borehole.

Current technology:

- Tools to measure downhole conditions such as temperature and thermal conductivity are an industry standard, but conditions during measurement must be adequately documented to reduce error from disturbance of downhole conditions through drilling or poor rock contact.
- The inclusion of additional data such as radiogenic heat flux, basement heat transfer properties and thermal conductivity properties from stratigraphic logs has been shown to drastically improve heat flow estimates at depth – to the order of +/-50°C (50%) in some cases.

Technology/approach needed to develop SHR:

- Improved downhole tools that can sample temperature and thermal conductivity properties must be designed to rapidly survey boreholes at SHR temperatures.
- Further work constraining radiogenic heat flow in the basement must be conducted, as this is a primary control on heat flow but is often oversimplified in heat flow modelling.

4.2 Stress and pore pressure at depth

The regional and local 3D stress fields—amplitude and orientation—must be quantified to optimize reservoir engineering (see Section 3.3). Stress measurements can be performed with borehole breakouts analysis and core-based methods. Principal (vertical) stress or overburden pressure can be estimated by multiplying rock density, gravity, and rock thickness. Accurate estimates require understanding the variation of rock stress states, including minimum and maximum principal (horizontal) stresses. These measurements inform the drilling program; for example, drilling conditions should ideally orient the drill hole to avoid alignment perpendicular to the maximum horizontal stress (Zang & Stephansson, 2009). Failure to do so may result in drilling complications, drilling failure, compromised well stability, poor fracture connectivity, or challenges during well completion.

Another crucial parameter to estimate is the pore fluid pressure during drilling. Although many SHR projects target areas with very low permeability, formations above the target reservoir may have variable pore pressure, which require adjustments to the drilling fluid pressure as they are drilled. If pore pressure is not properly predicted—for example, if mud/fluid drilling pressure is higher than pore pressure—the contrast in pore fluid pressures can result in induced fractures (e.g., fracture pressure), mud loss, or well instability (Zhang, 2011). Conversely, if the mud weight pressure is lower than the normal or hydrostatic pore pressure of subsurface formations, formation fluids can flow into the wellbore, causing drilling kicks and wellbore instability. Improper measurement or prediction of pore

fluid pressure at any depth can lead to well instability, affect drilling fluid design, and result in unsafe and inefficient operations.

Pore pressure can be predicted based on petroleum industry practices—for example, Eaton's method (Zhang, 2011). A significant study on pore fluid pressure was conducted in the St. Gallen Geothermal field (Switzerland) using 1) earthquake hypocenters and earthquake focal mechanisms to estimate stress patterns, and 2) slip vectors for predicting excess pore fluid pressure (De Matteis et al., 2024). While this method focuses on how excess pore fluid pressure causes earthquakes or occurs during fluid injection, applying it in other geothermal fields may predict pore fluid pressure for SHR development, extraction, and monitoring.

Anisotropy of geophysical properties also provides important information about the orientation of stress and structures in the subsurface. A local (10 km x 10 km) case study of seismic anisotropy was conducted in the potential SHR reservoir at Kuju volcano, Japan. Surface wave methods were used to identify cold and faulted/fractured regions (high anisotropic structure in low-velocity zones), while areas were targeted with high velocity and high anisotropy or low anisotropy, although these interpretations also depend on the litho-strata of the ductile subsurface (Chhun et al., 2024).

Gaps:

- Most logging tools can currently withstand a temperature of less than 250°C.
- Well logs are direct tools attached to the well bore, which can be influenced by casing or borehole breakout (e.g., fracture induced by drilling) or mud invasion. Therefore, the stress measurement to control log pressure versus the ambient pressure field needs to be balanced.

Current technology:

- All techniques have been used in exploration and reservoir extraction.

Technology needed to develop SHR:

- Tools must be improved for use in superhot rock conditions (see ongoing efforts detailed in Cladouhos & Callahan, 2024a; Pearce & Pink, 2024; Petty et al., 2020; Suryanarayana et al., 2024).

4.3. Structures and permeability

Geophysical and geological mapping of structures (faults, intrusions, dikes, basement depth) is a key input to conceptual models that inform many aspects of design and decision-making, including drilling and stimulation plans. The joint interpretation/inversion of varied datasets gives more confidence in the interpretation of the heat, stress, and permeability of the reservoir. In this section we focus on detailed downhole methods for mapping permeability, which is assumed to be dominated by fractures and faults in geothermal settings.

Borehole televiewer and formation micro-imager, which depend on acoustic waves or electrical pulses to scan the borehole walls, are techniques that provide a high-resolution structure of the borehole surface. They are useful for characterizing subsurface properties such as litho-strata, rock features, fracture direction, fracture density, intensity, and aperture.

Fracture seismic imaging based on micro-seismic events is a technique focusing on imaging fractures around the borehole. It involves passive seismic data and seismic reflection processing schemes to map fracture or connected flow pathways. Fracture growth or fluid-filled fractures can provide the source of pulses in the frequency band of 1 to 100Hz (Sicking & Malin, 2019). The key processing steps of fracture seismic imaging include removing cultural and industrial noises, applying elevation correction and residual statics, velocity model analysis, and one-way travel-time depth migration for a continuous signal source, then stacking and applying amplitude analysis to obtain fracture intensity maps (Malin et al., 2020; Sicking & Malin, 2019).

Becker et al. (2020) conducted a study on mapping reservoir fractures and permeability at the Mirror Lake Fractured Rock Hydrology site in New Hampshire. They used DAS as a distributed hydraulic sensor in both field and laboratory experiments. DAS was deployed along boreholes within two crystalline rock intervals (e.g., granitoids intruding the pelitic schist country rock) and validated through laboratory analysis. The DAS instruments in boreholes FSE9 and FSE10 measured oscillating strain responses from hydraulically active areas, induced by stimulation in well FSE6. This stimulation involved alternating injection and pumping, generating either periodic step or approximately sinusoidal hydraulic signals. These signals induced periodic strain in the formation, which was recorded for DAS displacement amplitude analysis. The study confirmed that their tests were highly sensitive to hydraulic strain signals, detecting hydraulic displacements as small as 1 nm. However, further research is needed to directly convert the displacement amplitudes into hydraulic stress or permeability. DAS is a promising technology for SHR reservoirs but also relies on developing and testing fiber optic cables that can withstand SHR conditions.

Gaps:

- Passive geophone/seismometers can capture unwanted signals, not only fractures around the boreholes but also from various types of noise such as environmental and equipment noises.
- Heterogeneity in the geothermal/SHR subsurface can cause seismic wave scattering or attenuation, affecting fracture resolution.
- The fracture intensity map/interpretation can be derived from amplitude artifacts and distortions.

Current technology:

- Multiple component sensors and high-density sampling recordings (e.g., DAS) have been developed for detailed fluid-filled fracture imaging

Technology needed to develop SHR:

- Advanced processing techniques and high temperature sensors for SHR regions in boreholes are needed to record signals.
- Long recording and integrating techniques with a full waveform inversion can improve the results. However, advanced data processing, noise filtering, or new algorithms/methods are needed to remove amplitude artifacts and enhance signals for velocity analysis or seismic attribute analysis (e.g., fracture intensity maps).
- The current techniques focused on active fracture zones are not applicable to SHR conditions.

5. Monitoring

Characterization efforts and conceptual model development offer a baseline understanding of reservoir changes as a result of stimulation and production. Ongoing characterization throughout the project life cycle is key for monitoring reservoir changes and guiding development decision-making. These activities are important for managing conventional geothermal reservoirs, but to this point there is limited relevant experience with longer-term management of EGS reservoirs and none in SHR reservoirs (to be economically viable energy production should continue for at least 20 years).

5.1 Induced seismicity mitigation

Seismicity can be caused by natural factors (i.e., cracks, volcanic inflation or deflation, and the ambient stress field resulting in pore pressurization, which can move and activate seismogenic fracture slip). It can also be caused by changes in the pore fluid pressure of the subsurface, such as due to fluid injection/production in oil and gas producing fields and geothermal power plants, which is known as *induced seismicity.* Induced seismicity is a necessary outcome of fluid injection in the subsurface (and provides invaluable data on reservoir properties and the location of engineering activities outcomes), but the maximum magnitude of events must be mitigated to avoid damage to infrastructure and push-back from the local community. There are a few infamous cases (e.g., Basal, Switzerland, and Pohang, Korea) where projects have been shut down due to damaging induced events.

Commonly, seismicity detection and location are based on the distribution of seismometers, depending on the arrival of the P-wave and S-wave of the seismicity event. Earthquake epicenters can be determined based on the arrival time difference recorded by multiple seismometers (Maurer et al., 2020) or using machine learning algorithms (Mousavi et al., 2020). Using the travel time difference and velocity of the P wave or S wave, the hypocenter of seismicity can be estimated (e.g., hypo inverse). Therefore, accurate velocity models are important to reduce the uncertainty in location estimates.

In the Geysers geothermal-producing field, seismic detection has been conducted using 45 seismometers from LBNL, USGS, and Calpine, covering an area of 20 x 25 sq km (Hartline, 2024; Kwiatek et al., 2015). Hartline et al. (2024) conducted a seismicity event analysis in this field, and they found that the clusters of seismicity patterns resulted from natural fluid flow paths, EGS, or long-term steam production (~330 wells) and water injection (~50 wells) within the reservoir compartments. Notably, this seismicity result was later combined with well data (e.g., lithology, temperature, permeability), heat flow, and surface structural maps to build a 3D structural model. This model was used for interpreting the plutonic structure complex related to the heat source, flow pathways, fault planes, and geothermal reservoir boundaries.

In the same study area, Kwiatek et al. (2015) specifically studied the induced seismicity effects from long-term fluid injection wells over 7 years. The two wells, namely Prati-9 and Prati-29, are a few hundred meters apart and at a depth of 1.5-2.5 km below sea level in the northwest part of the field. They estimated seismicity (1776 events) and source attributes by adopting the relocated Hypoinverse 1D and USGS FORTRAN computer program for calculating and displaying earthquake fault-plane

solutions (Reasenberg and Oppenheimer, 1986). As a result, they found spatiotemporal seismic clouds close to these injection wells, clearly indicated and induced by pore pressure increase along with thermal water expansion from fluid injection and migration into greater depths (Kwiatek et al., 2015; Leptokaropoulos et al., 2018). They also suggested that this can be attributed to seasonal changes in injection rates.

The protocol to reduce induced seismicity (termed adaptative traffic light system, ATLS) includes continuous seismic monitoring, limiting the frequency and magnitude of events by controlling water injection rate and pressure for reservoir fracture enhancement (Calpine, 2022). The seismicity in this region has been reported to be under control (not exceeding 3.0 Mw), and the company has continued working with DOE to improve seismicity detection, site characterization, and risk-based decision-making by adopting a probabilistic seismic hazard/risk method coupled with a physics-based approach. The Geysers was the first geothermal site to employ an ATLS for induced seismicity mitigation, but there has since been numerous studies of induced seismicity derived from geothermal fluid stimulation/extraction and mitigation efforts, including in Korea (e.g., Kim et al., 2018, 2022), France (e.g., Maurer et al., 2020), Germany (e.g., Bruhn et al., 2011), Switzerland (e.g., De Matteis et al., 2024; Kraft et al., 2020; Wiemer et al., 2017), and Finland (e.g., Eulenfeld et al., 2023; Kwiatek et al., 2019).

Gaps:

- Improved understanding of induced seismicity hazard in ductile rock.

Current technology:

- By adjusting injection and stimulation parameters (Bromley, 2020), the level of seismicity can be controlled (e.g., a modified traffic-light approach for adaptive response of seismicity levels).
- Advanced seismic detection methods continue to be developed, for example EQ-T (Mousavi et al., 2020) is an open tool for detecting seismicity using machine learning techniques.

Technology/approach needed to develop SHR:

- One aim of developing SHR in the ductile transition is to reduce seismicity. Seismicity is expected to be minimized within the ductile transition zone; however, this is uncertain, and hazards remain due to fracture creation and the local stress field. Therefore, monitoring fluid/fracture and rock stress during injection and production is still required.

5.2. Permeability enhancement stimulation monitoring

5.2.1 Seismic monitoring

Micro-seismicity monitoring is important to detect fracture activity within the producing field (Bromley, 2020), and to trace fluid movement and fractures (Hartline, 2024). Thus, the boundary or geometry of the reservoir can be mapped using microseismic locations. In the EGS demonstration project at Newberry Volcano, fracture reservoir stimulation, production well planning, and microseismic monitoring were applied over five years (Fang et al., 2018; Cladouhos et al., 2016). Newberry Volcano is a large caldera that has been active for approximately 500,000 years. EGS stimulation technologies created a fracture network in well 29-55, located on the northwest flank of Newberry Volcano, using

hydro-shearing (multizone stimulation and thermally degradable zonal isolation material). During the first phase of EGS reservoir testing in 2012, fracture stimulation occurred at wellhead pressures of 120-167 bar, causing a micro-seismicity cloud up to 800 meters from the injection well. Micro-seismicity locations were also interpreted as being due to casing hole leakage. In 2014, 2.5 million gallons of water were injected at rates of 0.009–0.045 l/s/bar at wellhead pressures >165 bar over four weeks. During this period, 398 micro-seismic events were recorded. Fang et al. (2018) studied the microearthquake stress-drop model for mapping fracture permeability during the EGS stimulation in Newberry Volcano. They used microearthquake monitoring data to map *in situ* reservoir permeability during and after EGS hydro-shearing stimulation. By applying Oda's crack tensor theory and a cubic-law-based analog, they successfully mapped the *in situ* permeability of fractures induced by stimulation. The resulting permeability distribution maps, derived from dense micro-seismicity data, served as a crucial reference for the siting of this geothermal field development's production well.

Further work has been conducted in this site demonstration using microseismic data in conjunction with well log and moment tensor data to design an optimal well path for a second well at Newberry. The lessons learned, parameters, design of EGS reservoir stimulation, and microseismicity data are used as reference models to optimize future well targets. An advanced technique in this EGS stimulation area involves using moment tensor and microseismicity monitoring data to optimize well paths. Aguiar & Myers, (2019) employed the relative polarity method to compute focal mechanisms from microseismicity data (Fang et al., 2018). Prior to stimulation, the stress field, characterized by a normal faulting/extensional regime, exhibited a vertical maximum stress direction and a north-south maximum horizontal stress, based on regional studies and borehole breakouts. Post-stimulation, six clusters were identified: deeper parts featured east-west striking normal faults, while shallower parts exhibited strike-slip faults with east-west motion close to the top of the open hole section. Hydro-shearing fractures should have been predominantly east-west, a preferred orientation that facilitates fracture opening in the direction of least resistance, perpendicular to the minimum horizontal stress direction. However, the focal mechanism results revealed a complex orientation of faults/fractures at different depths of the open hole section. This complexity can be attributed to the quality of microseismicity data, variations in the stress field with depth, and the presence of preexisting fractures during EGS fracture stimulation.

Gaps:

- Vertical errors of seismicity derived from an inaccurate velocity model and noisy data.

Current technology:

- DAS provides a high sampling rate, but handling big data in real-time can be a challenge. Also, DAS can be easily affected by noise or unwanted signals.

Technology/approach needed to develop SHR:

- Seismicity is expected to be minimized within the ductile transition zone; however, this is uncertain, and hazards remain due to fracture creation and the local stress field. Monitoring fluid/fracture and rock stress during injection and production is still required.
- Estimating hypocenters still requires an accurate subsurface velocity model, which is challenging to map using measurements based on seismometer array tomography. Improving the velocity

model based on advanced seismic tomography and/or conducting joint analysis can reduce uncertainty. Additionally, calibrating with true velocity data from borehole sonic logs, if available in SHR regions, can further improve results.

5.2.2 Electromagnetic monitoring

Electromagnetic methods are sensitive to the electrolytic properties of fluids and their migration pathways at depth. Based on this principle, it may be possible to extend the application of EM methods to SHR reservoir monitoring, particularly for EGS-type reservoir stimulation where hot-dry rock is hydro-sheared and injected with a working fluid, causing a distinct change in its fluid content and EM resistivity properties.

A handful of studies have detected signatures of permeability enhancement and fluid migration patterns in EGS reservoirs with MT (Section 4.3.1) data that warrant further investigation. In Parlana, South Australia, an >240°C EGS reservoir at 3.6 km depth in a granitic basement was monitored with 11 broadband MT receivers pre- and post-injection over four days. Results showed a 5-10% decrease in resistivity post-injection. Also, EM signatures of fluid migration followed the strike of a fault network, indicating hydraulic connectivity. These results were well correlated with microseismic data (Peacock et al., 2012). Furthermore, at the Habanero and Parlana EGS sites, post-injection maximum phase tensor residual responses resolved that the direction of working fluid migration was perpendicular to the maximum compressive stress field, yielding insights into fracture propagation trends at depth (Balfour et al., 2015; Didana et al., 2017; Theil 2017). Similarly, in the Otway Basin, Australia, anisotropy ratios in the MT data indicated north-northwest-trending preferential permeability at depth (2.5-3.5 km), aligning with the orientations of mapped faults (Kirkby et al., 2015). This was later verified with borehole permeability measurements that correlated with the regional stress field (Thiel, 2017). As permeability and fracture connectivity at depth are difficult yet essential properties to monitor in SHR reservoirs over their life cycle, the use of MT in these applications should be further studied through robust synthetic tests or with archival datasets with coeval petrophysical data.

Despite these promising findings, the question of MT's sensitivity to small fractures remains. CSEM/CSMT (introduced in Section 4.3.2) may offer improved resolution of resistive structure in the near-surface (<3 km) due to its higher signal-to-noise ratio than classic MT (Darnet et al., 2020). The applicability of CSEM for stimulation monitoring was tested during the injection of the IDDP-2 RN-15 well in the Reykjanes Geothermal field in 2016/2017. Lower frequencies (<2 Hz) and longer transmitter-receiver offsets (>5,000 m) yielded the highest sensitivity to resistive anomalies, with a high degree of repeatability to reduce the error range to <1% required for temporal studies. Challenges included terrain that limited long-offset CSEM configurations, as well as high levels of cultural noise from the geothermal plant. Overall, while the CSEM measurements were highly repeatable, no temporal change related to the IDDP-2 stimulation was observed. Further synthetic study revealed that this is related to the volume of the stimulated area, which must be >500 m in width to be detectable by CSEM. The IDDP-2 injection occurred at a depth between 3 and 3.4 km, with 100,000 m^3 of water injected over one month. Thus, the lateral extent is likely below the detectable threshold. Borehole or even denser CSEM configurations may be required to increase sensitivity for a target of this volume (Darnet et al., 2020).

Börner et al. (2015) explored the application of downhole TEM (introduced in Section 4.3.3) for deep (>5,000 m) reservoir modelling. The simulation used a detailed geological model of a region in Germany prospected for a deep geothermal system, characterized by shales, granites, and phyllites, including *a priori* information on porosity, electrical resistivity, permeability, faults, fractures, and geological contacts. An array of three-component receivers was deployed in several borehole configurations that sampled the decay of the secondary fields generated by a transmitter. It was observed that an optimal configuration of TEM sensors can detect a >25% change in resistivity, with signal strength dependent on the resistivity of the stimulated rock and the time window during monitoring. TEM receivers deployed below 5,000 m into temperatures above 150°C would need dewar-encapsulated borehole equipment that would suffice for the few hours of sampling (Börner et al., 2015). TEM arrays should be deployed in existing borehole networks to validate this study.

Gaps:

- While MT can detect changes in bulk resistivity, changes in resistivity from stimulated reservoir fractures may be too small to detect.
- CSEM data can monitor EGS stimulation, but only if the stimulated volume is above 500 m width based on synthetic studies. This has not been verified in-field.
- TEM shows potential for deep (greater than 5,000 m) reservoir modelling in a synthetic case. This requires field testing.

Current technology:

- MT has been shown to resolve changes in EM resistivity at depth during EGS injection with adequate coverage and station repeatability. Several studies have resolved permeability and fracture connectivity properties at depth through MT data, but these observations need further validation.
- CSEM may resolve subsurface changes in resistivity due to SHR reservoir stimulation within a 3 km depth with long-offset configurations.
- Synthetic studies have been performed on the effectiveness of TEM for EGS stimulation monitoring. With an optimal array of borehole sensors, a 25% change in resistivity can be detected. This needs in-field validation and TEM sensors that can be deployed at >150°C.

Technology/approach needed to develop SHR:

- Methods for fluid migration through fracture networks reviewed by Theil (2017) should be adopted for future EM monitoring of reservoir stimulation. The findings from Peacock et al. (2012), Didana et al. (2015) and Kirkby et al. (2015) should be further validated with future or archival MT datasets at EGS geothermal plays.
- Experimentation at existing SHR or analog sites must be performed to validate the applicability of CSEM in reservoir monitoring
- Borehole TEM monitoring of EGS stimulation must be tested in-field.

5.3 Life cycle analysis: Thermal drawdown, mass balance, and fluid-rock interaction

For the upfront investment in developing a geothermal project to pay off, the reservoir must keep producing economically for a minimum of about 20 years. So, throughout this time-period, the state of the reservoir must be monitored for heat depletion, changes in permeability, and water/stream content. The production of fluid can have large effects on the reservoir state, with accompanying measurable changes in its geophysical properties. Engineering actions, such as reinjecting wastewater, can help to maintain reservoir mass balance, but effective monitoring of reservoir changes is needed to plan and optimize these actions.

Most high-enthalpy geothermal systems contain a steam cap that accumulates under the clay-rich cap rock. The extent of this steam cap can grow due to production-driven decompression boiling, and thus will be a key property for the operation and economics of a SHR project. Sánchez-Pastor et al. (2023) showed that Seismic Noise Interferometry (SNI) can effectively and economically monitor changes in the steam content during production of the Hengill geothermal field in Iceland.

To sustain reservoir longevity, both geophysical and fluid monitoring should be conducted; the cost of passive gravity and seismic measurements is inexpensive (Omollo & Nishijima, 2023; Hartline, 2024), compared to 4D seismic reflection survey monitoring. Microgravity monitoring, surface deformation, or 4D time-lapse surveys can provide insight into reservoir mass balance and help evaluate the effectiveness and efficiency of injection and production strategies. Monitoring the subsidence rate is widely used in many geothermal fields, such as the Olkaria domes (Omollo & Nishijima, 2024). In addition, numerical reservoir modelling that integrates a conceptual model, geological conditions, and geophysical properties from field and well data can predict long-term reservoir performance, such as reservoir permeability, mass flow rate, enthalpies, recharge zone locations, etc. (e.g., Jalilinasrabady et al., 2021). This modelling also facilitates monitoring to validate and ensure longevity and efficiency throughout the reservoir life cycle. Injection fluid is generally far from chemical equilibrium, with the reservoir rock and high temperatures accelerating reaction kinetics, so extensive fluid-rock interaction can be expected. Dissolution and precipitation reactions on fracture surfaces can cause mechanical and hydrological changes in the reservoir, which are potentially observable through geophysical monitoring. The state of our understanding of geochemistry in these supercritical environments is limited (reviewed in Section 2.1.7). The chemical composition of produced fluids is also a major concern, as wellbore and surface equipment must be designed to handle expected corrosion (see companion reports on well design and construction, Suryanarayana et al., 2024, and power production, Brown et al., 2024).

Kioka & Nakagawa (2021) present a novel approach to preventing corrosion and scaling in conventional geothermal power plants. They used environmentally friendly, inexpensive, and easy-to-deploy nanobubbles as inhibitors in geothermal fluids to prevent precipitated minerals, such as calcium carbonate and silica, from causing scaling and corrosion during well drilling and production. This study could be useful for application and validation in SHR power plants.

Gaps:

- Lack of the chemical data of supercritical fluids in different geological settings to establish a general characterization and understand the mechanisms occurring in the deeper levels of hydrothermal systems
- Lack of understanding of chemical processes expected in wells under supercritical conditions.
- Lack of thermodynamic formulation for supercritical temperature and pressure conditions.

Current technology:

- Microgravity monitoring, surface deformation, or 4D time-lapse seismic surveys can constrain reservoir mass balance and help evaluate the effectiveness and efficiency of injection and production strategies
- Numerical reservoir modelling integrating a conceptual model, geological conditions, and geophysical and geochemical properties from field and well data can predict long-term reservoir performance.

Technology/approach needed to develop SHR:

- Geochemical tools development in areas of active volcanic-geothermal activity or supercritical fluids zones will be relevant for SHR resources.
- Geochemical studies are important during reservoir development, production, and environment assessment. Those analyses can predict scale deposition and corrosion from geothermal fluids.

6. Proposed paths forward

The advancement of SHR characterization requires multiple steps. We propose refining the PFA methodology to exclusively target SHR plays. This approach should emphasize the integration of datasets to identify favorable conditions for the creation of superhot EGS reservoirs (e.g., stress state) and elevated heat flow areas. Dataset integration requires incorporating SHR-specific evidence layers and developing models that target the various geological settings where SHR resources exist. Additionally, the refinement of the SHR PFA should integrate machine learning, advanced statistical methods, expert-driven approaches, and physics-based modelling. Currently, data-driven methods are hampered by the lack of applicable, openly accessible data. In order to improve the statistical robustness of our understanding of SHR conditions and their effect on geophysical observables across rock types, more data collection and validation are needed, both in the field and laboratory.

Most of the technology for direct and indirect measurement in geophysics already exists and is ready to apply and improve for SHR through gained experience, but a standardized approach to data collection and analysis would improve the widespread use of these methods and extrapolation of lessons learned between projects. Establishing a standardized approach to SHR site characterization would also de-risk SHR exploration, as developers will have followed an effective, pre-determined exploration strategy devised by experts. Conducting retroactive studies with archival datasets from developed SHR resources would be a cost- and time-effective method to identify the optimal geophysical techniques for characterizing SHR plays in a range of settings, informing the standardization of SHR geothermal exploration.

Laboratory rock physics work at SHR conditions is difficult due to equipment costs and limitations, but experimental solutions are available and further data collection and analysis is needed to improve interpretation, while field drilling tests in a range of relevant lithologies for *in situ* validation are vital (Bromley, 2020; Bromley et al., 2020; Bromley & Carey, 2023; Cladouhos & Callahan, 2024b). Exploration drilling involves very high upfront costs, so substantial subsidies, tax incentives, research funding, and company investment are needed to support and encourage research development of these next-generation technologies while promoting public understanding and acceptance.

6.1 Conclusions

In this report, we reviewed existing SHR characterization and siting studies and techniques at various scales. Our analysis focused on identifying the key components and methods for SHR development. We identify (at different scales) heat, stress, structures, and permeability as the main components to constrain for a SHR-play.

At the exploration scale, we outline work on heat mapping, stress regime, and hazards. Geodynamic setting provides needed context to properly interpret the locations of the heat source, depth to 400°C, reservoir rock properties, expected temperature ranges, fluid geochemistry, and state of stress. Therefore, sub-types of SHR-plays may have different signatures and may require different approaches. Heat mapping is a critical first step to identify preferable locations for exploration. Identifying regions with high geothermal gradient (i.e., shallower depth to 400°C) remains a complex task. Global

temperature maps lack the granularity needed to identify local high heat flow anomalies and instead capture broad regional patterns and are limited in modelling non-steady state (i.e convective) heat flow. However, they may be useful to guide initial assessments and can be improved by incorporating higher resolution data. The stress regime is also fundamental to engineering permeability enhancement. The scarcity of data in some regions results in a low-resolution map that relies on extensive spatial extrapolations. For each of the factors evaluated, increasing the granularity or resolution of the models was identified as a main technological advancement required to advance SHR.

At the reservoir scale (10s - sub km), we review work on heat at depth, stress and pore pressure at depth, and structures and permeability. At this scale, estimating the temperature isotherms (i.e., estimation of temperature at depth) depends upon a combination of direct measurements of heat flow from boreholes and petrophysical properties of core samples. Temperature estimation can incorporate proxies for thermal conductivity and geophysical information to constrain the maps, offering additional paths in places where borehole data are insufficient or non-existent. Stress measurement and pore pressure estimation are important factors in reservoir design, and in preventing drilling complications and failures. For example, a perpendicular alignment between the drill hole and the maximum horizontal stress should be avoided to prevent issues, requiring knowledge of the stress amplitude and orientation at depth, while pore pressure must be determined to calibrate fluid drilling pressure. Seismic methods offer a promising way to map structures (i.e., fracture networks) and permeability in SHR, but present technical gaps in obtaining robust data and interpretation. These factors are fundamental for the development of a superhot engineered reservoir.

For monitoring, induced seismicity offers some of the most detailed remotely sensed information about the reservoir state, while also representing a significant hazard for production. There is hope that approaching the Brittle-Ductile transition will limit the potential for large, damaging events, but this requires further laboratory and field studies to confirm and fully understand. Adaptive Traffic Light Systems (ATLS) will need to be developed to address the unique situations in SHR fields and require sufficient real-time microseismic monitoring arrays. Joint seismic and electromagnetic monitoring also offers significant potential for tracking permeability enhancement during stimulation, but more work is needed to validate the interpretation of these signals in SHR environments. Long-term lifecycle analysis will be required to track heat depletion, mass balance, and fluid-rock interaction in the reservoir, but these efforts are still in their infancy, requiring more SHR field demonstration sites and long-term production.

One main conclusion from this report is that existing geophysical techniques can be transferred to SHR characterization and siting procedures. However, there are very limited examples where SHR conditions have been validated. As such, we don’t yet have sufficient statistics to robustly relate geophysically observable properties (seismic velocity and attenuation, electrical conductivity, magnetic susceptibility, density, etc.) and the rock properties essential to SHR characterization (temperature, stress/fracture conditions, permeable structures, fluid content, etc.). Machine learning offers a lot of potential to improve data interpolation, interpretation, and prediction. However, there remains a severe lack of data to sufficiently inform these techniques. In this way, we need more field-validated data sets and laboratory experiments to draw robust connections between observables and variables of interest.

7. Acknowledgements

This paper was published simultaneously with the Clean Air Task Force under the title "A Survey of Methods, Challenges, and Pathways Forward for Superhot Rock Siting and Characterization." We appreciate our advisory committee and others for their invaluable comments and suggestions, which greatly enhanced the quality of our report: Matthew Pritchard (Cornell U.), Trenton Cladouhos (Quaise Energy), Vala Hjörleifsdóttir (Reykjavík U.), Douglas Blankenship (DOE), Amanda Kolker (NREL), William Cumming (Cumming Geoscience), Philip Ball (Geothermal Energy Advisors), Joseph Moore (EGI), and John McClennan (EGI). We thank the Clean Air Task Force (Terra Rogers and Jenna Hill) for their constructive comments and leadership in this report. We also thank Shaun J. Doherty for his support and assistance. This study was supported by the Cornell Atkinson Center for Sustainability and Cascade Institute.

8. References

Afonso, J. C., Salajegheh, F., Szwillus, W., Ebbing, J., & Gaina, C. (2019). A global reference model of the lithosphere and upper mantle from joint inversion and analysis of multiple data sets. *Geophysical Journal International*, *217*(3), 1602–1628.

Aghahosseini, A., & Breyer, C. (2020). From hot rock to useful energy: A global estimate of enhanced geothermal systems potential. *Applied Energy*, *279*, 115769.

Agrawal, M. G., Bernard, M. J., Hedegaard, M. M., Makthoum, M. M., Soni, M. A., & Wohrer, M. P. (2016). *A framework for international collaboration on lunar missions*.

Aguiar, A. C., & Myers, S. C. (2019). Microseismic focal mechanisms and implications for changes in stress during the 2014 Newberry EGS stimulation. *Bulletin of the Seismological Society of America*, *109*(5), 1653–1660.

Aizawa, K., Utsugi, M., Kitamura, K., Koyama, T., Uyeshima, M., Matsushima, N., Takakura, S., Inagaki, H., Saito, H., & Fujimitsu, Y. (2022). Magmatic fluid pathways in the upper crust: insights from dense magnetotelluric observations around the Kuju Volcanoes, Japan. *Geophysical Journal International*, *228*(2), 755–772.

Aljubran, M. J., & Horne, R. N. (2024). Thermal Earth model for the conterminous United States using an interpolative physics-informed graph neural network. *Geothermal Energy*, *12*(1), 1–48.

Allis, R., Moore, J., Davatzes, N., Gwynn, M., Hardwick, C., Kirby, S., McLennan, J., Pankow, K., Potter, S., & Simmons, S. (2016). EGS concept testing and development at the Milford, Utah FORGE site. *Proceedings*.

Ardid, A., Archer, R., Sepulveda, F., & Dempsey, D. (2021). Measuring heat flux dynamics through the clay cap in the Wairakei-Tauhara geothermal field. *Proceedings 43nd New Zealand Geothermal Workshop*.

Árnason, K., Eysteinsson, H., & Hersir, G. P. (2010). Joint 1D inversion of TEM and MT data and 3D inversion of MT data in the Hengill area, SW Iceland. *Geothermics*, *39*(1), 13–34.

Ars, J.-M., Tarits, P., Hautot, S., Bellanger, M., Coutant, O., & Maia, M. (2019). Joint inversion of gravity and surface wave data constrained by magnetotelluric: application to deep geothermal exploration of crustal fault zone in felsic basement. *Geothermics*, *80*, 56–68.

Asanuma, H., Mogi, T., Tsuchiya, N., Watanabe, N., Naganawa, S., Ogawa, Y., Fujimitsu, Y., Kajiwara, T., Osato, K., & Shimada, K. (2020). Japanese supercritical geothermal project for drastic increase of geothermal power generation in 2050. *Proceedings of the World Geothermal Congress*, *1*.

Balfour, N. J., Cummins, P. R., Pilia, S., & Love, D. (2015). Localization of intraplate deformation through fluid-assisted faulting in the lower-crust: The Flinders Ranges, South Australia. *Tectonophysics*, *655*, 97–106.

Ball, P. J., Banks, G., Montgomery, M., & Afonso, J. C. (2024). Global screening of superhot rock geothermal energy: geodynamic settings, heat endowment and extraction techniques. In *Geothermal Energy Engineering*. Elsevier.

Barison, E., Poletto, F., Böhm, G., Farina, B., Carrasco-Núñez, G., Norini, G., Giordano, G., & Pinna, G. (2023). Processing and interpretation of seismic reflection data from the Los Humeros super-hot geothermal system. *Geothermics*, *113*, 102771.

Batir, J., & Richards, M. (2022). Determining geothermal resources in three texas counties. *Texas Water Journal*, *13*(1), 27–44.

Bedrosian, P. A. (2007). MT+, integrating magnetotellurics to determine earth structure, physical state, and processes. *Surveys in Geophysics*, *28*(2–3), 121–167. https://doi.org/10.1007/s10712-007-9019-6

Bedrosian, P. A., Unsworth, M. J., Egbert, G. D., & Thurber, C. H. (2004). Geophysical images of the creeping segment of the San Andreas fault: implications for the role of crustal fluids in the earthquake process. *Tectonophysics*, *385*(1–4), 137–158.

Bégué, F., Deering, C. D., Gravley, D. M., Chambefort, I., & Kennedy, B. M. (2017). From source to surface: Tracking magmatic boron and chlorine input into the geothermal systems of the Taupo Volcanic Zone, New Zealand. *Journal of Volcanology and Geothermal Research*, *346*, 141–150.

Bennett, C. R., Nash, G. D., Sorkhabi, R., Moore, J., Simmons, S., Brandt, A., Barker, B., & Swanson, B. (2015). *The Convergence of Heat, Groundwater & Fracture Permeability. Innovative Play Fairway Modelling Applied to the Tularosa Basin Phase 1 Project Report*. Ruby Mountain Inc., Salt Lake City, UT (United States).

Benson, P. M., Austria, D. C., Gehne, S., Butcher, E., Harnett, C. E., Fazio, M., Rowley, P., & Tomas, R. (2020). Laboratory simulations of fluid-induced seismicity, hydraulic fracture, and fluid flow. *Geomechanics for Energy and the Environment*, *24*, 100169.

Bertani, R., Büsing, H., Buske, S., Dini, A., Hjelstuen, M., Luchini, M., Manzella, A., Nybo, R., Rabbel, W., & Serniotti, L. (2018). The first results of the Descramble project. *Proceedings, 43rd Workshop on Geothermal Reservoir Engineering, Stanford University, Stanford, California*.

Bertrand, E. A., Caldwell, T. G., Bannister, S., Soengkono, S., Bennie, S. L., Hill, G. J., & Heise, W. (2015). Using array MT data to image the crustal resistivity structure of the southeastern Taupo Volcanic Zone, New Zealand. *Journal of Volcanology and Geothermal Research*, *305*, 63–75.

Bielicki, J. M., Adams, B. M., Choi, H., Jamiyansuren, B., Saar, M. O., Taff, S. J., Buscheck, T. A., & Ogland-Hand, J. D. (2016). Sedimentary basin geothermal resource for cost-effective generation of renewable electricity from sequestered carbon dioxide. *41st Workshop on Geothermal Reservoir Engineering Stanford University*.

Biggs, J., Ayele, A., Fischer, T. P., Fontijn, K., Hutchison, W., Kazimoto, E., Whaler, K., & Wright, T. J. (2021). Volcanic activity and hazard in the East African Rift Zone. *Nature Communications*, *12*(1), 6881.

Biggs, J., Robertson, E., & Cashman, K. (2016). The lateral extent of volcanic interactions during unrest and eruption. *Nature Geoscience*, *9*(4), 308–311.

Blackwell, D. D., Richards, M. C., Frone, Z. S., Batir, J. F., Williams, M. A., Ruzo, A. A., & Dingwall, R. K. (2011). *SMU geothermal heatflow map of the conterminous United States, 2011, Supported by Google. org*.

Boness, N. L., & Zoback, M. D. (2006). A multiscale study of the mechanisms controlling shear velocity anisotropy in the San Andreas Fault Observatory at Depth. *Geophysics*, *71*(5), F131–F146.

Börner, J. H., Bär, M., & Spitzer, K. (2015). Electromagnetic methods for exploration and monitoring of enhanced geothermal systems–a virtual experiment. *Geothermics*, *55*, 78–87.

Bromley, C. (2020). Induced Seismicity-a Perspective on Monitoring, Mechanisms and Public Acceptability for Hydrothermal Systems. *Proceedings World Geothermal Congress*, 1.

Bromley, C., Axelsson, G., Asanuma, H., Manzella, A., & Dobson, P. (2020). Supercritical Fluids–Learning about the Deep Roots of Geothermal Systems from OEA Geothermal Collaboration. *Proceedings World Geothermal Congress*, *1*.

Bromley, C., & Carey, B. (2023). Ultra Hot-Supercritical Geothermal-IEA Geothermal Collaboration. *Proceedings*, 15–17.

Brown, S., Coolbaugh, M., DeAngelo, J., Faulds, J., Fehler, M., Gu, C., Queen, J., Treitel, S., Smith, C., & Mlawsky, E. (2020). Machine learning for natural resource assessment: An application to the blind geothermal systems of Nevada. *Transactions-Geothermal Resources Council*, *44*.

Bruhn, D., Huenges, E., Ágústsson, K., Zang, A., Kwiatek, G., Rachez, X., Wiemer, S., Van Wees, J.-D., Calcagno, P., & Kohl, T. (2011). Geothermal engineering integrating mitigation of induced seismicity in reservoirs-The European GEISER Project. *Transactions/Geothermal Resources Council*, *35*, 1623–1626.

Bürgmann, R., & Dresen, G. (2008). Rheology of the lower crust and upper mantle: Evidence from rock mechanics, geodesy, and field observations. *Annu. Rev. Earth Planet. Sci.*, *36*(1), 531–567.

Burns, E., DeAngelo, J., and Williams, C. F. (2024). *Updated three-dimensional temperature maps for the Great Basin, USA*. 49th Workshop on Geothermal Reservoir Engineering.

Cabrera-Pérez, I., Soubestre, J., D'Auria, L., Barrancos, J., Martín-Lorenzo, A., van Dorth, D. M., Padilla, G. D., Przeor, M., & Pérez, N. M. (2023). Geothermal and structural features of La Palma island (Canary Islands) imaged by ambient noise tomography. *Scientific Reports*, *13*(1), 12892.

Campillo, M., & Paul, A. (2008). *Long-range correlations in the diffuse seismic coda*.

Capdeville, Y., Cupillard, P., & Singh, S. (2020). An introduction to the two-scale homogenization method for seismology. In *Advances in Geophysics* (Vol. 61, pp. 217–306). Elsevier.

Caraccioli, P. D., Mordensky, S. P., Lindsey, C. R., DeAngelo, J., Burns, E., & Lipor, J. (2023). Don't Let Negatives Hold You Back: Accounting for Underlying Physics and Natural Distributions of Hydrothermal Systems When Selecting Negative Training Sites Leads to Better Machine Learning Predictions. *Geothermal Resources Council Transactions*, *47*, 1672–1693.

Carrillo, J., Perez-Flores, M. A., Gallardo, L. A., & Schill, E. (2022). Joint inversion of gravity and magnetic data using correspondence maps with application to geothermal fields. *Geophysical Journal International*, *228*(3), 1621–1636.

Chambefort, I., & Stefánsson, A. (2020). Fluids in geothermal systems. *Elements: An International Magazine of Mineralogy, Geochemistry, and Petrology*, *16*(6), 407–411.

Chave, A. D., & Jones, A. G. (2012). *The magnetotelluric method: Theory and practice*. Cambridge University Press.

Chave, A. D., & Thomson, D. J. (2003). A bounded influence regression estimator based on the statistics of the hat matrix. *Journal of the Royal Statistical Society: Series C (Applied Statistics)*, *52*(3), 307–322.

Chhun, C., Tsuji, T., & Ikeda, T. (2024). Potential fluid flow pathways and the geothermal structure of Kuju revealed by azimuthal anisotropic ambient noise tomography. *Geothermics*, *119*, 102932.

Cladouhos, T. T., Petty, S., Swyer, M. W., Uddenberg, M. E., Grasso, K., & Nordin, Y. (2016). Results from newberry volcano EGS demonstration, 2010–2014. Geothermics, 63, 44-61.

Cladouhos, T. T., & Callahan, O. A. (2024a). *Bridging the Gaps: A Survey of Methods, Challenges, and Pathways Forward for Superhot Rock Heat Extraction*.

Cladouhos, T. T., & Callahan, O. A. (2024b). *Heat Extraction from SuperHot Rock-Technology Development*.

Coblentz, D., van Wijk, J., Carmichael, J., Johnson, C., Delorey, A., Chai, C., Maceira, M., & Richardson, R. M. (2024). New approaches to an old problem: addressing spatial gaps in the World Stress Map. *Geological Society, London, Special Publications*, *546*(1), 47–68. https://doi.org/10.1144/SP546-2023-27

Cumming, W. (2009). Geothermal resource conceptual models using surface exploration data. *Proceedings*, 9–11.

Cumming, W., & Mackie, R. (2010). Resistivity imaging of geothermal resources using 1D, 2D and 3D MT inversion and TDEM static shift correction illustrated by a Glass Mountain case history. *Proceedings World Geothermal Congress*, 25–29.

Darnet, M., Wawrzyniak, P., Coppo, N., Nielsson, S., Schill, E., & Fridleifsson, G. Ó. (2020). Monitoring geothermal reservoir developments with the controlled-source electro-magnetic method—a calibration study on the Reykjanes geothermal field. *Journal of Volcanology and Geothermal Research*, *391*, 106437.

Davarpanah, S. M., Sharghi, M., Narimani, S., Török, Á., & Vásárhelyi, B. (2023). Brittle-ductile transition stress of different rock types and its relationship with uniaxial compressive strength and Hoek–Brown material constant (mi). *Scientific Reports*, *13*(1), 1186.

Davide, P., & Luca, S. (2019). Drilling in supercritical condition: the DESCRAMBLE project. *European Geothermal Congress 2019*, 11–14.

DeAngelo, J., Burns, E., Mordensky, S. P., and Lindsey, C. R. (2023a). Detrending Great Basin elevation to identify structural patterns for identifying geothermal favorability. *Geothermal Resources Council Transactions, 47*, 1694-1702. https://pubs.usgs.gov/publication/70250639

DeAngelo, J., Burns, E. R., Gentry, E., Batir, J. F., Lindsey, C. R., and Mordensky, S. P. (2023b). *New maps of conductive heat flow in the Great Basin, USA: Separating conductive and convective influences*. 48th Workshop on Geothermal Reservoir Engineering.

De Franco, R., Petracchini, L., Scrocca, D., Caielli, G., Montegrossi, G., Santilano, A., & Manzella, A. (2019). Synthetic seismic reflection modelling in a supercritical geothermal system: An image of the K-horizon in the Larderello Field (Italy). *Geofluids*, *2019*(1), 8492453.

De Matteis, R., Massa, B., Adinolfi, G. M., Amoroso, O., Terakawa, T., & Convertito, V. (2024). Pore fluid pressure in St. Gallen geothermal field (Switzerland) based on earthquake focal mechanisms. *Geophysical Research Letters*, *51*(6), e2023GL105127.

Didana, Y. L., Heinson, G., Thiel, S., & Krieger, L. (2017). Magnetotelluric monitoring of permeability enhancement at enhanced geothermal system project. *Geothermics*, *66*, 23–38.

Dingwell, D. B. (1997). The brittle–ductile transition in high-level granitic magmas: material constraints. *Journal of Petrology*, *38*(12), 1635–1644.

Doughty, C., Dobson, P. F., Wall, A., McLing, T., & Weiss, C. (2018). *GeoVision analysis supporting task force report: Exploration*.

Driesner, T., & Heinrich, C. A. (2007). The system H2O–NaCl. Part I: Correlation formulae for phase relations in temperature–pressure–composition space from 0 to 1000 C, 0 to 5000 bar, and 0 to 1 XNaCl. *Geochimica et Cosmochimica Acta*, *71*(20), 4880–4901.

Ekström, G., Abers, G. A., & Webb, S. C. (2009). Determination of surface-wave phase velocities across USArray from noise and Aki's spectral formulation. *Geophysical Research Letters*, *36*(18).

Elbarbary, S., Zaher, M. A., Saibi, H., Fowler, A.-R., Ravat, D., & Marzouk, H. (2022). Thermal structure of the African continent based on magnetic data: Future geothermal renewable energy explorations in Africa. *Renewable and Sustainable Energy Reviews*, *158*, 112088.

Eulenfeld, T., Hillers, G., Vuorinen, T. A. T., & Wegler, U. (2023). Induced earthquake source parameters, attenuation, and site effects from waveform envelopes in the Fennoscandian Shield. *Journal of Geophysical Research: Solid Earth*, *128*(4), e2022JB025162.

Fang, H., Yao, H., Zhang, H., Huang, Y.-C., & van der Hilst, R. D. (2015). Direct inversion of surface wave dispersion for three-dimensional shallow crustal structure based on ray tracing: methodology and application. *Geophysical Journal International*, *201*(3), 1251–1263.

Fang, Y., Elsworth, D., & Cladouhos, T. T. (2018). Reservoir permeability mapping using microearthquake data. *Geothermics*, *72*, 83–100.

Farina, B., Parisio, F., & Poletto, F. (2022). A seismic-properties and wave-propagation analysis for the long-term monitoring of supercritical geothermal systems. *Geothermics*, *104*, 102451.

Farina, B., Poletto, F., Mendrinos, D., Carcione, J. M., & Karytsas, C. (2019). Seismic properties in conductive and convective hot and super-hot geothermal systems. *Geothermics*, *82*, 16–33.

Faulds, J. E., Hinz, N. H., Coolbaugh, M., Ayling, B., Glen, J., Craig, J. W., McConville, E., Siler, D., Queen, J., & Witter, J. (2021). *Discovering Blind Geothermal Systems in the Great Basin Region: An Integrated Geologic and Geophysical Approach for Establishing Geothermal Play Fairways: All Phases*. Univ. of Nevada, Reno, NV (United States); ATLAS Geosciences, Inc., Reno, NV.

Faulds, J., Hinz, N., Coolbaugh, M., dePolo, C., Siler, D., Shevenell, L., Hammond, W., Kreemer, C., & Queen, J. (2015). Discovering geothermal systems in the Great Basin region: An integrated geologic, geochemical, and geophysical approach for establishing geothermal play fairways. *PROCEEDINGS, 41st Workshop on Geothermal Reservoir Engineering*, *DOE-UNR-06731-06*.

Faulds, J., Hinz, N., Coolbaugh, M., Sadowski, A., Shevenell, L., McConville, E., Craig, J., Sladek, C., & Siler, D. (2017). Progress report on the Nevada Play Fairway Project: integrated geological, geochemical,

and geophysical analyses of possible new geothermal systems in the Great Basin region. *Proceedings, 42nd Workshop on Geothermal Reservoir Engineering, Stanford University*, *DOE-UNR-06731-04*.

Folsom, M., Libbey, R., Feucht, D., Warren, I., & Garanzini, S. (2020). Geophysical observations and integrated conceptual models of the San Emidio geothermal field, Nevada. *Proceedings of the 45th Workshop on Geothermal Reservoir Engineering, Stanford University, Stanford, CA, USA 21p*.

Fomel, S. (2009). Velocity analysis using AB semblance. *Geophysical Prospecting*, *57*(3), 311–321.

Fournier, R. O. (1999). Hydrothermal processes related to movement of fluid from plastic into brittle rock in the magmatic-epithermal environment. *Economic Geology*, *94*(8), 1193–1211.

Fuchs, S., Norden, B., Neumann, F., Kaul, N., Tanaka, A., Kukkonen, I. T., Pascal, C., Christiansen, R., Gola, G., & Šafanda, J. (2023). Quality-assurance of heat-flow data: The new structure and evaluation scheme of the IHFC Global Heat Flow Database. *Tectonophysics*, *863*, 229976.

Fullea, J., Lebedev, S., Martinec, Z., & Celli, N. L. (2021). WINTERC-G: mapping the upper mantle thermochemical heterogeneity from coupled geophysical–petrological inversion of seismic waveforms, heat flow, surface elevation and gravity satellite data. *Geophysical Journal International*, *226*(1), 146–191.

Fulton, P. M., & Saffer, D. M. (2009). Potential role of mantle-derived fluids in weakening the San Andreas Fault. *Journal of Geophysical Research: Solid Earth*, *114*(B7). https://doi.org/https://doi.org/10.1029/2008JB006087

Gallardo, L. A., & Meju, M. A. (2011). Structure-coupled multiphysics imaging in geophysical sciences. *Reviews of Geophysics*, *49*(1).

Gasperikova, E., & Cumming, W. (2020). How geophysics can help the geothermal industry. *SEG International Exposition and Annual Meeting*, D021S019R005.

Gasperikova, E., Newman, G., Feucht, D., & Arnason, K. (2011). 3D MT characterization of two geothermal fields in Iceland. *GRC Trans*, *35*(1–2), 1667–1671.

Georgsson, L. S. (2009). Geophysical methods used in geothermal exploration. *Short Course on Surface Exploration for Geothermal Resources*.

Gola, G., Bertini, G., Bonini, M., Botteghi, S., Brogi, A., De Franco, R., Dini, A., Donato, A., Gianelli, G., & Liotta, D. (2017). Data integration and conceptual modelling of the Larderello geothermal area, Italy. *Energy Procedia*, *125*, 300–309.

Goto, R., Watanabe, N., Sakaguchi, K., Miura, T., Chen, Y., Ishibashi, T., Pramudyo, E., Parisio, F., Yoshioka, K., & Nakamura, K. (2021). Creating cloud-fracture network by flow-induced microfracturing in superhot geothermal environments. *Rock Mechanics and Rock Engineering*, *54*, 2959–2974.

Grasby, S. E., Jessop, A., Kelman, M., Ko, M., Chen, Z., Allen, D. M., Bell, S., Ferguson, G., Majorowicz, J., & Moore, M. (2011). *Geothermal energy resource potential of Canada*.

Grobbe, N., Revil, A., Zhu, Z., & Slob, E. (2020). *Seismoelectric exploration: Theory, experiments, and applications* (Vol. 252). John Wiley & Sons.

Gudmundsson, Á., & Mortensen, A. K. (2015). Well locations consideration of purpose, objectives and achievement with emphasis on recent drilling in the Krafla geothermal area. *Proceedings of the World Geothermal Congress*.

Gunnlaugsson, E., Ármannsson, H., Thorhallsson, S., & Steingrímsson, B. (2014). Problems in geothermal operation–scaling and corrosion. *Goethermal Training Program, United Nations University*, 1–18.

Hakami, H. (2006). *Numerical studies on spatial variation of the in situ stress field at Forsmark-a further step. Site descriptive modelling Forsmark-stage 2.1*.

Halter, W. E., & Webster, J. D. (2004). The magmatic to hydrothermal transition and its bearing on ore-forming systems. In *Chemical Geology* (Vol. 210, Issues 1–4, pp. 1–6). Elsevier.

Hanneson, C., & Unsworth, M. J. (2023). Magnetotelluric imaging of the magmatic and geothermal systems beneath Mount Meager, southwestern Canada. *Canadian Journal of Earth Sciences*, *ja*.

Hardwick, C., Hurlbut, W., Gwynn, M., Allis, R., Wannamaker, P., & Moore, J. (2019). Geophysical surveys of the Milford, Utah, FORGE site—gravity and TEM. *Geothermal Characteristics of the Roosevelt Hot Springs System and Adjacent FORGE EGS Site*, 14.

Hartline, C. (2024). *Seismic Monitoring Advisory Committee Meeting*. https://geysers.com/smac

Hart-Wagoner, N., Coolbaugh, M., Faulds, J. E., Mlawsky, E., Lindsey, C., Trainor-Guitton, W., & Brown, S. (n.d.). *Preliminary Regional Play Fairway Workflow for the Great Basin Region, USA*.

Hasterok, D., & Chapman, D. S. (2008). Global heat flow: a new database and a new approach. *AGU Fall Meeting Abstracts*, *2008*, T21C-1985.

Heidbach, O., Rajabi, M., Cui, X., Fuchs, K., Müller, B., Reinecker, J., Reiter, K., Tingay, M., Wenzel, F., & Xie, F. (2018). The World Stress Map database release 2016: Crustal stress pattern across scales. *Tectonophysics*, *744*, 484–498.

Henley, R. W., & Seward, T. M. (2018). Gas–solid reactions in arc volcanoes: Ancient and modern. *High Temperature Gas-Solid Reactions in Earth and Planetary Processes*, 309–350.

Heřmanská, M., Kleine, B. I., & Stefánsson, A. (2019). Supercritical fluid geochemistry in geothermal systems. *Geofluids*, *2019*(1), 6023534.

Heřmanská, M., Stefánsson, A., & Scott, S. (2019). Supercritical fluids around magmatic intrusions: IDDP-1 at Krafla, Iceland. *Geothermics*, *78*, 101–110.

Hersir, G. P., Flóvenz, O. G., Bruhn, D., Liotta, D., van Wees, J.-D., Halldórsdóttir, S., & Manzella, A. (2021). Geothermal exploration and reservoir assessment in magmatic systems the image project. *Proceedings World Geothermal Congress2020+1*.

Hinze, W. J., Von Frese, R. R. B., Von Frese, R., & Saad, A. H. (2013). *Gravity and magnetic exploration: Principles, practices, and applications*. Cambridge University Press.

Hokstad, K., & Kruber, C. (2023). Multigeophysical Inversion for Geothermal Exploration. *GRC Transactions47*, *2939*.

Hokstad, K., & Tanavasuu-Milkeviciene, K. (2017). Temperature prediction by multigeophysical inversion: application to the IDDP-2 well at Reykjanes, Iceland. *Geotherm Resource Council*, *41*, 1141–1152.

Hu, S., Luo, S., & Yao, H. (2020). The frequency-Bessel spectrograms of multicomponent cross-correlation functions from seismic ambient noise. *Journal of Geophysical Research: Solid Earth*, *125*(8), e2020JB019630.

Huang, X., Yu, Z., Wang, W., & Wang, F. (2023). JointNet: A Multimodal Deep Learning-Based Approach for Joint Inversion of Rayleigh Wave Dispersion and Ellipticity. *Bulletin of the Seismological Society of America*, *114*(2), 627–641. https://doi.org/10.1785/0120230199

Hurst, T., Heise, W., Hreinsdottir, S., & Hamling, I. (2016). Geophysics of the Taupo Volcanic Zone: A review of recent developments. *Geothermics*, *59*, 188–204.

Hurwitz, S., & Lowenstern, J. B. (2014). Dynamics of the Yellowstone hydrothermal system. *Reviews of Geophysics*, *52*(3), 375–411.

Hutapea, F. L., Tsuji, T., Katou, M., & Asakawa, E. (2020). Data processing and interpretation schemes for a deep-towed high-frequency seismic system for gas and hydrate exploration. *Journal of Natural Gas Science and Engineering*, *83*, 103573.

Hutchings, L., Bonner, B., Saltiel, S., Jarpe, S., & Nelson, M. (2019). Rock physics interpretation of tomographic solutions for geothermal reservoir properties. *Applied Geophysics with Case Studies on Environmental, Exploration and Engineering Geophysics*.

Ilic, O., Sigmundsson, F., Lavallée, Y., Mortensen, A. K., Eichelberger, J., Markusson, S. H., Papale, P., & Thordarson, T. (2020). Geological Risk Associated with Drilling into Magma at Krafla Caldera, Iceland: Preliminary Evaluation. *Proceedings of the World Geothermal Congress*, *1*.

Ishitsuka, K., Kobayashi, Y., Watanabe, N., Yamaya, Y., Bjarkason, E., Suzuki, A., Mogi, T., Asanuma, H., Kajiwara, T., & Sugimoto, T. (2021). Bayesian and neural network approaches to estimate deep temperature distribution for assessing a supercritical geothermal system: evaluation using a numerical model. *Natural Resources Research*, *30*(5), 3289–3314.

Ishizu, K., Ogawa, Y., Mogi, T., Yamaya, Y., & Uchida, T. (2021). Ability of the magnetotelluric method to image a deep conductor: Exploration of a supercritical geothermal system. *Geothermics*, *96*, 102205.

Jalilinasrabady, S., Tanaka, T., Itoi, R., & Goto, H. (2021). Numerical simulation and production prediction assessment of Takigami geothermal reservoir. *Energy*, *236*, 121503.

Jenkins, A. P., Rust, A. C., Blundy, J., & Biggs, J. (2023). Magnetotelluric investigations at andean volcanoes: partial melt or saline magmatic fluids? *Journal of Volcanology and Geothermal Research*, *440*, 107852.

Jiang, C., & Denolle, M. A. (2020). NoisePy: A new high-performance python tool for ambient-noise seismology. *Seismological Research Letters*, *91*(3), 1853–1866.

Jordan, T. E. (2015). Final Report: *Low Temperature Geothermal Play Fairway Analysis for the Appalachian Basin.* Cornell University. https://data.openei.org/submissions/

Kalberkamp, U. (2007). Exploration of geothermal high enthalpy resources using magnetotellurics-an example from Chile. *Proceedings 22nd Colloquium Electromagnetic Depth Research, Děčín, Czech Republic*, 194–198.

Kamei, R., Pratt, R. G., & Tsuji, T. (2012). Waveform tomography imaging of a megasplay fault system in the seismogenic Nankai subduction zone. *Earth and Planetary Science Letters*, *317*, 343–353.

Kana, J. D., Djongyang, N., Raïdandi, D., Nouck, P. N., & Dadjé, A. (2015). A review of geophysical methods for geothermal exploration. *Renewable and Sustainable Energy Reviews*, *44*, 87–95.

Kasahara, J., Hasada, Y., & Yamaguchi, T. (2019). Seismic imaging of supercritical geothermal reservoir using full-waveform inversion method. *Proceedings*.

Keilis-Borok, V. I., & Yanovskaja, T. B. (1967). Inverse Problems of Seismology (Structural Review). *Geophysical Journal International*, *13*(1–3), 223–234. https://doi.org/10.1111/j.1365-246X.1967.tb02156.x

Kelbert, A., Meqbel, N., Egbert, G. D., & Tandon, K. (2014). ModEM: A modular system for inversion of electromagnetic geophysical data. *Computers & Geosciences*, *66*, 40–53.

Khankishiyev, O., Salehi, S., Hasanov, G., & Hu, Z. (n.d.). *Application of Distributed Temperature Sensing (DTS) in Geothermal Wells*.

Khodaei, P., Karimpouli, S., Balcewicz, M., & Saenger, E. H. (2022). Computing wave velocity of rock sample using rock chips and cuttings. *Journal of Petroleum Science and Engineering*, *209*, 109849.

Kim, K.-I., Min, K.-B., Kim, K.-Y., Choi, J. W., Yoon, K.-S., Yoon, W. S., Yoon, B., Lee, T. J., & Song, Y. (2018). Protocol for induced microseismicity in the first enhanced geothermal systems project in Pohang, Korea. *Renewable and Sustainable Energy Reviews*, *91*, 1182–1191.

Kim, K.-I., Yoo, H., Park, S., Yim, J., Xie, L., Min, K.-B., & Rutqvist, J. (2022). Induced and triggered seismicity by immediate stress transfer and delayed fluid migration in a fractured geothermal reservoir at Pohang, South Korea. *International Journal of Rock Mechanics and Mining Sciences*, *153*, 105098.

Kioka, A., & Nakagawa, M. (2021). Theoretical and experimental perspectives in utilizing nanobubbles as inhibitors of corrosion and scale in geothermal power plant. *Renewable and Sustainable Energy Reviews*, *149*(111373), 111373.

Kirkby, A., Czarnota, K., Huston, D. L., Champion, D. C., Doublier, M. P., Bedrosian, P. A., Duan, J., & Heinson, G. (2022). Lithospheric conductors reveal source regions of convergent margin mineral systems. *Scientific Reports*, *12*(1), 8190.

Kirkby, A., Funnell, R., Scadden, P., Seward, A., Sagar, M., Mortimer, N., & Sanders, F. (2024). Towards a New Zealand Heat Flow Model. *Proceedings, 49th Workshop on Geothermal Reservoir Engineering. Stanford, California*.

Kirkby, A., Heinson, G., Holford, S., & Thiel, S. (2015). Mapping fractures using 1D anisotropic modelling of magnetotelluric data: a case study from the Otway Basin, Victoria, Australia. *Geophysical Journal International*, *201*(3), 1961–1976.

Kitamura, K., Fujii, Y., Inagaki, H., Aizawa, K., Ishibashi, J., Saito, H., & Fujimitsu, Y. (2023). Evaluation of a potential supercritical geothermal system in the Kuju region, central Kyushu, Japan. *Geothermics*, *107*, 102602.

Kohrn, S. B., Bonet, C., DiFrancesco, D., & Gibson, H. (2011). Geothermal exploration using gravity gradiometry—A Salton Sea example. *Geothermal Resources Council Transactions*, *35*, 1699–1702.

Kolker, A., Taverna, N., Dobson, P., Benediksdottir, A., Warren, I., Pauling, H., Sonnenthal, E., Hjorleifsdottir, V., Hokstad, K., & Caliandro, N. (2022). *Exploring for Superhot Geothermal Targets in Magmatic Settings: Developing a Methodology*. National Renewable Energy Lab.(NREL), Golden, CO (United States).

Koulakov, I., D'Auria, L., Prudencio, J., Cabrera-Pérez, I., Barrancos, J., Padilla, G. D., Abramenkov, S., Pérez, N. M., & Ibáñez, J. M. (2023). Local earthquake seismic tomography reveals the link between crustal structure and volcanism in Tenerife (Canary Islands). *Journal of Geophysical Research: Solid Earth*, *128*(3), e2022JB025798.

Koulakov, I., Komzeleva, V., Smirnov, S. Z., & Bortnikova, S. B. (2021). Magma-fluid interactions beneath Akutan volcano in the Aleutian arc based on the results of local earthquake tomography. *Journal of Geophysical Research: Solid Earth*, *126*(3), e2020JB021192.

Koulakov, I., Shapiro, N. M., Sens-Schönfelder, C., Luehr, B. G., Gordeev, E. I., Jakovlev, A., Abkadyrov, I., Chebrov, D. V, Bushenkova, N., & Droznina, S. Y. (2020). Mantle and crustal sources of magmatic activity of Klyuchevskoy and surrounding volcanoes in Kamchatka inferred from earthquake tomography. *Journal of Geophysical Research: Solid Earth*, *125*(10), e2020JB020097.

Kraft, T., Roth, P., & Wiemer, S. (2020). *Good Practice Guide for Managing Induced Seismicity in Deep Geothermal Energy Projects in Switzerland*. ETH Zurich.

Kummerow, J., & Raab, S. (2015a). Temperature dependence of electrical resistivity-Part I: Experimental investigations of hydrothermal fluids. *Energy Procedia*, *76*, 240–246.

Kummerow, J., & Raab, S. (2015b). Temperature dependence of electrical resistivity–part II: A new experimental set-up to study fluid-saturated Rocks. *Energy Procedia*, *76*, 247–255.

Kwiatek, G., Martínez-Garzón, P., Dresen, G., Bohnhoff, M., Sone, H., & Hartline, C. (2015). Effects of long-term fluid injection on induced seismicity parameters and maximum magnitude in northwestern part of The Geysers geothermal field. *Journal of Geophysical Research: Solid Earth*, *120*(10), 7085–7101.

Kwiatek, G., Saarno, T., Ader, T., Bluemle, F., Bohnhoff, M., Chendorain, M., Dresen, G., Heikkinen, P., Kukkonen, I., & Leary, P. (2019). Controlling fluid-induced seismicity during a 6.1-km-deep geothermal stimulation in Finland. *Science Advances*, *5*(5), eaav7224.

Lachmar, T. E., Freeman, T. G., Kessler, J. A., Batir, J. F., Evans, J. P., Nielson, D. L., Shervais, J. W., Chen, X., Schmitt, D. R., & Blackwell, D. D. (2019). Evaluation of the geothermal potential of the western Snake River Plain based on a deep corehole on the Mountain Home AFB near Mountain Home, Idaho. *Geothermal Energy*, *7*, 1–15.

Lautze, N., Thomas, D., Hinz, N., Apuzen-Ito, G., Frazer, N., & Waller, D. (2017). Play fairway analysis of geothermal resources across the State of Hawaii: 1. Geological, geophysical, and geochemical datasets. *Geothermics*, *70*, 376–392.

Lavallée, Y., & Kendrick, J. E. (2021). A review of the physical and mechanical properties of volcanic rocks and magmas in the brittle and ductile regimes. *Forecasting and Planning for Volcanic Hazards, Risks, and Disasters*, 153–238.

Lehujeur, M., Vergne, J., Schmittbuhl, J., Zigone, D., Le Chenadec, A., & Team, E. (2018). Reservoir imaging using ambient noise correlation from a dense seismic network. *Journal of Geophysical Research: Solid Earth*, *123*(8), 6671–6686.

Leptokaropoulos, K., Staszek, M., Lasocki, S., Martínez-Garzón, P., & Kwiatek, G. (2018). Evolution of seismicity in relation to fluid injection in the North-Western part of The Geysers geothermal field. *Geophysical Journal International*, *212*(2), 1157–1166.

Li, C.-F., Lu, Y., & Wang, J. (2017). A global reference model of Curie-point depths based on EMAG2. *Scientific Reports*, *7*(1), 45129.

Li, Y., & Oldenburg, D. W. (1998). 3-D inversion of gravity data. *Geophysics*, *63*(1), 109–119.

Li, Z., Zhou, J., Wu, G., Wang, J., Zhang, G., Dong, S., Pan, L., Yang, Z., Gao, L., & Ma, Q. (2021). CC-FJpy: A python package for extracting overtone surface-wave dispersion from seismic ambient-noise cross correlation. *Seismological Research Letters*, *92*(5), 3179–3186.

Lin, F.-C., Ritzwoller, M. H., & Snieder, R. (2009). Eikonal tomography: surface wave tomography by phase front tracking across a regional broad-band seismic array. *Geophysical Journal International*, *177*(3), 1091–1110.

Lindsey, N. J., & Martin, E. R. (2021). Fiber-optic seismology. *Annual Review of Earth and Planetary Sciences*, *49*(1), 309–336.

Liu, C., Yao, H., Yang, H., Shen, W., Fang, H., Hu, S., & Qiao, L. (2019). Direct inversion for three-dimensional shear wave speed azimuthal anisotropy based on surface wave ray tracing: Methodology and application to Yunnan, southwest China. *Journal of Geophysical Research: Solid Earth*, *124*(11), 11394–11413.

Lucazeau, F. (2019). Analysis and mapping of an updated terrestrial heat flow data set. *Geochemistry, Geophysics, Geosystems*, *20*(8), 4001–4024.

Majorowicz, J., & Grasby, S. E. (2010). Heat flow, depth–temperature variations and stored thermal energy for enhanced geothermal systems in Canada. *Journal of Geophysics and Engineering*, *7*(3), 232–241.

Malin, P. E., Leary, P. C., Cathles, L. M., & Barton, C. C. (2020). Observational and critical state physics descriptions of long-range flow structures. *Geosciences*, *10*(2), 50.

Maliva, R., & Missimer, T. (2012). Remote Sensing. In *Arid Lands Water Evaluation and Management* (pp. 435–456). Springer Berlin Heidelberg. https://doi.org/10.1007/978-3-642-29104-3_18

Martins, J. E., Weemstra, C., Ruigrok, E., Verdel, A., Jousset, P., & Hersir, G. P. (2020). 3D S-wave velocity imaging of Reykjanes Peninsula high-enthalpy geothermal fields with ambient-noise tomography. *Journal of Volcanology and Geothermal Research*, *391*, 106685.

Mather, B., & Fullea, J. (2019). Constraining the geotherm beneath the British Isles from Bayesian inversion of Curie depth: integrated modelling of magnetic, geothermal, and seismic data. *Solid Earth*, *10*(3), 839–850.

Maubana, W., Maryanto, S., & Nadir, A. (2019). Geochemical Analysis of Mount Pandan Geothermal Area in East Java Indonesia. *Jurnal Internasional Inovatif Energi Dan Teknik*, *6*(1), 137–141.

Maurer, V., Gaucher, E., Grunberg, M., Koepke, R., Pestourie, R., & Cuenot, N. (2020). Seismicity induced during the development of the Rittershoffen geothermal field, France. *Geothermal Energy*, *8*(1), 5.

Mavko, G., Mukerji, T., & Dvorkin, J. (2009). *The Rock Physics Handbook. Cambridge University Press*.

Mejía-Fragoso, J. C., Flórez, M. A., & Bernal-Olaya, R. (2024). Predicting the geothermal gradient in Colombia: A machine learning approach. *Geothermics*, *122*, 103074. https://doi.org/https://doi.org/10.1016/j.geothermics.2024.103074

Mendrinos, D., Karytsas, C., Karytsas, S., Poletto, F., Farina, B., & Barison, E. (2020). Seismic Velocities and Elastic Moduli Correlations with Temperature in a Superhot and an Enhanced Geothermal System. *Proceedings World Geothermal Congress*, 1.

Meyer, G. G., Garrison, G., & Violay, M. (2022). *Permeability of Basalt Through the Brittle-Ductile Transition, Implications for Superhot Rock Geothermal*.

Meyer, G. G., Shahin, G., Cordonnier, B., & Violay, M. (2024). Permeability partitioning through the brittle-to-ductile transition and its implications for supercritical geothermal reservoirs. *Nature Communications*, *15*(1), 7753.

Mhana, N., Julian, B. R., Foulger, G. R., Sabin, A., & Meade, D. (2018). Time-Dependent Seismic Tomography at the Coso Geothermal Area. *Proceedings*.

Miller, J. D. A. (1980). Principles of microbial corrosion. *British Corrosion Journal*, *15*(2), 92–94.

Minissale, A. (1991). The Larderello geothermal field: a review. *Earth-Science Reviews*, *31*(2), 133–151.

Miranda, M. M., Giordano, N., Raymond, J., Pereira, A. J. S. C., & Dezayes, C. (2020). Thermophysical properties of surficial rocks: a tool to characterize geothermal resources of remote northern regions. *Geothermal Energy*, *8*(1), 4. https://doi.org/10.1186/s40517-020-0159-y

Moeck, I. S. (2014). Catalog of geothermal play types based on geologic controls. *Renewable and Sustainable Energy Reviews*, *37*, 867–882.

Momita, M., Tokita, H., Matsudo, K., Takagi, H., Soeda, Y., Tosha, T., & Koide, K. (2000). Deep geothermal structure and the hydrothermal system in the Otake–Hatchobaru Geothermal Field. *22nd New Zealand Geothermal Workshop, Auckland, New Zealand*, 8–10.

Moorkamp, M., Heincke, B., Jegen, M., Roberts, A. W., & Hobbs, R. W. (2011). A framework for 3-D joint inversion of MT, gravity and seismic refraction data. *Geophysical Journal International*, *184*(1), 477–493.

Mordensky, S. P., Burns, E. R., Lipor, J. J., & DeAngelo, J. (2023b). Cursed? Why one does not simply add new data sets to supervised geothermal machine learning models. *Geothermal Resources Council Transactions*, *47*, 1288-1313.

Mordensky, S. P., Burns, E., DeAngelo, J., and Lipor, J. (2023c). Predicting Large Hydrothermal Systems. *Geothermal Resources Council Transactions*, 47, 1763-1796.

Mordensky, S. P., Lipor, J., Burns, E., & Lindsey, C. R. (2022). What did they just say? Building a Rosetta stone for geoscience and machine learning. *2022 Geothermal Rising Conference*, *46*.

Mordensky, S. P., Lipor, J. J., DeAngelo, J., Burns, E. R., & Lindsey, C. R. (2023a). When less is more: How increasing the complexity of machine learning strategies for geothermal energy assessments may not lead toward better estimates. *Geothermics*, *110*, 102662.

Morency, C., Matzel, E., Grobbe, N., Brito, D., Bordes, C., Bernardo, N., Barucq, H., Diaz, J., Heta, A., & Bellanger, M. (2022). Seismoelectric effects for geothermal resources assessment and monitoring:

Overview and preliminary results. *Proc. of the 47th Workshop on Geothermal Reservoir Engineering*.

Moreno, T., Wallis, S. R., Kojima, T., & Gibbons, W. (2016). *The geology of Japan*. Geological Society London.

Mousavi, S. M., Ellsworth, W. L., Zhu, W., Chuang, L. Y., & Beroza, G. C. (2020). Earthquake transformer—an attentive deep-learning model for simultaneous earthquake detection and phase picking. *Nature Communications*, *11*(1), 3952.

Muanza, P., Jónsdóttir, I., Kristinsson, S., Einarsson, G., & Björnsson, G. (2024). *Geothermal mapping and remote sensing of thermal anomalies at Grændalur area, Hveragerði, SW Iceland*.

Mudunuru, M. K., Ahmmed, B., Frash, L., & Frijhoff, R. (2023). Deep Learning for Modeling Enhanced Geothermal Systems. *PROCEEDINGS of 48th Workshop on Geothermal Reservoir Engineering. Presented at the Workshop on Geothermal Reservoir Engineering, Stanford University, Stanford, California*.

Mudunuru, M. K., Vesselinov, V. V, & Ahmmed, B. (2022). GeoThermalCloud: Machine Learning for Geothermal Resource Exploration. *Journal of Machine Learning for Modeling and Computing*, *3*(4).

Mukumoto, K., Capdeville, Y., Singh, S., & Tsuji, T. (2024). Accounting for subwavelength heterogeneities in full waveform inversion based on wavefield gradient measurements. *Geophysical Journal International*, *238*(1), 235–256.

Munoz, G. (2014). Exploring for Geothermal Resources with Electromagnetic Methods. *Surveys in Geophysics*, *35*(1), 101–122. https://doi.org/10.1007/s10712-013-9236-0

Munoz, G., & Ritter, O. (2013). Pseudo-remote reference processing of magnetotelluric data: a fast and efficient data acquisition scheme for local arrays. *Geophysical Prospecting*, *61*(sup1), 300–316.

Nibe, T., & Matsushima, J. (2022). Cross-well seismic attenuation tomography with correction for coupling effects at source and receiver positions in the Yutsubo geothermal field, Japan. *Geothermics*, *105*, 102550.

Nimiya, H., Ikeda, T., & Tsuji, T. (2020). Three-dimensional S wave velocity structure of central Japan estimated by surface-wave tomography using ambient noise. *Journal of Geophysical Research: Solid Earth*, *125*(4), e2019JB019043.

Nimiya, H., Ikeda, T., & Tsuji, T. (2023). Multimodal Rayleigh and Love wave joint inversion for S-wave velocity structures in Kanto basin, Japan. *Journal of Geophysical Research: Solid Earth*, *128*(1), e2022JB025017.

Nthaba, B., Ikeda, T., Nimiya, H., Tsuji, T., & Iio, Y. (2022). Ambient noise tomography for a high-resolution 3D S-wave velocity model of the Kinki Region, Southwestern Japan, using dense seismic array data. *Earth, Planets and Space*, *74*(1), 96.

Nthaba, B., Ikeda, T., Tsuji, T., & Iio, Y. (2023). High-resolution three-dimensional azimuthal velocity anisotropy of S-waves in southern-central Japan, based on ambient noise tomography. *Earth, Planets and Space*, *75*(1), 102.

Núñez Demarco, P., Prezzi, C., & Sánchez Bettucci, L. (2021). Review of Curie point depth determination through different spectral methods applied to magnetic data. *Geophysical Journal International*, *224*(1), 17–39.

Obermann, A., & Hillers, G. (2019). Seismic time-lapse interferometry across scales. In *Advances in geophysics* (Vol. 60, pp. 65–143). Elsevier.

Ogawa, Y., Ichiki, M., Kanda, W., Mishina, M., & Asamori, K. (2014). Three-dimensional magnetotelluric imaging of crustal fluids and seismicity around Naruko volcano, NE Japan. *Earth, Planets and Space*, *66*, 1–13.

Okoroafor, E. R., Smith, C. M., Ochie, K. I., Nwosu, C. J., Gudmundsdottir, H., & Aljubran, M. J. (2022). Machine learning in subsurface geothermal energy: Two decades in review. *Geothermics*, *102*, 102401.

Omollo, P., & Nishijima, J. (2023). Analysis and interpretation of the gravity data to delineate subsurface structural geometry of the Olkaria geothermal reservoir, Kenya. *Geothermics*, *110*, 102663.

Omollo, P., & Nishijima, J. (2024). Inception of time-lapse micro-gravity monitoring of the great Olkaria geothermal field, Kenya. *Geothermics*, *117*, 102891.

Pandarinath, K., Shankar, R., Torres-Alvarado, I. S., & Warrier, A. K. (2014). Magnetic susceptibility of volcanic rocks in geothermal areas: application potential in geothermal exploration studies for identification of rocks and zones of hydrothermal alteration. *Arabian Journal of Geosciences*, *7*, 2851–2860.

Parisio, F., Yoshioka, K., Sakaguchi, K., Goto, R., Miura, T., Pramudyo, E., Ishibashi, T., & Watanabe, N. (2021). A laboratory study of hydraulic fracturing at the brittle-ductile transition. *Scientific Reports*, *11*(1), 22300.

Pauling, H., Taverna, N., Trainor-Guitton, W., Witter, E., Kolker, A., Warren, I., Robins, J., & Rhodes, G. (2023). *Geothermal Play Fairway Analysis Best Practices*. National Renewable Energy Laboratory (NREL), Golden, CO (United States).

Peacock, J. R., & Siler, D. L. (2021). Bottom-Up and Top-Down Control on Hydrothermal Resources in the Great Basin: An Example from Gabbs Valley, Nevada. *Geophysical Research Letters*, *48*(23), e2021GL095009.

Peacock, J. R., Thiel, S., Reid, P., & Heinson, G. (2012). Magnetotelluric monitoring of a fluid injection: Example from an enhanced geothermal system. *Geophysical Research Letters*, *39*(18).

Pearce, R. K., Sánchez de la Muela, A., Moorkamp, M., Hammond, J. O. S., Mitchell, T. M., Cembrano, J., Araya Vargas, J., Meredith, P. G., Iturrieta, P., & Pérez-Estay, N. (2020). Reactivation of fault systems by compartmentalized hydrothermal fluids in the Southern Andes revealed by magnetotelluric and seismic data. *Tectonics*, *39*(12), e2019TC005997.

Pearce, R., & Pink, T. (2024). *A Survey of Methods, Challenges, and Pathways Forward for Superhot Rock Drilling*.

Pérouse, E., & Wernicke, B. P. (2017). Spatiotemporal evolution of fault slip rates in deforming continents: The case of the Great Basin region, northern Basin and Range province. *Geosphere*, *13*(1), 112–135.

Petrini, C., Madonna, C., & Gerya, T. (2021). Inversion in the permeability evolution of deforming Westerly granite near the brittle–ductile transition. *Scientific Reports*, *11*(1), 24027.

Petty, S., Cladouhos, T., Watz, J., & Garrison, G. (2020). Technology Needs for SuperHot EGS Development. *45th Workshop on Geothermal Reservoir Engineering*.

Piana Agostinetti, N., Licciardi, A., Piccinini, D., Mazzarini, F., Musumeci, G., Saccorotti, G., & Chiarabba, C. (2017). Discovering geothermal supercritical fluids: a new frontier for seismic exploration. *Scientific Reports*, *7*(1), 14592.

Planès, T., Obermann, A., Antunes, V., & Lupi, M. (2020). Ambient-noise tomography of the Greater Geneva Basin in a geothermal exploration context. *Geophysical Journal International*, *220*(1), 370–383.

Poletto, F., Farina, B., & Carcione, J. M. (2018). Sensitivity of seismic properties to temperature variations in a geothermal reservoir. *Geothermics*, *76*, 149–163.

Pollack, H. N., Hurter, S. J., & Johnson, J. R. (1993). Heat flow from the Earth's interior: analysis of the global data set. *Reviews of Geophysics*, *31*(3), 267–280.

Poux, B., & O'Brien, J. (2020). A Conceptual Approach to 3-D Play Fairway Analysis for Geothermal Exploration and Development. *Proceedings 42nd New Zealand Geothermal Workshop*, *24*, 26.

Preston, L. (2010). *P-and S-body wave tomography of the state of Nevada.* Sandia National Laboratories (SNL), Albuquerque, NM, and Livermore, CA ….

Rawlinson, N., & Sambridge, M. (2003). Seismic traveltime tomography of the crust and lithosphere. *Advances in Geophysics*, *46*, 81–199.

Reath, K., Pritchard, M., Poland, M., Delgado, F., Carn, S., Coppola, D., Andrews, B., Ebmeier, S. K., Rumpf, E., & Henderson, S. (2019). Thermal, deformation, and degassing remote sensing time series (CE 2000–2017) at the 47 most active volcanoes in Latin America: Implications for volcanic systems. *Journal of Geophysical Research: Solid Earth*, *124*(1), 195–218.

Reinsch, T., Dobson, P., Asanuma, H., Huenges, E., Poletto, F., & Sanjuan, B. (2017). Utilizing supercritical geothermal systems: a review of past ventures and ongoing research activities. *Geothermal Energy*, *5*(1), 1–25.

Richards, C., Tape, C., Abers, G. A., & Ross, Z. E. (2021). Anisotropy variations in the Alaska subduction zone based on shear-wave splitting from intraslab earthquakes. *Geochemistry, Geophysics, Geosystems*, *22*(5), e2020GC009558.

Rosenkjaer, G. K., Gasperikova, E., Newman, G. A., Arnason, K., & Lindsey, N. J. (2015). Comparison of 3D MT inversions for geothermal exploration: Case studies for Krafla and Hengill geothermal systems in Iceland. *Geothermics*, *57*, 258–274.

Rowland, J. V, & Simmons, S. F. (2012). Hydrologic, Magmatic, and Tectonic Controls on Hydrothermal Flow, Taupo Volcanic Zone, New Zealand: Implications for the Formation of Epithermal Vein Deposits. *Economic Geology*, *107*, 427–457.

Sadeghisorkhani, H., Gudmundsson, Ó., & Tryggvason, A. (2018). GSpecDisp: a matlab GUI package for phase-velocity dispersion measurements from ambient-noise correlations. *Computers & Geosciences*, *110*, 41–53.

Samrock, F., Grayver, A., Dambly, M. L. T., Müller, M. R., & Saar, M. O. (2023). Geophysically guided well siting at the Aluto-Langano geothermal reservoir. *Geophysics*, *88*(5), WB105–WB114.

Sanada, N., Kurata, Y., Nanjo, H., Kim, H., Ikeuchi, J., & Lichti, K. A. (2000). IEA deep geothermal resources subtask C: materials, progress with a database for materials performance in deep and acidic geothermal wells. *Proc World Geothermal Congress, Kyushu, Tohoku, Japan*, 2411–2416.

Sánchez-Pastor, P., Obermann, A., Reinsch, T., Ágústsdóttir, T., Gunnarsson, G., Tómasdóttir, S., Hjörleifsdóttir, V., Hersir, G. P., Ágústsson, K., & Wiemer, S. (2021). Imaging high-temperature geothermal reservoirs with ambient seismic noise tomography, a case study of the Hengill geothermal field, SW Iceland. *Geothermics*, *96*, 102207.

Sánchez-Pastor, P., Wu, S.-M., Hokstad, K., Kristjánsson, B., Drouin, V., Ducrocq, C., Gunnarsson, G., Rinaldi, A., Wiemer, S., & Obermann, A. (2023). Steam caps in geothermal reservoirs can be monitored using seismic noise interferometry. *Communications Earth & Environment*, *4*(1), 453. https://doi.org/10.1038/s43247-023-01122-8

Sandwell, D., Mellors, R., Tong, X., Wei, M., & Wessel, P. (2011). *GMTSAR: An InSAR processing system based on generic mapping tools*.

Sanjuan, B., Millot, R., Asmundsson, R., Brach, M., & Giroud, N. (2014). Use of two new Na/Li geothermometric relationships for geothermal fluids in volcanic environments. *Chemical Geology*, *389*, 60–81.

Santilano, A., Giodio, A., Manzella, A., Menghini, A., Rizzo, E., & Romano, G. (2015). Electromagnetic and DC methods for geothermal exploration in Italy–case studies and future developments. *First Break*, *33*(8).

Sayers, C. M. (1994). The elastic anisotrophy of shales. *Journal of Geophysical Research: Solid Earth*, *99*(B1), 767–774.

Sellars, J., Ball, P. J., Gould, K., & Afonso, J. C. (2023). Mapping the 450 C isotherm: Mapping uncertainties and the potential of deep geothermal in Canada. *THE MAGAZINE OF CANADIAN ENERGY GEOSCIENTISTS*, *Reservoir* (4).

Sewell, S. M., Addison, S. J., Hernandez, D., Azwar, L., & Barnes, M. L. (2015). Rotokawa conceptual model update 5 years after commissioning of the 138 MWe NAP plant. *Proc. NZ Geothermal Workshop*.

Shapiro, N. M., & Campillo, M. (2004). Emergence of broadband Rayleigh waves from correlations of the ambient seismic noise. *Geophysical Research Letters*, *31*(7).

Shervais, J. W., DeAngelo, J., Glen, J. M., Nielson, D. L., Garg, S., Dobson, P., Gasperikova, E., Sonnenthal, E., Liberty, L. M., & Newell, D. L. (2024). Geothermal play fairway analysis, part 1: Example from the Snake River Plain, Idaho. *Geothermics*, *117*, 102865.

Shervais, J. W., Evans, J. P., Newell, D. L., Glen, J. M., DeAngelo, J., Siler, D., Peacock, J., Dobson, P., Gasperikova, E., and Sonnenthal, E. (2021). *Play Fairway Analysis of the Snake River Plain, Idaho.*

Shevenell, L., Coolbaugh, M., Hinz, N., Stelling, P., Melosh, G., & Cumming, W. (2015). *Geothermal Potential of the Cascade and Aleutian Arcs, with Ranking of Individual Volcanic Centers for their Potential to Host Electricity-Grade Reservoirs*. ATLAS Geosciences, Inc., Reno, NV (United States).

Shi, Y., Rop, E., Wang, Z., Jiang, G., Wang, S., & Hu, S. (2021). Characteristics and formation mechanism of the Olkaria geothermal system, Kenya revealed by well temperature data. *Geothermics*, *97*, 102243.

Sicking, C., & Malin, P. (2019). Fracture seismic: Mapping subsurface connectivity. *Geosciences*, *9*(12), 508.

Siler, D. L., Pepin, J. D., Vesselinov, V. V, Mudunuru, M. K., & Ahmmed, B. (2021). Machine learning to identify geologic factors associated with production in geothermal fields: a case-study using 3D geologic data, Brady geothermal field, Nevada. *Geothermal Energy*, *9*, 1–17.

Siler, D. L., Witter, J. B., Craig, J. W., Faulds, J. E., Glen, J. M., Earney, T. E., Schermerhorn, W. D., Peacock, J. R., & Fournier, D. (2020). Using 3D gravity inversion modeling to iteratively refine 3D geologic maps: The Nevada play fairway project, southern Gabbs Valley. *Nevada: Geothermal Resources Council Transactions*, *44*, 20.

Simmons, S. F., Kirby, S., Bartley, J., Allis, R., Kleber, E., Knudsen, T., Miller, J., Hardwick, C., Rahilly, K., & Fischer, T. (2019). Update on the geoscientific understanding of the Utah FORGE site. *Proceedings*.

Simpson, F., & Bahr, K. (2005). *Practical magnetotellurics*. Cambridge University Press.

Soyer, W., Mackie, R., Pavesi, A., Hallinan, S., & Miorelli, F. (2018). Multi-physics Imaging of a High Enthalpy Geothermal Field: the Darajat Case. *First EAGE/IGA/DGMK Joint Workshop on Deep Geothermal Energy*, cp-577-00002.

Spichak, V., & Manzella, A. (2009). Electromagnetic sounding of geothermal zones. *Journal of Applied Geophysics*, *68*(4), 459–478.

Spichak, V. V. (2020). Modern Methods for Joint Analysis and Inversion of Geophysical Data. *Russian Geology and Geophysics*, *61*(3), 341–357. https://doi.org/10.15372/RGG2019092

Stephansson, O., & Zang, A. (2014). ISRM suggested methods for rock stress estimation—part 5: establishing a model for the in situ stress at a given site. In *The ISRM Suggested Methods for Rock Characterization, Testing and Monitoring: 2007-2014* (pp. 187–201). Springer.

Stockwell Jr, J. W. (1999). The CWP/SU: seismic Un∗ x package. *Computers & Geosciences*, *25*(4), 415–419.

Sudo, Y., & Matsumoto, Y. (1998). Three-dimensional P-wave velocity structure in the upper crust beneath Kuju Volcano, central Kyushu, Japan. *Bulletin of Volcanology*, *60*, 147–159.

Suemoto, Y., Tsuji, T., & Ikeda, T. (2022). Temporal variation and frequency dependence of ambient noise on Mars from polarization analysis. *Authorea Preprints*.

Suryanarayana, S., Krishnamurthy, R. M., & Bour, D. (2024). *A Survey of Methods, Challenges, and Pathways Forward for Superhot Rock Well Design and Construction*.

Takei, Y. (2017). Effects of partial melting on seismic velocity and attenuation: A new insight from experiments. *Annual Review of Earth and Planetary Sciences*, *45*(1), 447–470.

Taverna, N., Pauling, H., Trainor-Guitton, W., Kolker, A., Mibei, G., Dobson, P., Sonnenthal, E., Tu, X., & Schultz, A. (2024). De-risking superhot EGS development through 3D play fairway analysis: Methodology development and application at Newberry Volcano, Oregon, USA. *Geothermics*, *118*, 102909.

Telford, W. M., Geldart, L. P., & Sheriff, R. E. (1990). *Applied geophysics*. Cambridge university press.

Tester, J. W., Anderson, B. J., Batchelor, A. S., Blackwell, D. D., DiPippo, R., Drake, E. M., Garnish, J., Livesay, B., Moore, M. C., & Nichols, K. (2006). The future of geothermal energy. *Massachusetts Institute of Technology*, *358*, 1–3.

Thiel, S. (2017). Electromagnetic monitoring of hydraulic fracturing: Relationship to permeability, seismicity, and stress. *Surveys in Geophysics, 38*(5), 1133–1169.

Thompson, R. R. (1936). The seismic electric effect. *Geophysics*, *1*(3), 327–335.

Toledo, T., Obermann, A., Verdel, A., Martins, J. E., Jousset, P., Mortensen, A. K., Erbas, K., & Krawczyk, C. M. (2022a). Ambient seismic noise monitoring and imaging at the Theistareykir geothermal field (Iceland). *Journal of Volcanology and Geothermal Research*, *429*, 107590.

Toledo, T., Obermann, A., Verdel, A., Martins, J. E., Jousset, P., Mortensen, A. K., Erbas, K., & Krawczyk, C. M. (2022b). Ambient seismic noise monitoring and imaging at the Theistareykir geothermal field (Iceland). *Journal of Volcanology and Geothermal Research*, *429*, 107590.

Tomac, I., & Sauter, M. (2018). A review on challenges in the assessment of geomechanical rock performance for deep geothermal reservoir development. *Renewable and Sustainable Energy Reviews*, *82*, 3972–3980.

Trainor-Guitton, W. J., Hoversten, G. M., Nordquist, G., & Intani, R. G. (2017). Value of MT inversions for geothermal exploration: accounting for multiple interpretations of field data & determining new drilling locations. *Geothermics*, *66*, 13–22.

Trainor-Guitton, W., Ramirez, A., Ziagos, J., Mellors, R., and Roberts, J. (2013). *An initial value of information (VOI) framework for geophysical data applied to the exploration of geothermal energy*. In PROCEEDINGS, 38th Workshop on Geothermal Reservoir Engineering Stanford University, Stanford, California, February 11-13, 2013.

Treitel, S., & Lines, L. (2001). Past, present, and future of geophysical inversion—A new millennium analysis. *Geophysics*, *66*(1), 21–24.

Tsuji, S., Araki, E., Yokobiki, T., Nishida, S., Machida, Y., Zumberge, M., & Takahashi, K. (2023). Precise tilt measurement by seafloor borehole tiltmeters at the Nankai Trough subduction zone. *Earth, Planets and Space*, *75*(1), 188.

Tsuji, T., Ikeda, T., Matsuura, R., Mukumoto, K., Hutapea, F. L., Kimura, T., Yamaoka, K., & Shinohara, M. (2021). Continuous monitoring system for safe managements of CO2 storage and geothermal reservoirs. *Scientific Reports*, *11*(1), 19120.

Tsuji, T., Kamei, R., & Pratt, R. G. (2014). Pore pressure distribution of a mega-splay fault system in the Nankai Trough subduction zone: Insight into up-dip extent of the seismogenic zone. *Earth and Planetary Science Letters*, *396*, 165–178.

Tsvankin, I., Gaiser, J., Grechka, V., Van Der Baan, M., & Thomsen, L. (2010). Seismic anisotropy in exploration and reservoir characterization: An overview. *Geophysics*, *75*(5), 75A15-75A29.

Tu, X., & Zhdanov, M. S. (2021). Joint Gramian inversion of geophysical data with different resolution capabilities: Case study in Yellowstone. *Geophysical Journal International*, *226*(2), 1058–1085.

Ulberg, C. W., Creager, K. C., Moran, S. C., Abers, G. A., Thelen, W. A., Levander, A., Kiser, E., Schmandt, B., Hansen, S. M., & Crosson, R. S. (2020). Local source Vp and Vs tomography in the Mount St. Helens region with the iMUSH broadband array. *Geochemistry, Geophysics, Geosystems*, *21*(3), e2019GC008888.

Uno, M., Koyanagawa, K., Kasahara, H., Okamoto, A., & Tsuchiya, N. (2022). Volatile-consuming reactions fracture rocks and self-accelerate fluid flow in the lithosphere. *Proceedings of the National Academy of Sciences*, *119*(3), e2110776118.

Van der Meer, F., Hecker, C., van Ruitenbeek, F., van der Werff, H., de Wijkerslooth, C., & Wechsler, C. (2014). Geologic remote sensing for geothermal exploration: A review. *International Journal of Applied Earth Observation and Geoinformation*, *33*, 255–269.

Van Leeuwen, T., & Mulder, W. A. (2010). A correlation-based misfit criterion for wave-equation traveltime tomography. *Geophysical Journal International*, *182*(3), 1383–1394.

Vatankhah, S., Renaut, R. A., Huang, X., Mickus, K., & Gharloghi, M. (2022). Large-scale focusing joint inversion of gravity and magnetic data with Gramian constraint. *Geophysical Journal International*, *230*(3), 1585–1611.

Vernik, L. (2016). *Seismic petrophysics in quantitative interpretation*. Society of Exploration Geophysicists.

Vesselinov, V. V., Ahmmed, B., Mudunuru, M. K., Pepin, J. D., Burns, E. R., Siler, D. L., Karra, S., & Middleton, R. S. (2022). Discovering hidden geothermal signatures using non-negative matrix factorization with customized k-means clustering. *Geothermics*, *106*, 102576.

Wallace, P. J., Plank, T., Edmonds, M., & Hauri, E. H. (2015). Volatiles in magmas. In *The encyclopedia of volcanoes* (pp. 163–183). Elsevier.

Wang, S., Xu, W., & Guo, T. (2024). Advances in Thermal Infrared Remote Sensing Technology for Geothermal Resource Detection. *Remote Sensing*, *16*(10), 1690.

Wannamaker, P. E., Caldwell, T. G., Jiracek, G. R., Maris, V., Hill, G. J., Ogawa, Y., Bibby, H. M., Bennie, S. L., & Heise, W. (2009). Fluid and deformation regime of an advancing subduction system at Marlborough, New Zealand. *Nature*, *460*(7256), 733–736.

Wannamaker, P. E., Pankow, K. L., Moore, J. N., Nash, G. D., Maris, V., Simmons, S. F., & Hardwick, C. L. (2016). Play fairway analysis for structurally controlled geothermal systems in the eastern Great Basin extensional regime, Utah. *Proceedings* 41st Workshop on Geothermal Reservoir Engineering Stanford University, Stanford, California, February 22-24, 2016.

Watanabe, N., Abe, H., Okamoto, A., Nakamura, K., & Komai, T. (2021). Formation of amorphous silica nanoparticles and its impact on permeability of fractured granite in superhot geothermal environments. *Scientific Reports*, *11*(1), 5340.

Watanabe, N., Egawa, M., Sakaguchi, K., Ishibashi, T., & Tsuchiya, N. (2017). Hydraulic fracturing and permeability enhancement in granite from subcritical/brittle to supercritical/ductile conditions. *Geophysical Research Letters*, *44*(11), 5468–5475.

Watanabe, N., Numakura, T., Sakaguchi, K., Saishu, H., Okamoto, A., Ingebritsen, S. E., & Tsuchiya, N. (2017). Potentially exploitable supercritical geothermal resources in the ductile crust. *Nature Geoscience*, *10*(2), 140–144.

Watanabe, N., Sakaguchi, K., Goto, R., Miura, T., Yamane, K., Ishibashi, T., Chen, Y., Komai, T., & Tsuchiya, N. (2019). Cloud-fracture networks as a means of accessing superhot geothermal energy. *Scientific Reports*, *9*(1), 939.

Webster, J. D., Kinzler, R. J., & Mathez, E. A. (1999). Chloride and water solubility in basalt and andesite melts and implications for magmatic degassing. *Geochimica et Cosmochimica Acta*, *63*(5), 729–738.

Wenning, Q. C., Madonna, C., de Haller, A., & Burg, J.-P. (2018). Permeability and seismic velocity anisotropy across a ductile–brittle fault zone in crystalline rock. *Solid Earth*, *9*(3), 683–698.

White, R. S., Edmonds, M., Maclennan, J., Greenfield, T., & Agustsdottir, T. (2019). Melt movement through the Icelandic crust. *Philosophical Transactions of the Royal Society A*, *377*(2139), 20180010.

Wiemer, S., Kraft, T., Trutnevyte, E., & Roth, P. (2017). *"Good practice" guide for managing induced seismicity in deep geothermal energy projects in Switzerland*. ETH Zurich.

Williams, C. F., Reed, M. J., Mariner, R. H., DeAngelo, J., & Galanis, S. P. (2008). *Assessment of moderate- and high-temperature geothermal resources of the United States*. Geological Survey (US).

Witter, J. B., Siler, D. L., Faulds, J. E., & Hinz, N. H. (2016). 3D geophysical inversion modeling of gravity data to test the 3D geologic model of the Bradys geothermal area, Nevada, USA. *Geothermal Energy*, *4*, 1–21.

Zahedi, R., Daneshgar, S., Seraji, M. A. N., & Asemi, H. (2022). Modeling and interpretation of geomagnetic data related to geothermal sources, Northwest of Delijan. *Renewable Energy*, *196*, 444–450.

Zang, A., & Stephansson, O. (2009). *Stress Field of the Earth's Crust*. Springer Science & Business Media.

Zhang, J. (2011). Pore pressure prediction from well logs: Methods, modifications, and new approaches. *Earth-Science Reviews*, *108*(1–2), 50–63.

Zhang, J., Xingyao, Y., Zhang, G., Yipeng, G., and Xianggang, F. (2020). Prediction method of physical parameters based on linearized rock physics inversion. P*etroleum Exploration and Development, 47*(1), 59-67.

Zoback, M., Hickman, S., Ellsworth, W., & Team, S. S. (2011). Scientific drilling into the San Andreas fault zone–an overview of SAFOD's first five years. *Scientific Drilling*, *11*, 14–28.